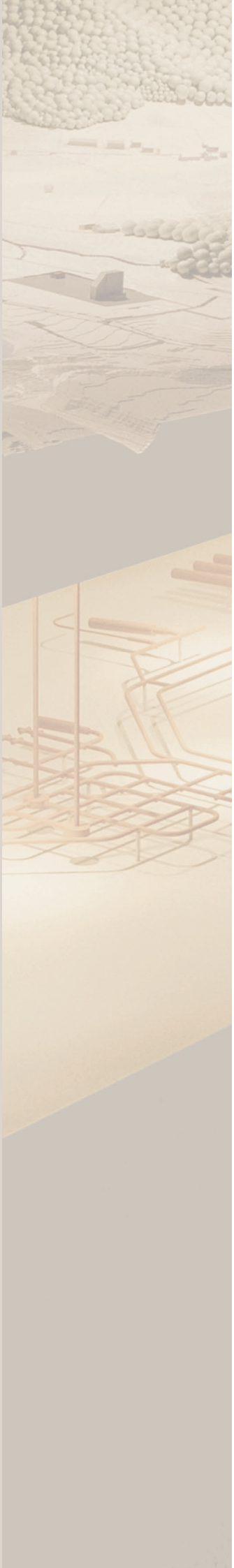

nagra.

ARBEITSBERICHT NAB 23-21

Evolution of the Sealing System Porosity and its Impact on Performance

September 2023

Nagra | National Cooperative for the Disposal of Radioactive Waste
Hardstrasse 73 | 5430 Wettingen | Switzerland
+41 56 437 11 11 | info@nagra.ch | nagra.ch

nagra.

ARBEITSBERICHT NAB 23-21

Evolution of the Sealing System Porosity and its Impact on Performance

September 2023

L. Martin[1], G. Kosakowski[2]
A. Papafotiou[1,3] & P.A. Smith[4]

[1]Nagra

[2]Paul Scherrer Institute (PSI)

[3]Intera

[3]Safety Assessment Management (Switzerland) GmbH

KEYWORDS
Sealing system, cement-clay interaction, diffusion, gas transport, clogging, performance assessment

Nagra | National Cooperative for the Disposal of Radioactive Waste
Hardstrasse 73 | 5430 Wettingen | Switzerland
+41 56 437 11 11 | info@nagra.ch | nagra.ch

Nagra Arbeitsberichte ("Working Reports") present the results of work in progress that have not necessarily been subject to a comprehensive review. They are intended to provide rapid dissemination of current information..

Table of Contents

List of Tables

List of Figures

List of Acronyms

BFE	Bundesamt für Energie (Swiss federal office for energy)
COx	Callovo Oxfordian Claystone
CI	Cement-Opalinus Clay interaction experiment at the Mont Terri rock laboratory
C-S-H	Cement phase: Calcium-silicate-hydrate
CV	Coefficient of variation
D	Apparent diffusion coefficient
D_e	Effective diffusion coefficient
DGR	Deep geological repository
D_W	Gas specific diffusion coefficient in water
EDL	Electric double layers
ENSI	Swiss Federal Nuclear Safety Inspectorate
EDZ	Excavation Damage Zone
FEBEX	Full-scale Engineered Barriers Experiment at the Grimsel test site
FIB-nt	Focussed Ionbeam Nano-tomography
GAST	Gas Permeable Seal Test, experiment at the Grimsel test site
GMT	Gas Migration Test, experiment at the Grimsel test site
HCM	Hydro-chemo mechanical behaviour
HET	Heterogeneous nucleation
HG-D	Reactive gas transport in argillaceous fromation experiment at the Mont Terri rock laboratory
HLW	High-level waste (spent fuel assemblies and high-level waste from reprocessing)
HOM	Homogeneous nucleation
HT	Hydrogen transfer experiment at the Mont Terri rock laboratory
HTO	Tritium (^{3}H)-bearing water
IAEA	International Atomic Energy Agency
ILW	Intermediate level waste
IUPAC	International Union of Pure and Applied Chemistry
k	Intrinsic permeability [m^2]
KEG	Kernenergie Gesetz (Swiss Nuclear Energy Act)
L/ILW	Low- and intermediate-level waste
MA	Microbial activity experiment at the Mont Terri rock laboratory

MIR	Radioactive waste from medicine, industry and research
M-S-H	Cement phase: Magnesium silicate hydrate
NL	Siting region of Nördlich Lägern
OPA	Opalinus Clay rock
OPC	Ordinary Portland Cement, referring to CEM I according to SN EN 197-1
PEBS project	Long-term performance of the engineered barrier system project
PSI	Paul Scherrer Institute
REV	Representative elementary volume
RH	Relative humidity
RTM	Reactive Transport Models
SEM	Scanning Electron Microscopy
SF	Spent fuel
SFOE	Swiss federal office for energy
SNT	Supersaturation nucleation time
TEM	Transmission Electron Microscopy
TOT	tetrahedral-octahedral-tetrahedral layer structure of clay minerals
V	Sealing element
VE	Ventilation experiment at the Mont Terri rock laboratory
VF	Tunnel backfill

1 Introduction

1.1 Background and aims

In Switzerland, the Nuclear Energy Law requires the disposal of all types of radioactive waste in deep geological repositories (KEG 2003). The basic feasibility of the safe disposal of radioactive waste in a deep geological repository in a clay host rock was demonstrated by Nagra in Project Entsorgungsnachweis (the term translates into English as "demonstration of disposal feasibility") at the end of 2002. This feasibility study was based on the Opalinus Clay host rock option in the Zürcher Weinland area in northern Switzerland and was supported by a detailed safety case (Nagra 2002a, Nagra 2002b). At the time, two types of repositories were foreseen in Switzerland:

- a repository for the disposal of low- and intermediate-level waste (L/ILW) arising from the operation and decommissioning of Swiss nuclear power plants, from medicine, industry and research and from those operations in reprocessing that produce only low-level technological waste
- a repository for the disposal of high-level waste (HLW), comprising spent nuclear fuel (SF) and vitrified HLW, as well as long-lived intermediate-level waste (ILW), primarily resulting from fuel reprocessing

Project Entsorgungsnachweis considered only the repository for SF/HLW/ILW, referred to in the following as the HLW repository.

The choice of both Opalinus Clay and the Zürcher Weinland was the result of preliminary, safety-based evaluation of potential host rocks, in which other possible options were also evaluated but set aside by Nagra; host-rock and site selection were later carried out in a more systematic manner following the sectoral plan for deep geological repositories.

The sectoral plan for deep geological repositories (BFE 2008) specifies how sites for deep geological radwaste repositories are to be selected in Switzerland. The concept for the sectoral plan for deep geological repositories was developed by the Swiss Federal Office of Energy (SFOE) together with other agencies and organisations and was approved by the Federal Council in 2008. This procedure set out in the sectoral plan allows a transparent and fair choice of siting locations in three stages:

- Stage 1: Selection of geological siting regions
- Stage 2: Selection of at least two sites
- Stage 3: Selection of one site

In September 2022, as part of Stage 3 of the siting procedure, Nagra formally proposed the siting region Nördlich Lägern (NL), which lies within cantons Zürich and Aargau, as the site for a combined repository for all waste types, with Opalinus Clay as the selected host rock (Nagra 2022). Nagra is currently in the process of preparing a general licence application for this site, supported by a safety case, that it will submit at the end of 2024. The Federal Council and the Swiss Parliament will decide on the granting of the general licence and a national referendum can be called for on this decision.

The present report is one of several in support of the safety case for the general licence application that will address the requirement that the long-term behaviour of the repository barrier system must be understood (KEG 2003). The specific barrier addressed by this report is the sealing system, i.e., the sealing and backfilling of the underground openings and the access structures. The sealing system is designed to provide a strong and stable barrier to radionuclide transport. In addition, it provides a transport and storage system for repository-generated gas that prevents the build-up of potentially adverse gas pressures in the disposal areas, as well as mechanical

stabilisation of the host rock following the degradation of the excavation support. It also reduces the probability of human intrusion into the repository. The sealing system must continue to perform these functions as it evolves over time due to a range of physical and, most importantly in the context of this report, chemical processes. The overarching aim of this report is to examine the ways in which the porosity of the sealing system could evolve in response to these processes and the resulting impact on sealing system performance, including, in particular, the impact on the fate of repository-generated gas.

The report reviews and summarises current understanding of the chemical processes that could lead to porosity changes, i.e., to mineral dissolution and, most importantly from the point of view of gas transport and storage, to precipitation of minerals in relevant porous media and the resulting implications for the design and performance of the sealing system. Because it is critical to the occurrence of these chemical processes and to the evolution of gas pressures, the saturation history of the repository is also described, based on the results of two-phase flow modelling carried out as part of Stage 2 of the sectoral plan. In the course of ongoing work, these results will be updated and documented as part of the gas synthesis report (Nagra NTB 24-23 *planned*) and of the performance assessment synthesis (Nagra NTB 24-22 *planned*), along with a description of model abstraction and validation.

With currently available state-of-the-art numerical codes, it is not possible to simulate the sealing system porosity evolution in a holistic way, taking into account all physical and (bio-)chemical processes and their couplings at the necessary level of detail. For this reason, this report is based on a set of theoretical arguments and considerations supported by literature reviews on potentially relevant processes in combination with numerical simulations. These simulations investigate specific aspects of (sub-)system evolution by considering only selected processes and their couplings. The simulation codes that are used are validated in terms of their numerical correctness via numerical tests and code comparison (benchmarking) studies. Details of model conceptualisation and model validation are given in Nagra NTB 24-22 *(planned)* and in the reference therein. In terms of application, the results of numerical simulations are compared with published experimental and numerical studies on related systems. This approach is in line with IAEA Safety Glossary 2022 definition on “validation on process level” (IAEA 2022).

It is to be noted that porosity evolution and its impact on performance is assessed for a flexible sealing system design, which is part of a provisional engineered barrier system design developed specifically to support the general licence application by demonstrating that safe disposal in the NL siting region can be achieved. It is expected that these provisional designs will be reviewed and revised as necessary over the forthcoming years as part of the continuing licencing process.

1.2 Disposal concept

1.2.1 General repository layout

The combined repository proposed by Nagra at NL contains two separate disposal areas: an HLW disposal area for SF and vitrified HLW and an L/ILW disposal area (Nagra 2021b). Waste will be disposed of in a set of emplacement drifts in the HLW disposal area and in caverns in the L/ILW disposal area in the centre of a host rock layer.

The drifts and caverns are accessed by interconnected underground openings, including the access structures, which are shafts in the current reference concept that connect the repository to the surface. The emplacement caverns and drifts will be backfilled in parallel with the emplacement of the waste, and a sealing system will then be installed to close the repository and transfer it to a passive state.

A generic layout of the combined repository is shown in Nagra (2021b).

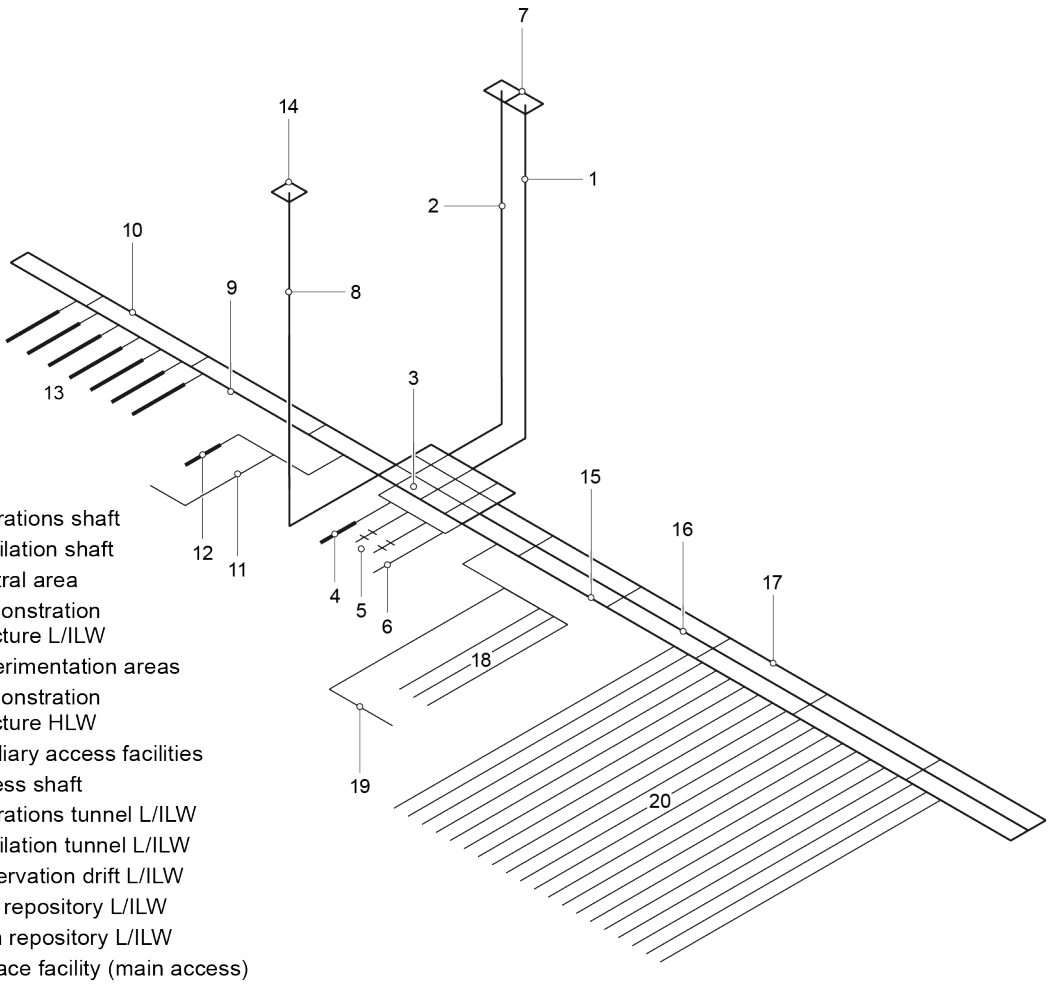

1 Operations shaft
2 Ventilation shaft
3 Central area
4 Demonstration structure L/ILW
5 Experimentation areas
6 Demonstration structure HLW
7 Auxiliary access facilities
8 Access shaft
9 Operations tunnel L/ILW
10 Ventilation tunnel L/ILW
11 Observation drift L/ILW
12 Pilot repository L/ILW
13 Main repository L/ILW
14 Surface facility (main access)
15 Operations tunnel HLW
16 Ventilation tunnel HLW
17 Construction tunnel HLW
18 Pilot repository HLW
19 Observation drift HLW
20 Main repository HLW

Fig. 1-1: Layout of the underground facilities of a generic combined repository
Nagra (2021b)

Access to the repository during the construction and operational phases is provided by:

- the access shaft (labelled 8 in the figure)
- the operating shaft (labelled 1)
- the ventilation shaft (labelled 2)

These three shafts connect the surface to the central area (labelled 3) at the disposal level, from where the HLW and L/ILW disposal areas are constructed and accessed during repository operations. Facilities for underground geoscientific investigations and demonstrations (labelled 4, 5 and 6) are also accessed from this central area.

The HLW disposal area (labelled 20) consists of parallel emplacement drifts, connected to the central area by three tunnels:

- the service tunnel (labelled 15)
- the ventilation tunnel (labelled 16)
- the construction tunnel (labelled 17)

Separate construction and service tunnels are required in the HLW disposal area for the sequence of operations foreseen during waste emplacement, which take place in parallel with the successive excavation of individual emplacement drifts. Each drift is backfilled continuously as emplacement of canisters for SF and vitrified HLW proceeds. Once emplacement and backfilling of a drift are complete, the drift is closed as quickly as possible with a seal (part of the overall sealing system described in Chapter 2). Rapid closure serves to limit the possibilities for inadvertent or unauthorised human intrusion and reduces the likelihood of damage to the repository, e.g., due to accidents such as repository flooding, and transfers the emplacement drifts to a passive state.

The L/ILW disposal area (labelled 13) consists of parallel dead-end emplacement caverns. The emplacement caverns are connected to the central area by two tunnels:

- the service tunnel (labelled 9)
- the ventilation tunnel (labelled 10)

The service tunnel also serves the role, during the construction phase, of a construction tunnel; the type of parallel operation foreseen for the HLW disposal area is not planned for the L/ILW disposal area. Containers for L/ILW will be emplaced in cavern sections, each of which will be backfilled once waste emplacement in that section is complete. Once the whole cavern is backfilled, it will be closed as quickly as possible (for the same reasons as in the case of the SF/HLW drifts) using a seal of sufficient gas permeability to prevent the build-up of potentially damaging gas pressures that could otherwise arise from gas generation processes inside the cavern.

In each disposal area, the emplacement drifts and caverns are connected to the service tunnels by branch tunnels. The service tunnels have diameters of about 5 to 6 m. Rock support for the service tunnels and for the branch tunnels that connect them to the emplacement drifts and caverns will either be formed of sliding arches and shotcrete or will follow the same two-shell principal that is envisaged for the L/ILW emplacement drifts (cf. Chapter 1.2.3).

In addition to the main HLW and L/ILW disposal areas, there are pilot facilities for SF/HLW disposal (labelled 18) and for L/ILW disposal (labelled 12), in which the behaviour of the wastes, the backfill, the seals and the host rock is monitored until the end of a decades-long monitoring phase. Each pilot facility has an associated control tunnel for monitoring purposes (labelled 19 and 11, respectively). Access to the pilot facilities is via short tunnels that branch from the service tunnels for the main HLW and L/ILW disposal areas.

After ten years of monitoring, the disposal area accesses will be backfilled and sealed. In a next step, after completing the entire monitoring phase, the remainder of the sealing system will be installed within the underground openings and access structures.

1.2.2 HLW emplacement drifts

The current provisional emplacement drift design for SF and vitrified HLW is illustrated in Fig. 1-2. The dead-end drifts will be created using tunnel boring machines for reasons of engineering practicability, to reduce damage of the host rock and the extent of the excavation damage zone (EDZ) and to obtain an appropriate tunnel geometry. The drifts will have an excavation diameter in the order of 3.5 to 3.7 m and are several hundred meters in length where the waste can be stored. During tunnelling, a prefabricated single-shell segmental liner consisting, in the reference design, of pre-cast concrete tubbing elements will be installed. The liner is designed to provide stable conditions during construction and operation. The annular gap between the liner and the rock will be filled completely with a highly fluid grout.

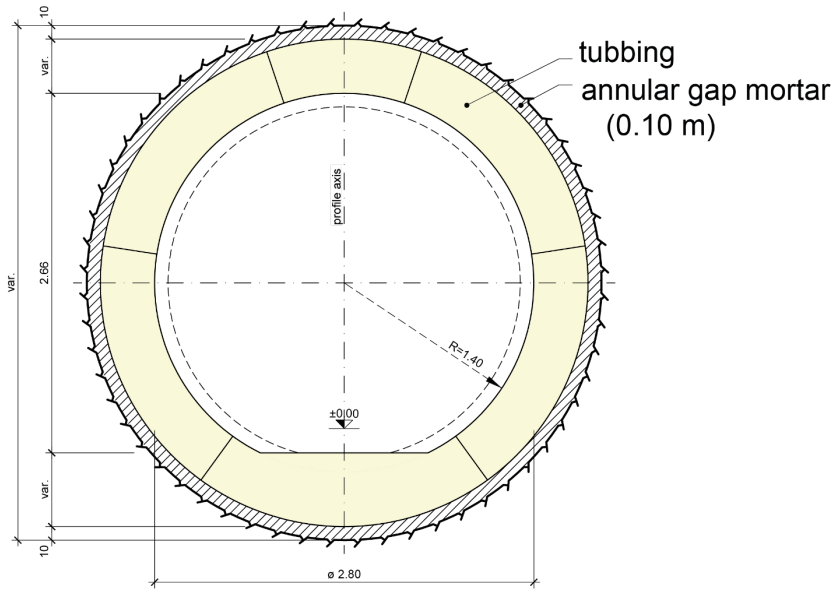

Fig. 1-2: Reference design profile of emplacement drift: tubbing thickness 0.4 m

Each SF/HLW disposal canister will be placed on a pedestal of highly compacted bentonite blocks, and the remaining void spaces backfilled with highly compacted granular bentonite. Together, the pedestal and granular bentonite are termed the bentonite buffer. Seals will be emplaced at the end of each drift after the waste has been emplaced and the cavern is backfilled.

1.2.3 L/ILW and its emplacement

The provisional emplacement cavern design for L/ILW is illustrated in Fig. 1-3. The dead-end caverns have an internal width of about 11.5 m and a height of about 12.5 m. The length of each cavern is approximately 230 to 250 m.

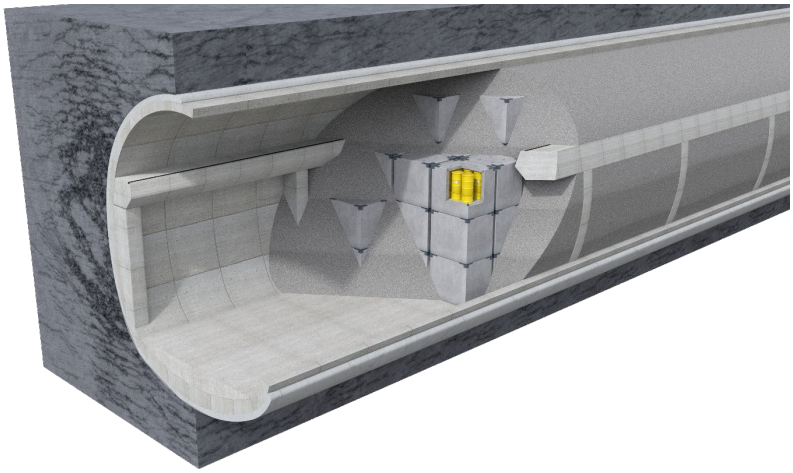

Fig. 1-3: Graphical illustration of provisional design of an emplacement cavern for L/ILW disposal

The caverns will be connected to the operation tunnel by branch tunnels, each of which has an enlarged section adjoining the cavern entrance.

The lining of the caverns will, according to the current concept, be constructed using a two-shell principle. The outer shell consists of reinforced shotcrete and has a temporary function as short-term rock support. The shotcrete layer will be emplaced directly on the exposed rock surface. The inner liner shell consists of unreinforced concrete which will be placed in-situ using formwork and is designed to withstand the final ground loads. The base and the top vault of the tunnel will consist of concrete and the sole will be filled with poured concrete.

Once the L/ILW disposal containers have been emplaced, the void spaces between the cavern walls and the L/ILW containers, as well as any gaps between containers, will be filled with a porous cementitious mortar. When all sections of a cavern have been backfilled, the enlarged section of its branch tunnel adjoining the cavern entrance will also be backfilled with mortar. A seal will be placed at the end of the branch tunnel furthest from the cavern.

1.3 Potential for porosity changes and effects on gas transport and storage

The sealing system is comprised of porous materials that are, to a large extent, only partially water-saturated on installation (see Chapter 2 and Nagra 2021c for more details). The surrounding rock contains a reservoir of water that will eventually saturate the sealing system, although saturation will be delayed due to the low permeability of the host rock, which slows water inflow. The increase of gas pressure in the repository due to repository-generated gas will further delay water flow into the repository. The transport and distribution of gas within the sealing system pores limits the build-up of gas pressure.

Gases will be generated within the repository principally by the anaerobic corrosion of metals, which produces H_2 (Diomidis et al. *in prep.*), and by microbial and chemical degradation of organic matter (Guillemot et al. 2023), which can produce gaseous compounds such as CO_2 and CH_4. The largest rates of gas production occur in the L/ILW emplacement caverns. The sealing system is designed to ensure controlled saturation of the repository, such that an adequate gas storage volume is maintained for as long as required to limit potentially damaging gas pressures produced by this repository-generated gas. The present report assesses the significance of processes that could detrimentally affect the capacity of the sealing system to fulfil this role.

The porous materials used in the sealing system are largely clay- and cement-based. Chemical interactions between these materials, which may lead to the dissolution of existing minerals and to the precipitation of new minerals, have been widely studied. As discussed in the present report, cement-clay interactions and the associated precipitation/dissolution of minerals and porosity changes are expected to occur on a timescale that is similar to that of gas production in the L/ILW disposal area and so should form an essential part of any account of the fate of repository-generated gas. It is critical for the role of the sealing system in providing for gas transport and storage that such interactions do not lead to the clogging of pores to the extent that either gas transport is significantly hindered or the gas storage capacity significantly reduced.

1.4 Structure of the remaining chapters of this report

The remaining chapters of this report are structured as follows:

- Chapter 2 describes the sealing system and its various elements; a more detailed description is provided in App. A, as well as in Nagra (2021c), where it is also explained how and when it is planned to emplace these elements in the current design.
- Chapter 3 gives a general account of chemical reactions and other processes leading to precipitation in porous media and potentially to pore clogging.
- Chapter 4 describes more specifically how precipitation can lead to pore clogging at the interfaces between clay- and cement-based materials.
- Chapter 5 discusses gas transport and storage in these materials and how they may be affected by pore clogging; relevant gas transport mechanisms are described in more detail in App. B.
- Chapter 6 discusses the implications for the design of the sealing system, i.e., how the potential for pore clogging can be avoided or reduced.
- Chapter 7 discusses the resulting saturation evolution of the sealing system and the fate of repository-generated gas.
- Finally, Chapter 8 provides a summary of the main findings of the report and presents some conclusions.

2 The sealing system

2.1 Types of seals and backfill materials

The sealing system will include multiple individual seals, together with the backfilling of the access structures and all other underground openings. The current design for the combined repository foresees three different types of seals:

V1 seals, which will be placed at the entrances to SF/HLW disposal drifts and L/ILW caverns in which the wastes will be emplaced. As elaborated in the following paragraphs, the design of the V1 seals for the SF/HLW drifts is somewhat different to those for the L/ILW caverns because of the requirement for the latter to be more gas permeable. Thus, the notation, V1-HLW and V1-L/ILW is adopted.

V2 seals, which will close off the disposal areas for L/ILW and for HLW, as well as the pilot facility for HLW and L/ILW, after the waste has been emplaced. Similar to the V1 seals, the notation, V2-HLW and V2-L/ILW is adopted.

V3 seals, which will be placed in the access- and ventilation shafts to seal the repository from the surface environment and protect it from external impacts, including the possibility of future human intrusion. No safety requirements are placed on components within the access shafts above the V3 seals[1].

Backfill material will be emplaced in the open tunnels and facilities between these different seals. Backfill material VF1 will be emplaced between the V1 and V2 seals and backfill material VF2 will be emplaced between V2 and V3 seals. The arrangement of the V1, V2 and V3 seals and the VF1 and VF2 backfill materials is illustrated in Fig. 2-1.

The operating shaft will be closed with a V3 seal immediately after the emplacement of all the V2 seals. The access and ventilation shafts will be closed later, again with V3 seals, after the end of the final monitoring phase. When this is done, the repository as a whole will have been transferred to a passive state.

[1] If a ramp were to be constructed, a seal would be installed with similar requirements as those applying to the V3 seal.

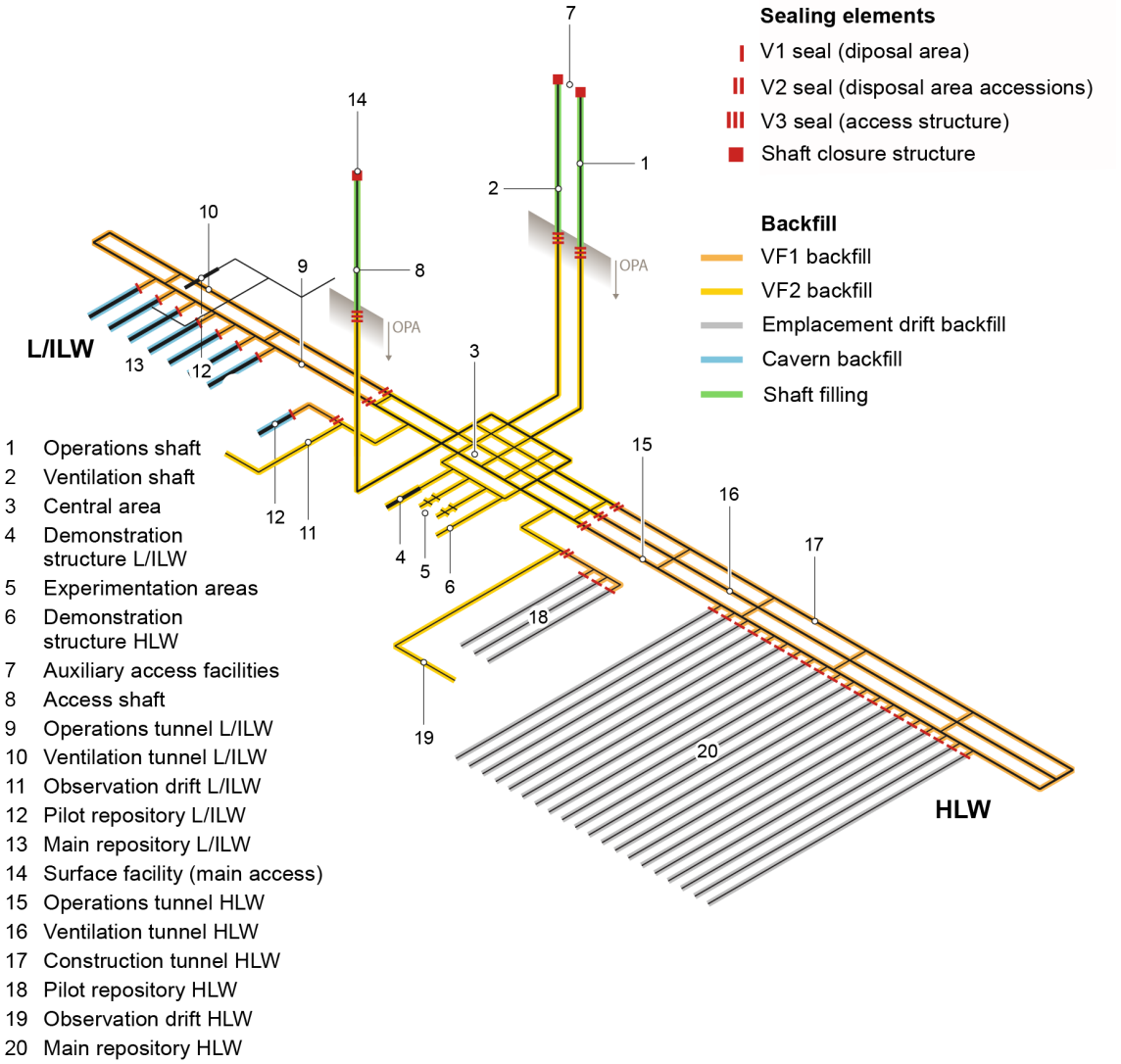

Fig. 2-1: The arrangement of the V1, V2 and V3 seals and the VF1 and VF2 backfill within the generic layout shown in Fig. 1-1

2.2 Principal components of the seals

The basic design concept is broadly similar for all types of seals and is illustrated in Fig. 2-2 (more detailed descriptions of each seal, based on Nagra (2021c), are given in App. A). The principal components of a seal comprise:

- one or more sealing elements composed of compacted bentonite clay or bentonite/sand
- one or more concrete abutments to hold the sealing elements in place, absorbing mechanical stresses and bentonite swelling pressure from the adjacent sealing elements
- one or more transition layers for the purpose of structural design and to provide physical separation of between clay and concrete components

2.2.1 Sealing elements

Each sealing element for the V1-HLW and V3 seals consists of compactable bentonite clay (currently assumed to be MX-80) in the form of fine-grained material, granules, pellets, shaped bricks, or a combination of these. Compacted bentonite swells as it takes up water and thus any gaps within and around the sealing element become sealed. Compacted bentonite is also currently planned to be used for the V2-HLW sealing elements (Nagra 2021c). The use of clay for the sealing elements minimises chemical interactions with the surrounding clay rock. On installation, the compacted bentonite has a dry density greater than 1'450 kg/m^3 to ensure both sufficient swelling pressure and that the intrinsic permeability[2] at complete saturation meets its design target: 10^{-19} to 10^{-18} m^2 for the V1-HLW, V3 seals and 10^{-19} to 10^{-17} m^2 for the V2-HLW seals; see design targets in Section 2.3, Tab. 2-1.

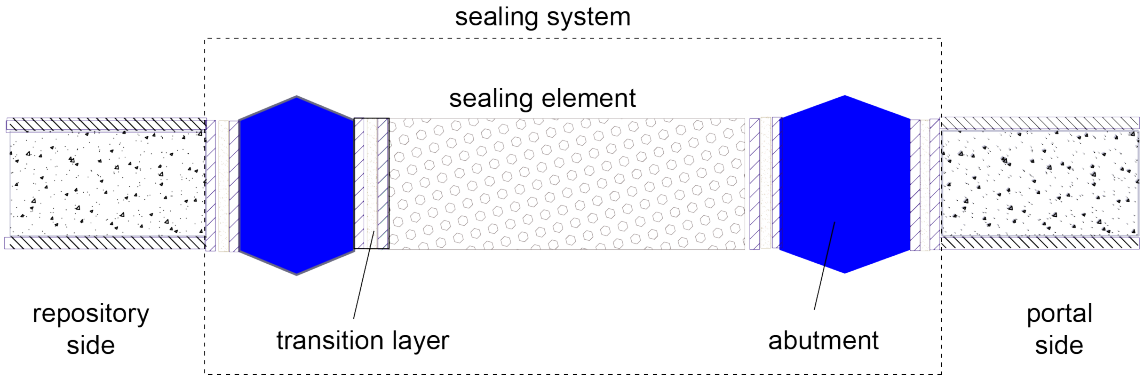

Fig. 2-2: Generic illustration of a seal, showing its principal components (not to scale)

For the V1-L/ILW and V2-L/ILW sealing elements, the bentonite is mixed with ca. 80 wt.-% of sand, which provides a grain-supported matrix and, compared with bentonite alone, more readily allows the passage of gases from in the L/ILW caverns, where the greatest rates of gas production occur. At the same time, the swelling of the bentonite in the sand-bentonite mixture still ensures sufficiently low intrinsic permeability, in the range 10^{-18} to 10^{-17} m^2 for both the V1-L/ILW and V2-L/ILW seals; see design targets in Tab. 2-1.

[2] Intrinsic permeability is a tensorial quantity (in m^2) that describes the permeability of a material for a given phase when no other phases are present (single-phase conditions). In general, it is a measure of the ability of the porous material to allow a fluid to pass through it. It is considered to be predominantly a property of the porous medium pore space, but may also depend on the properties of the fluid, so that intrinsic permeability of a material may differ, e.g., for gas and water.

2.2.2 Abutments

In its initial, unswollen state, the bentonite of the sealing elements does not have sufficient stiffness to act as the main load-bearing element of a seal. It is therefore necessary to install abutments next to the sealing elements to satisfy the load-bearing requirements. Although the function of the abutments is mainly to withstand both rock pressures and the swelling pressures that will develop in the sealing elements, other mechanical loads, including swelling pressures from the VF1 and VF2 backfill and the possibility of early exposure to hydrostatic pressures, e.g., due to accidental flooding before backfilling, must be taken into account in the design. The abutments are assigned no long-term safety functions other than they are compatible with surrounding materials.

In the current design, all abutments take the form of symmetrical double cones (see Fig. 2-2), hereafter called wedge plugs, which transfer the load into the rock via normal stresses rather than shear stresses, favouring positional stability. The dimensioning of the abutments is based on several factors: the lithostatic pressure and the pore pressures that will develop in the rock, the swelling pressure that will develop in the sealing elements, the selected concrete strength, the selected opening angle of the symmetrical wedge plug and the tunnel radius. To avoid stress increases due to bending effects, the length of each abutment is similar to its diameter according to the current desing. A widening angle in the range of approx. 20° to 25° ensures the load transfer into the surrounding host rock in the desired manner. Experience e.g., in the scope of the DOPAS project (Hansen et al. 2016), has shown that cuts in the rock of this size can be successfully implemented underground.

All abutments consist of an unreinforced, possibly low-pH, structural concrete (concrete formulation are to be fully defined in a later stage of the project). The use of low-pH concrete reduces, but does not entirely avoid, the potential for chemical reactions that could lead to precipitation, as discussed in Section 6.1.

In addition to their load-bearing function, the abutments are expected to make some contribution to the limitation of water flow, but this is likely to be small compared with the barrier provided by the sealing elements and is disregarded in the safety assessment. The abutments must also allow the flow of gas. As noted above, the design target for the intrinsic permeability of the V1-L/ILW and V2-L/ILW seals is 10^{-17} to 10^{-18} m^2 and the hydraulic conductivity of the abutments should be no lower than this so as not to unduly obstruct gas flow. As summarised by Lea & Hewlett (2004), dense concrete in a fully saturated state has a hydraulic conductivity between 10^{-12} and 10^{-11} m/s (corresponding to an intrinsic permeabilities of between ca. 10^{-19} and 10^{-18} m^2) when properly compacted[3]. The permeability of concrete can, however, be varied over a wide range by adjusting its formulation, e.g., the water/cement ratio, the cement/aggregate ratio and the size distribution of the aggregates[4]. More specifically, permeability could be increased by omitting an aggregate size fraction in the sieving curve (called gap-grading). Alternatively (or in addition), the capillarity of the cement paste within the concrete could be increased by employing

---

[3] Pores larger than about 100 nm in size in cement paste have a particularly strong influence on its permeability and diffusivity (Nyame & Illston 1981). Moreover, the permeability of concrete can be about 100 times greater than that of cement paste (Young 1988) due to the imperfect contact of the aggregates in concrete with the paste (Argiz & Saniuan 2017).

[4] As outlined e.g., an appropriate selection of aggregate size distribution affects the main properties of concrete, including not only permeability, but also workability of the concrete mix, mechanical strength and durability. The size distribution of aggregate particles can be either described by means of grading curves or obtained from sieve analysis. The Fuller curve (an example of a sieving curve which describes the aggregate size distribution) is one of the most widely used grading curves, used to ensure the desired aggregate packing and properties of concrete. There are other types of sieving curves, which also account for the angularity of the aggregates.

an elevated water/cement-ratio. Finally, it would be possible to reduce the amount of the cement paste relative to the aggregate contents to create concrete with a higher porosity and permeability. One or more of these measures could thus be employed to ensure a permeability higher than 10^{-17} m^2.

2.2.3 Transition layers

The transition layers provide a physical separation between the sealing elements, abutments and residual cavity fillings (i.e., fillings placed in breakouts from tunnel walls). Each transition layer occupies the entire tunnel cross-section. Part of the transitional layer should consist of a cohesion less material, e.g. varying sand and gravel layers, to fulfil filter criteria (Nagra 2008a)[5]. The pore sizes within the top transition layer should be large enough that capillary rise is significantly less than the tunnel height. Such relatively large pores favour the development of the gas saturated zone (at the top of the layer) and a liquid saturated zone (below), contributing to a connected gas transport pathway in the upper parts of the tunnels for as long as a gas phase is still present. Because chemical interactions between the bentonite of the sealing elements and the concrete of the abutments require water, and also because of the physical separation that they provide, the filter layers thus serve to limit such interactions, as discussed in later chapters of this report.

Only materials that are thermodynamically stable under alkaline conditions and do not influence the geochemical environment at all, or tend to influence it positively, are suitable for use within the transition layer. Suitable materials include pure $CaCO_3$, limestone sands, limestone gravels and limestone aggregates[6]. In the current design, the transition layer includes one or two partion walls to separate the cohesionless material from adjacent structures (Nagra 2021c). Factors that have an impact on the dimensions of the transition layer include the coarseness of the cohesionless material and the corresponding capillary rise that it produces. Further evaluation in support the optimisation of this design will happen in the later course of the project.

2.2.4 Backfill materials within the sealing system

The VF1 and VF2 backfill provides a storage volume for gas, in particular for gas released via the V1-L/ILW seals from the L/ILW emplacement caverns. As such, the backfill is required to maintain an intrinsic permeability greater than 10^{-16} m^2 (see design targets, Tab. 2-1), as well a gas-accessible porosity of around 40%. The backfill materials have the further role of ensuring mechanical stabilisation of the underground opening, preventing or limit convergence that might potentially cause damage to the geological barrier. These requirements can be fulfilled by a swelling clay mixed with a suitable grain-supported material. Candidate materials include excavated clay which would be mixed with sand and/or gravel, or a sand-bentonite mixture (specific requirements for the selection of backfill material are given in Nagra 2021c). Consequently, the general observations concerning sand-bentonite mixtures discussed in this report, can also be applied to the backfill materials (VF1 and VF2) within the sealing system, although the macro-porosity in the backfill material will be significantly higher. In addition, as

---

[5] In terms of porosity clogging, the intrusion of bentonite into transition layer should be not a problem for gas transport properties, as this will create an "extension" of the sand/bentonite layer with favourable gas transport properties due to its lower bentonite content.

[6] The terms "sand, gravel, aggregates" refer to the grain dimension and not the composition. All material should be $CaCO_3$.

the backfill material is rather coarse, the arguments concerning the capillary rise and clogging of large pores in the transition layer (see Sections 3.5.5 & 6.3) discussed within this report can also be applied to the backfill material (VF1 and VF2).

2.3 Design targets

Current long-term safety requirements on the backfill and seals are, in some cases, linked to one or more design targets. Most relevant for the present report are the design targets on the intrinsic permeability of the seals (or, more precisely the sealing elements) and backfill mentioned in the previous sections and summarised in Tab. 2-1.

The current design targets for the intrinsic permeabilities of the V1-HLW and V3 seals are set to relatively low values. Once saturated, these seals are intended to provide effective barriers to pore water and gas movement, consistent with the role of the sealing system of providing a strong and stable barrier to radionuclide transport. The design targets on the intrinsic permeability of the other seals are set to higher values. Although these intrinsic permeabilities describe seal properties at full water saturation, these higher values also imply higher permeabilities to gas at partial saturation. As notes earlier and described further in Chapter 6, the main sources of gas in the repository are in the L/ILW disposal caverns. The higher intrinsic permeabilities of the V1-L/ILW and V2 seals and the VF1 and VF2 backfill favour the transfer of this gas to the sealing system, where a high gas storage volume is provided. In this way, the sealing system fulfils its further role of preventing the build-up of potentially damaging gas pressures, especially in the L/ILW disposal area. The adequacy of these targets it tested in the calculations of the fate of gas summarised in Chapter 7.

Tab. 2-1: Current provisional design targets for the intrinsic permeability of the seals

Nagra (2021c)

Seal	**Design target**
V1-HLW	10^{-19} to 10^{-18} m^2
V1-L/ILW	10^{-18} to 10^{-17} m^2
VF1	$\geq 10^{-16}$ m^2
V2-HLW	10^{-19} to 10^{-17} m^2
V2-L/ILW	10^{-18} to 10^{-17} m^2
VF2	$\geq 10^{-16}$ m^2
V3	10^{-20} to $10^{-19}$$m^2$

With regard to precipitation and pore clogging, it is clearly important that these processes do not reduce the intrinsic permeabilities of the V1-L/ILW and V2-L/ILW seals and the VF1 and VF2 backfill to the extent that the design targets set for these indicators are violated. Design measures to ensure that this is the case are the topic of Chapter 6.

3 Processes potentially leading to clogging of porous media

3.1 Porosity definition and concepts

Porosity, or void fraction, is a measure of empty, or “non-solid”, volume within a material. It is expressed as a fraction of total volume and varies between zero and one. Alternatively, it can be expressed as a percentage and varies between 0% and 100%.

For most applications, including the analyses presented later in this report, porosity is defined at a continuum scale, i.e., porosity is a representative property of the medium. In order to establish a representative porosity for a porous medium, a representative elementary volume (REV) needs to exist (Fig. 3-1). The REV is the smallest volume over which a property, such as porosity, can be defined and yield a value representative of the whole (Bear 1972, Hill 1963).

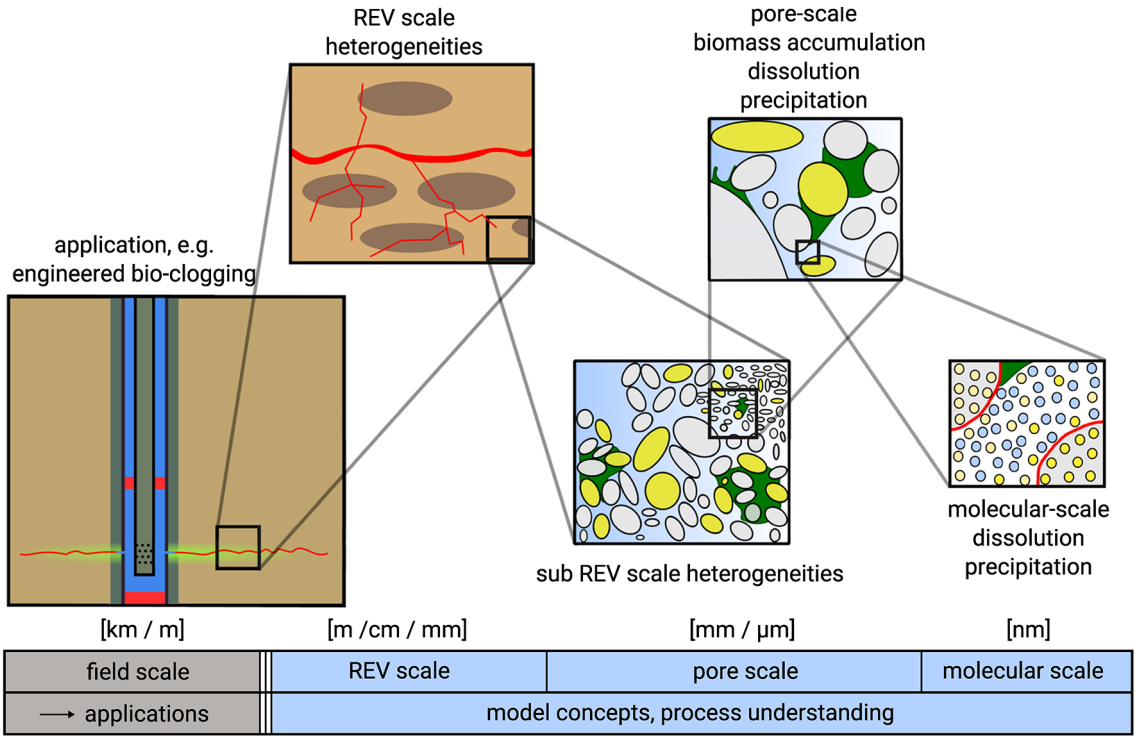

Fig. 3-1: Scales of a porous medium considered when developing process understanding and when developing and applying models

REV-scale = continuum scale

From Hommel et al. (2018).

Porosity does not in itself provide a geometric description of the pore space that is sufficient to relate, e.g., transport on a pore scale, to continuum-scale transport. Other important properties on a continuum scale are the tortuosity and the constrictivity. The tortuosity is a measure of the lengthening of transport pathways through the medium relative to the shortest distance between two points, while the constrictivity accounts for the variation of cross-sectional area of the transport pathways (van Brakel & Heertjes 1974).

Porosity can become an ill-defined parameter, especially in complex porous media such as clays and cements with complicated pore structures, wide distributions of pore sizes or electrically charged pore surfaces (c.f. Section 3.2). Furthermore, distinct physical and chemical processes might take place within different parts of the water- or gas-filled pore space. These considerations lead to additional concepts such as “connected pore space”, “dead end pores”, “open pores” and “closed pores”.

3.2 Pore structure

As described in detail in Chapter 2, the sealing system largely comprises both clay- and cement-based materials. Cements and concrete are used mainly within the sealing system in abutments adjacent to the sealing elements. They are also used in the L/ILW disposal area for waste immobilisation (at the waste package level), for the disposal containers and for tunnel/cavern backfill (see App. B) and are used throughout the repository for tunnel support. Regarding clays, as well as their use in the sealing elements and sealing system backfill, the repository is constructed in a clay host rock (Opalinus Clay) and compacted bentonite clay is used as a buffer material around SF/HLW disposal canisters in the HLW disposal area. It is the chemical interactions between these clay- and cement-based materials that is the primary concern in relation to pore clogging.

To understand these interactions, it is necessary to understand their highly heterogeneous pore structure. According to the International Union of Pure and Applied Chemistry (IUPAC), the pores in porous materials are divided according to their sizes (Fig. 3-2).

Beside macro-pores, also termed capillary pores, with sizes > 50 nm (Sing et al. 1985), clay- and cement-based materials contain considerable amounts of mesopores (2 – 50 nm) and micro-pores, also termed nano-pores (< 2 nm). The porosity of clay- and cement-based materials is the topic of the following paragraphs.

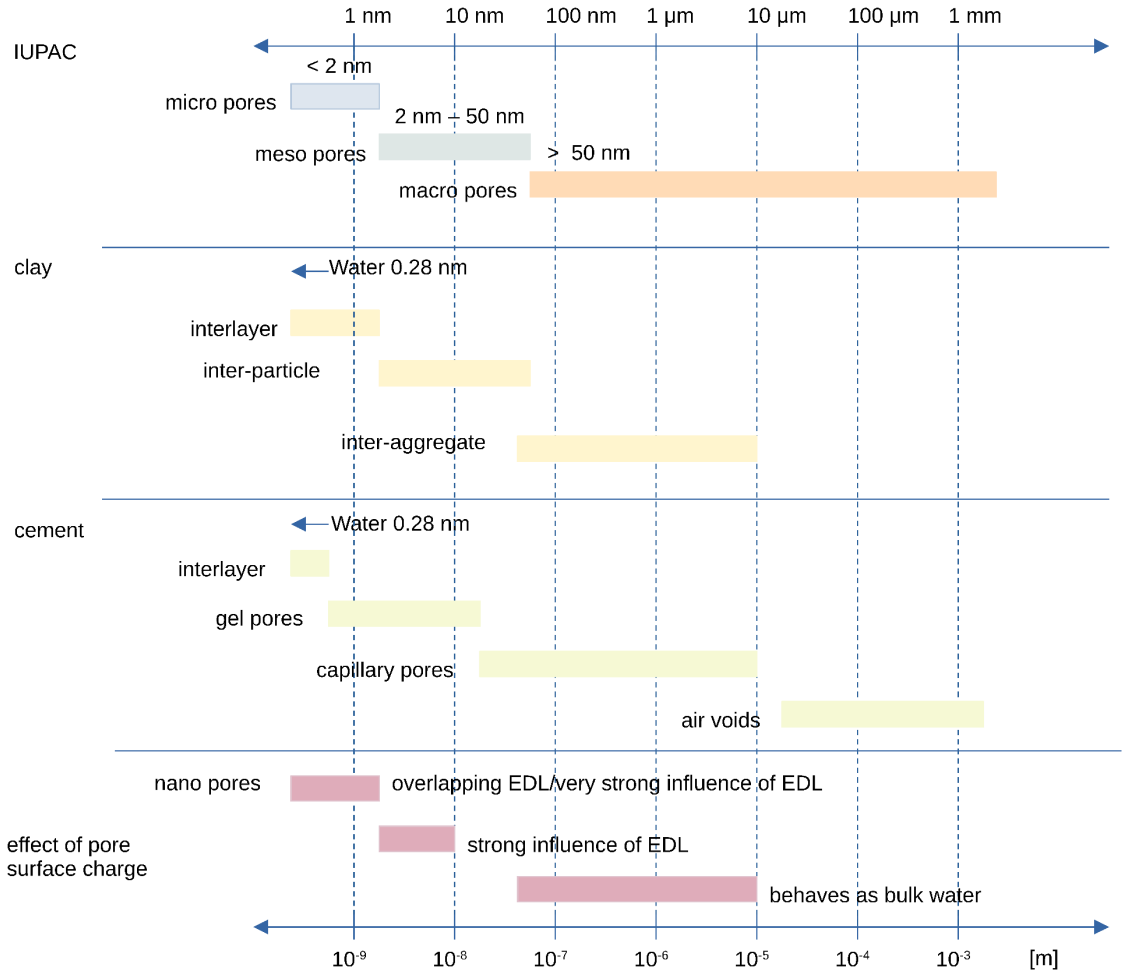

Fig. 3-2: Pore size definitions according to IUPAC, pore size definitions commonly used for clay (Section 3.2.1) and cement materials (Section 3.2.2) and pore size classes defined according to the influence of electrical double layers (EDL) in the case of charged pore surfaces

3.2.1 Clay-based materials

In clays, as described e.g., by Kuila & Prasad (2013), Nagra (2002b) and Yuan & Rezaee (2019) and illustrated in Fig. 3-3, the pore space is typically divided into:

- Inter-layer pores, lying between (for many clay materials) hydrated inter-layers and having widths of less than 2 nm, which are thus micro-pores in the IUPAC nomenclature, and
- intra-granular pores, consisting of inter-particle pores and inter-aggregate pores, which are respectively mesopores[7] and macro-pores in the IUPAC nomenclature.

[7] Nomenclature for the pore size classes in clays does not in all cases comply with the IUPAC nomenclature. For this report, inter-particle pores are referred to as mesopores, whereas in Fig. 3.3, they are referred to as macropores.

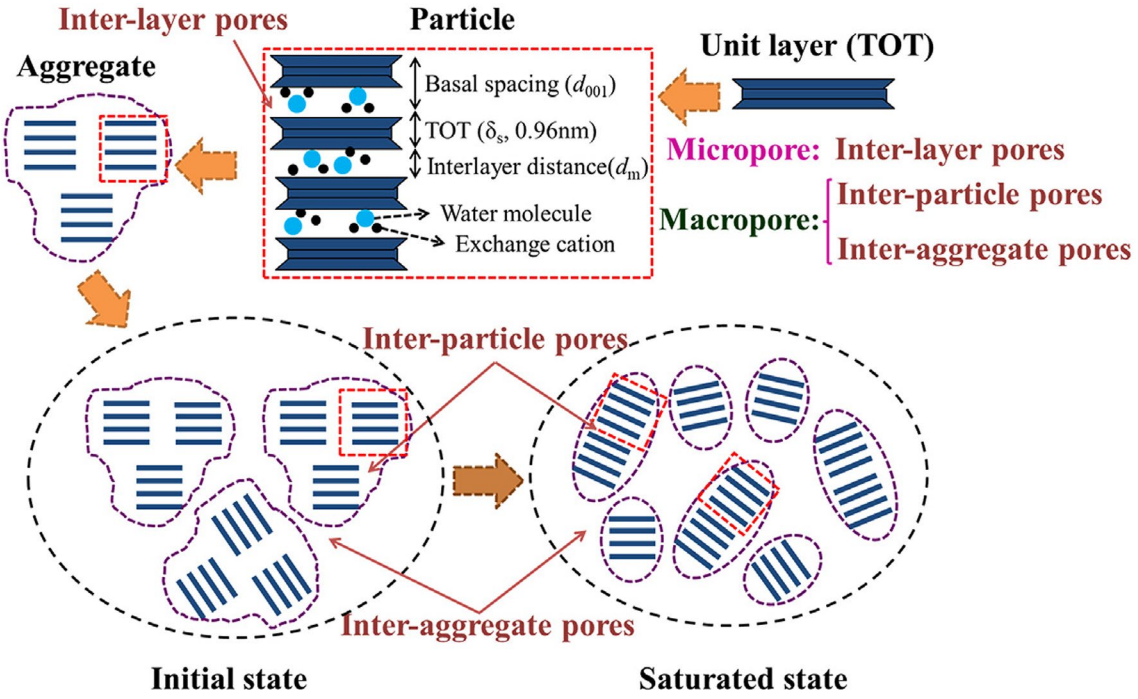

Fig. 3-3: Pores in bentonite clay

TOT = tetrahedral-octahedral-tetrahedral layer structure

From Ruan & Fu (2021)

Compacted clays and hard clay rocks contain a large fraction of inter-layer and inter-granular pores that are smaller than 10 nm. The existence of small pore throats and the presence of charged surfaces within these pores has a large effect on transport of solutes and on the possibility to drain the material (see Section 5.1).

Sand-bentonite mixtures are envisaged for use in some seals and as a backfill material in the repository sealing system (c.f. Chapter 2). In the case of the seals, the mixture consists of quartz sand and bentonite in a ratio of ca. 80/20 by dry mass. It has been shown that sand/bentonite mixtures with a moderate bentonite content of 20 – 30% are characterised by a multi-modal pore size distribution (Olsen 1969, Alonso et al. 1987, Collins & McGown 1974, Gens & Alonso 1992, Hoffmann et al. 2007, Ahlström 2015). The form of the pore-size distribution depends on a variety of factors, such as the degree of compaction and the water content of the sand/bentonite mixture. The design goal for the sand-bentonite mixtures used in the sealing system is that the sand provides a mechanical stable sand-grain skeleton. The mineralogical composition and the geotechnical characteristics of the bentonite and sand are given in Levasseur et al. (2020).

In the initial dry state, inter-layer distances of the clay material are small and clay particle stacks are arranged in aggregates, which gives rise to a relatively large amount of inter-aggregate macro-porosity associated with the gaps within the sand skeleton (Fig. 3-2). With increasing water content, the bentonite swells, i.e., clay inter-layers expand and clay minerals re-arrange to fill the available macro-porosity within the sand-grain skeleton. This is accompanied by an increase in the inter-layer porosity and a decrease in the macro-porosity. An effective bentonite density can be calculated from the dry density of the mixture and the swelling pressure using the regressions for pure bentonite at low density (Fig. 3-4). The resulting pore-size distribution in the sand-grain skeleton will then largely correspond to those of fully-wetted bentonite at the effective dry density.

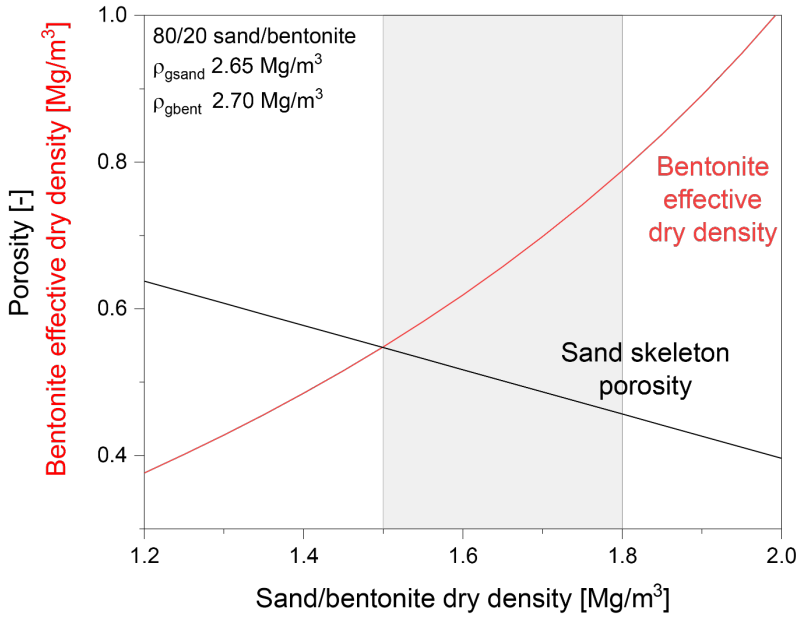

Fig. 3-4: Porosity and effective bentonite dry density (Mg/m^3) as functions of sand/bentonite dry density.

Bentonite is assumed to completely fill the sand-grain skeleton porosity. Grain density of sand ρ_{gsand} 2.65 Mg/m^3 and bentonite ρ_{gbent} 2.70 Mg/m^3.

From Lanyon et al. *planned*

3.2.2 Cement-based materials

Cement-based building materials like concrete and mortar are porous and have a complex internal pore system. They can be described as a compound of aggregate particles dispersed in a matrix of cement paste (Kaufmann et al. 2009). A concept for the partitioning of pore space into different domains has been developed for hydrated cement paste that is similar to that developed for clays (Fig. 3-2) (Feldman & Sereda 1968, Jennings et al. 2008, Jennings et al. 2002, Pinson et al. 2015). In a similar way to clay minerals, C-S-H crystals contain micro-pores in the form of hydrated inter-layers. The so-called "gel porosity" is composed of small mesopores, which are associated with the size and arrangement of C-S-H crystals. Capillary pores, which display a large range of pore sizes greater than 50 nm, occur in the gaps between cement minerals and aggregates that are not completely filled with these hydration products (Kaufmann et al. 2009) and are comparable with the macro-pores in clay materials. The corresponding pore sizes are illustrated in Fig. 3-2.

The amount and size distribution of capillary pores in cement paste after cement hydration depends on the water-cement ratio. Adding more water to the initial mix increases the porosity and also the fraction of gel pores. Of relevance to the amount of macro-porosity is the sieving curve (Taylor 1997), which describes the grain-size distribution of the aggregates with respect to the size and shape of the aggregate material. The denser the aggregates can be packed and filled with cement minerals in the interstitial macro-pores, the lower the porosity of the mortar or concrete. A 20 – 50 µm thick zone, the so-called interfacial transition zone, exists adjacent to the aggregates, where porosity is elevated and affects the transport and mechanical properties of

concrete (Leemann et al. 2010, Scrivener et al. 2004). Additionally, naturally- or deliberately-induced spherical "air voids" with relatively large diameters of more than 20 µm are present in cement-based materials, which remain gas-filled after hydration. Air voids are connected to the capillary pores and fluid and gas exchange between these pores can therefore occur.

Overall, as described in Kaufmann et al. (2009), the pore network of cement-based materials may be described as a network of large chambers connected together via smaller, capillary or gel pores.

3.3 Categories of pore clogging

According to review papers by Eddaoui et al. (2021), Gaol et al. (2021), Jeong et al. (2018) and Yang et al. (2021), pore clogging can be separated into three categories according to its causes:

- physical clogging, caused e.g., by filtration/sedimentation of suspended solids in water at pore walls and pore throats
- chemical clogging, mainly related to chemical/mineral precipitation. This process may become relevant if significant amounts of precipitated minerals accumulate *in situ*, e.g., in pore throats
- bio-clogging, due mainly to microorganism growth and the trapping of microorganisms in narrow pores (filtration)

These three categories are discussed further in the following sections. Other processes that can lead to changes in porosity, including temperature and pressure changes (Scott & Driesner 2018), are not discussed further in the present document.

3.4 Physical pore clogging

Physical clogging of pores can be caused by particle or colloid transport and by filtration/sedimentation processes at pore walls and pore throats (Torkzaban et al. 2015a). Physical clogging is often observed in granular media (e.g. Tang et al. 2020), but has also been observed in concrete (Kia et al. 2017). Physical clogging nearly always results in a change of constrictivity due to the accumulation of particles in pore throats, including particles with diameters larger than that of the pore throat (Kia et al. 2017). It is commonly observed that chemical changes and particle/colloid transport are interrelated (Liu et al. 2020, Torkzaban et al. 2015b). The physical clogging potentially caused by these particles/colloids is, however, probably less relevant than chemical clogging in the context of the repository sealing system, since advective transport processes are very slow in this system (see Section 7.2.4).

The extrusion of swelling bentonite into the pore space of adjacent materials (i.e., from the sealing elements into the adjacent transition layers and concretes) is not investigated in this report.

For the seals with sealing elements composed only of bentonite (the V1-HLW, V2-HLW and V3 seals; c.f., Ch. 2), the filter function of the transition layers will prevent excessive loss of bentonite from the sealing section. For the remaining seals, i.e., V1-L/ILW and V2-L/ILW, accumulation of bentonite in the cohesionless material would result, in effect, in the extension of the sealing section. In these seals, the sealing elements are composed of a sand-bentonite mixtures, with a much lower swelling pressure than pure bentonite. As long as the chemical composition of the pore water does not change significantly, it can be expected that during and after full saturation of these seals, only minor amounts of bentonite are extruded into neighbouring transition layers (see e.g. Yan et al. 2021). Low water fluxes will also result in limited mobilisation of bentonite particles. However, even if significant amounts of bentonite were to be mobilised, since the neighbouring layers will be probably composed of sand/gravel, their intrinsic permeabilities after intrusion of bentonite can be expected to be similar or lower to the permeabilities of the

sand/bentonite sealing element itself. Finally, bentonite extrusion from the sealing elements into the clay host rock (as well as particle and colloid transport into the host rock) is unlikely, as host rock pore sizes are much smaller than clay particle sizes. Overall, therefore, clogging of pore space in barrier components adjacent to the sealing elements due to this bentonite swelling and mobilisation seems unlikely.

3.5 Chemical pore clogging

In the following paragraphs, two types of precipitation processes potentially leading to chemical pore clogging are described: (i) precipitation caused by chemical interactions (Sections 3.5.1 to 3.5.4) and (ii) precipitation due to evaporation and water consumption (Section 3.5.5).

3.5.1 Precipitation caused by chemical interactions at interfaces

Changes in porosity can be caused by the dissolution and precipitation of mineral phases, driven by transport processes (Seigneur et al. 2019). Mineral precipitation and dissolution processes are nearly always associated with volume changes (porosity change and mineral volumes). Such changes are observed e.g., in reactive barriers (Claveau-Mallet & Comeau 2020, Indraratna et al. 2020, Mayer et al. 2001, Wantanaphong et al. 2006), in chemical reactors (Botes et al. 2018) and in relation to the extraction and injection of waters in oil/gas wells, in geothermal wells and in groundwater wells (Torkzaban et al. 2015b). Precipitation can lead to the clogging of some or, in extreme cases, all of the pores within a porous medium (Torkzaban et al. 2015b).

Suppose two geochemically different materials are in contact, e.g., quartz sand (a candidate material for the transition layers in the repository sealing system; see Section 2.2.3) and cement. As illustrated in Fig. 3-5, due to the diffusive mixing of pore waters at the interface between these materials, a mineral phase is precipitated, in this case calcium-silicate-hydrate (C-S-H), and the corresponding aqueous concentrations at the interface are decreased. The supply of reactants is provided by leaching of calcium from cement phases and by the dissolution of silica grains. For significant clogging of porosity to occur, the zone of mixing for reactants has to be stationary in order to allow the accumulation of precipitates.

In this example, the fronts of dissolving mineral phases on either side of the interface fix the aqueous equilibrium concentration of the reactants, while, in the mixing zone, the lower aqueous equilibrium concentrations of the reactants are controlled by the precipitated phase. Typically, for such situations, the diffusive fluxes, and hence the rate of precipitation, decreases with time due to the increasing distance of the reactions fronts from the mixing zone. Other types of situations that also involve the interaction between dissolution/precipitation reactions and transport of reactants are outlined in Section 2.5.2 of Prasianakis et al. (2022).

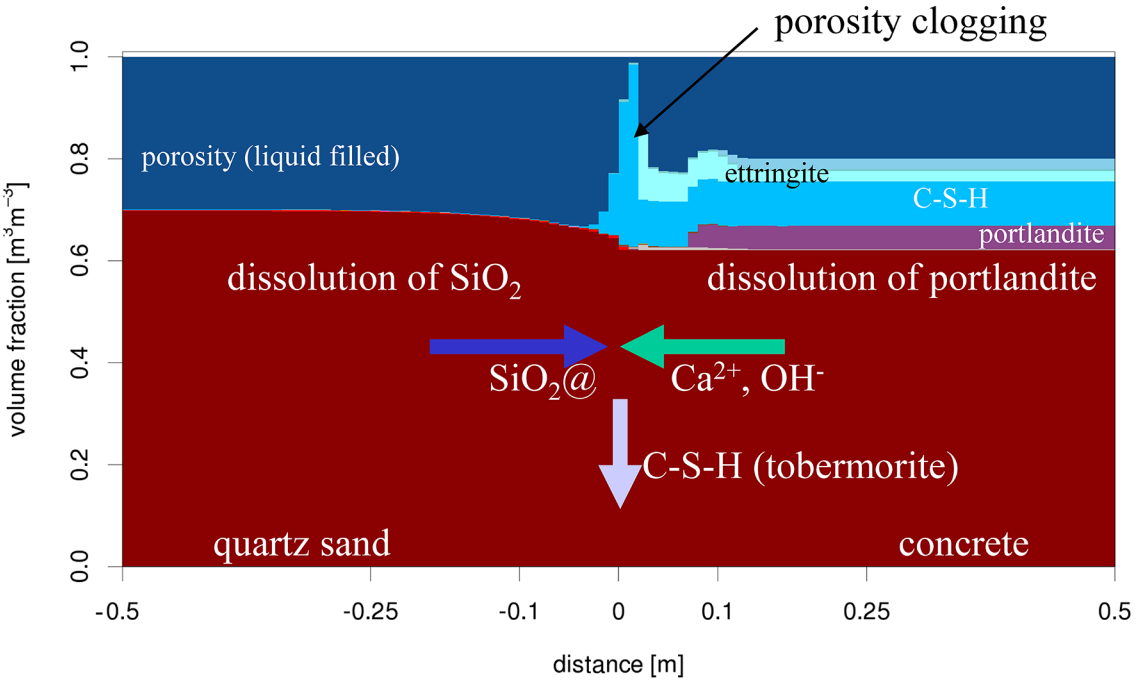

Fig. 3-5: Illustration of clogging at the interface between reactive quartz sand (left) and concrete (right) in a diffusive transport regime

The clogging is due to C-S-H precipitation at the interface

Fig. 1-3 from Kosakowski & Smith (2014)

The volumes of precipitated material produced at such interfaces can readily be assessed using reactive transport models (as in the example in Fig. 3-5) that utilise upscaled volume-averaged material properties on a mm to cm scale, or larger. However, while most such continuum scale chemical, mechanical and transport models describe macroscopic changes of porosity and other average properties, they do not account for microscopic changes, or for the interactions between different types of processes. It is not possible, for example, to calculate the impact of precipitation on the geometry of the pore space with such models. The geometry of the pore space is, however, a key factor determining various material properties, including, e.g., pore size distribution, connectivity, reactive surface area. These properties affect not only transport and mechanical properties of the material, but also chemical parameters such as reactivity and kinetic rates (Hommel et al. 2018). The inappropriate consideration of changes at a microscopic scale could thus potentially give rise to significant inaccuracy in formulation and parameterisation of kinetic control on mineral dissolution and precipitation at the macroscopic scale (Kurganskaya & Rohlfs 2020, Noiriel & Daval 2017). The issue of pore-size dependent precipitation is thus discussed further in the following sections, following a brief overview of nucleation theory, which concerns the initiation of precipitation.

3.5.2 Nucleation theory and the initiation of precipitation

Depending on the size of the pores, different chemical, physical and transport mechanisms can influence precipitation and dissolution of minerals. For example, at scales of a few nanometres, electrostatic forces have a strong influence on transport and, in some cases, may totally restrict the transport of specific ions. Reaction kinetics and crystallisation paths are also dependent on pore sizes. Very often, for the initiation of precipitation, a threshold supersaturation must be achieved, below which the solution remains in a metastable state. Classical nucleation theory or its extended variants may be used to model such processes.

Nucleation is the first step in the formation of either a new thermodynamic phase or a new structure via self-assembly or self-organisation. The model developed by Prieto (2014) can be used to calculate the Supersaturation-Nucleation-Time (SNT) dynamics for different types of nucleation, namely:

- homogeneous nucleation (HOM), where nuclei form inside a pore solution
- heterogeneous nucleation, (HET), where the nuclei are formed at existing mineral surfaces

The nucleation rate, J [m^3/s] varies exponentially with the free energy change ΔG_c associated with the formation of a nucleus of critical size:

$$J = \Gamma \exp\left(\frac{\Delta G_c}{kT}\right) \qquad 3\text{-}1$$

where k is the Boltzmann constant, T is the absolute temperature and is a Γ a pre-exponential factor.

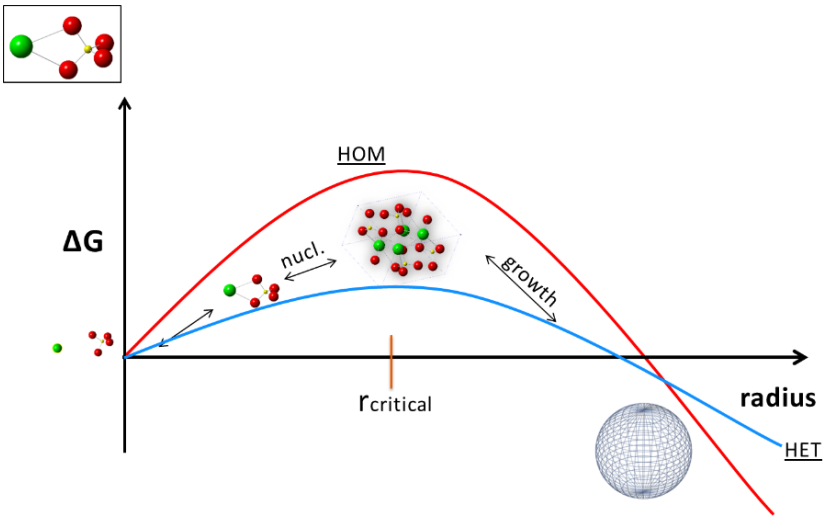

Fig. 3-6: Schematic plot of the Gibbs free energy change (ΔG) for homogeneous (HOM) and heterogeneous (HET) nucleation as functions of the radius of spherical nuclei

From Prasianakis et al. (2017)

Fig. 3-6 is a schematic plot of the total Gibbs free energy change (ΔG) for HOM and for HET as functions of the radius of a spherical nucleus. As soon as a nucleus of critical size is formed and the energetic barrier is exceeded (at the maximum of the ΔG curve), further growth of the nucleus is energetically more favourable than its disaggregation and precipitation starts. The nucleation energy barrier is highly dependent upon the interfacial tension σ and saturation index and is higher for HOM than for HET, which is why homogeneous nucleation requires higher levels of supersaturation to occur.

The induction time for nucleation, i.e., the time needed for nuclei to reach the critical size at which growth starts, depends on

- the volume in which nucleation happens, i.e., the size of a pore
- the number of nuclei
- the attachment rate for monomers that build the nuclei
- the local diffusion coefficients of these monomers in pore solution
- the degree of supersaturation, which is normally expressed in the form of a saturation index

The dependence of induction time on the saturation index in the case of barite ($BaSO_4$) precipitation is shown in Fig. 3-7 for two different pore sizes (1 μm and 10 μm) and for the HOM and HET crystallisation paths.

The figure shows how the larger pore size is more favourable to precipitation by both crystallisation paths. The HET crystallisation path is more likely to occur at low supersaturations. It is, however, also greatly facilitated when a compatible crystallographic template is available, meaning that HET nucleation kinetics depend on both the mineral that precipitates and the surface characteristics of the specific pore where precipitation takes place.

Once the mineral precipitates are formed, the local mass transport properties of the material change accordingly, including its diffusivity and permeability. Modelling results, based on multiscale lattice Boltzmann modelling, which are able to reproduce the characteristic features of the respective experiments, are shown on the right of Fig. 3-7: for the case of competitive celestite ($SrSO_4$) dissolution and barite precipitation. Results are shown for four different solution supersaturations, highlighting the effects of chemical conditions on pore-space evolution (Prasianakis et al. 2017).

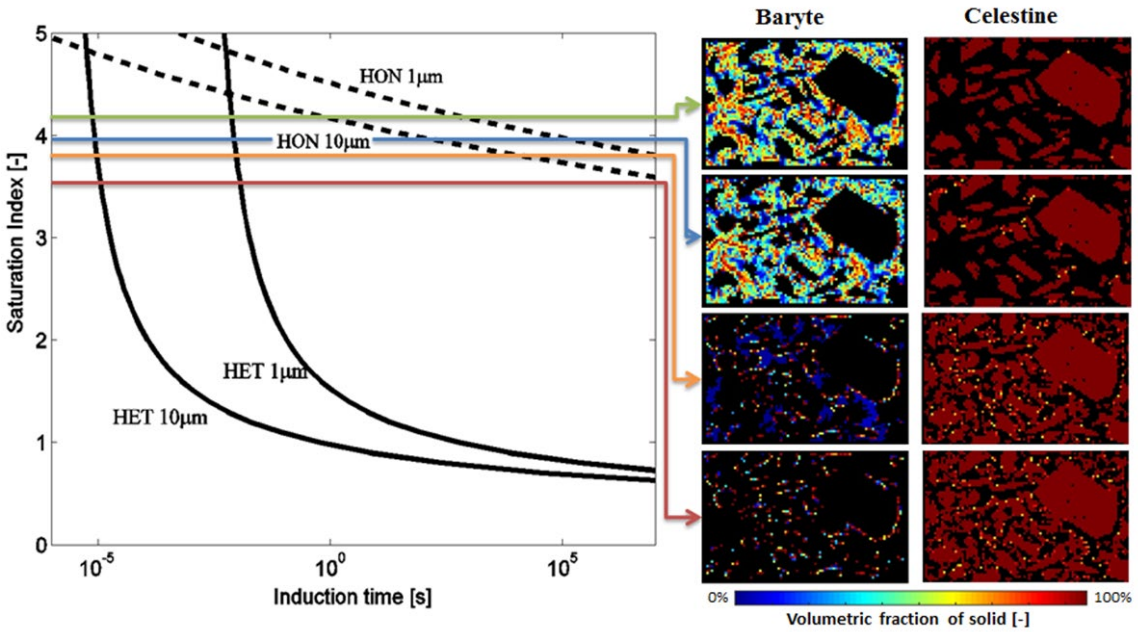

Fig. 3-7: Left: induction time as a function of saturation index in the case of barite precipitation for two different pore sizes (1 µm and 10 µm) and for the HON and HET crystallisation paths. Right: volumetric fractions of precipitating barite and of simultaneously dissolving celestite after 140 hours of reaction at saturation indices of 4.08, 3.96, 3.8 and 3.6 (top to bottom)

From Prasianakis et al. (2017)

3.5.3 Influence of liquid saturation

Most chemical reactions in a geological repository require the presence of a solvent, i.e., liquid water, to break or create bonds between atoms. In the absence of water, these reactions will not proceed. The presence or absence and the state of the solvent influence the chemical reactivity, i.e., solvents can affect solubility, stability and reaction rates. In chemical engineering, the choice of an appropriate solvent allows thermodynamic and kinetic control over chemical reactions (Reichardt 2007).

The presence and distribution of water in a porous medium depend on the pore size distribution and the saturation degree of the medium. Under partially saturated conditions, it is the smaller pores that are the most likely to be water-filled, due to the operation of capillary forces. In particular:

- upon desaturation, the largest pores will be desaturated first
- upon (re-)saturation, smaller pores will become water-filled first

Saturation may occur either by the migration of liquid water or by the condensation of water from the vapour phase. Capillary condensation is the *"process by which multilayer adsorption from the vapour into porous medium proceeds to the point at which pore spaces become filled with condensed liquid from the vapor"* (Schramm 1994). The Kelvin equation relates the equilibrium vapour pressure of a fluid to the curvature of the fluid-vapour interface and is consistent with the observation that vapour condensation will occur in pores or irregularities that are sufficiently small (Deinert & Parlange 2009). The ratio of equilibrium vapor pressure to saturation vapour

pressure can be thought of as a relative humidity of a gas phase (Hartley et al. 1980). The relative humidity of a gas phase is often used as a proxy to describe the change in chemical reactivity with the availability of water as a solvent. In such a concept, the chemical reactivity is a function of pore size distribution, of the fraction of pores that are completely or partially water filled and of the minimum water film thickness or pore size at which transport of reactants is still possible.

Generally, there is a threshold relative humidity below which specific reactions are suppressed. For example, it is well known that iron corrosion rates depend on relative humidity (Stefanoni et al. 2018) and that corrosion stops almost completely as soon as the relative humidity is lower than a threshold value (Roberge 2019). Threshold values can be different depending on the specific corrosion reactions that occur (Roberge 2019). For example, corrosion of an iron surface exposed to the atmosphere has been found to slow strongly as the relative humidity is decreased below a first threshold value of 55% and to be reduced even more below a second threshold value of 20% (Watkinson & Lewis 2004). For reactions in a porous medium, such thresholds will also depend on the pore size distribution via the Kelvin equation, which connects the (partial) water saturation of the medium with the relative humidity of the gas phase (Ahlström 2015).

Stefanoni et al. (2018) link the portion of steel area that is in contact with liquid-water-filled pores to the relative humidity and the saturation degree of the porous medium. At low relative humidity, large pores are gas filled and only a few monolayers of adsorbed water are present on steel and pore surfaces (see e.g., Gimmi & Churakov 2019). The electrochemical reactions are strongly limited in such thin films, because the transport of charged species involved in the anodic and cathodic processes responsible for steel corrosion is strongly inhibited (Stefanoni et al. 2018). Conversely, in water filled (capillary) pores, transport of charged species and electrochemical reactions can more readily occur. Harrison et al. (2017) used microfluidics experiments in partially water filled capillary pore networks to examine mineral dissolution-precipitations reactions. They found that the pore-scale distribution of gas-water mineral interfaces controls both the rate and the extent of reactions.

The importance of water films in partially saturated porous media, including the film thickness and the effect of pore size, pore solution chemistry and mineral type, was investigated by Nishiyama & Yokoyama (2013) and Nishiyama & Yokoyama (2021). They developed a model that allows the effects of water saturation on the dissolution of mineral grains to be predicted in situations where water flows in films, which is typical for water infiltration processes (Nishiyama & Yokoyama 2013). They found that the reactive surface area for mineral dissolution is largely independent of the saturation state of the porous medium, since, in air-filled pores, the mineral grain surfaces are still covered by thin water films. They showed that the film thickness for silica increases with decreasing ionic strength and with increasing pore radius and pH (Nishiyama & Yokoyama 2021). Furthermore, they state that the water film is thick when the sign of surface charge of the mineral is the same as that at the air/water interface, which is the case, e.g., for quartz and montmorillonite at neutral pH.

The progress of chemical reactions is largely controlled by the availability and transport of reactants in the liquid phase. Solute transport is heavily influenced by the liquid saturation of materials. Tyagi et al. (2013) and Gimmi & Churakov (2019) used numerical simulations on clay(stone) structure maps to estimate the effective diffusion coefficient of solutes in samples as a function of porosity and liquid saturation degree, with and without consideration of surface films. Fig. 3-8 summarises the saturation dependence of solute diffusivity for different structure maps. According to these results, the presence of gas in 10 – 20% of the pore space is sufficient to lead to a significant decrease of diffusivity, especially for anions.

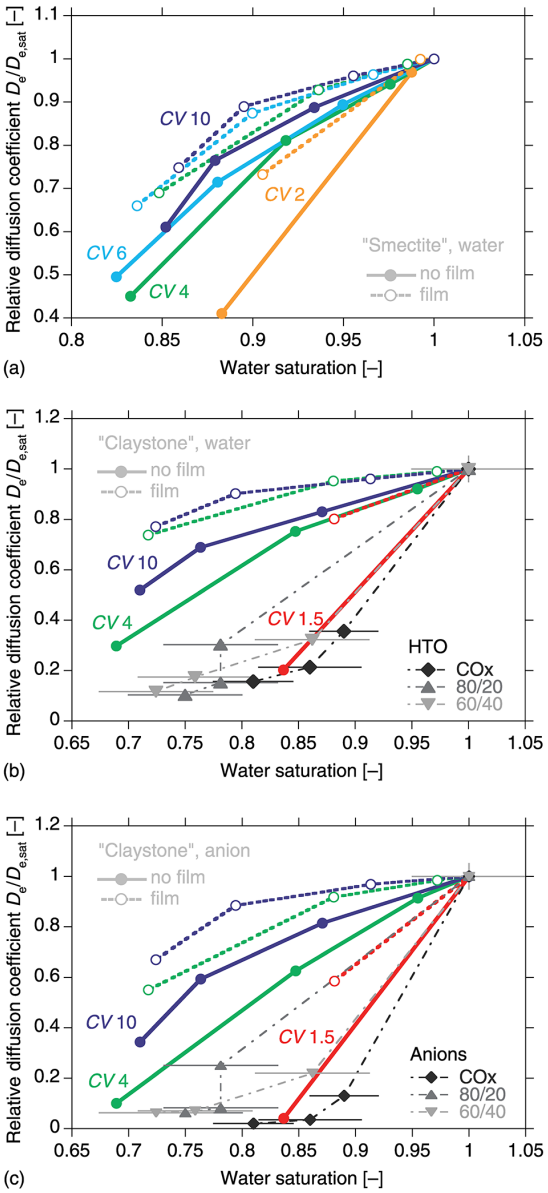

Fig. 3-8: Simulated diffusion coefficients $D_e/D_{e,\,sat}$ (parallel to bedding) for clay structure maps with various coefficients of variations[8] (CV) of the gamma distribution of pore widths as a function of water saturation

(a) Water in "smectite" structures. (b) Water in "claystone" structures (smectite and non-smectite particles). (c) Anion in "claystone" structures. Solid lines: only capillary condensation. Dashed lines: capillary condensation and surface films. Symbols with dash-dotted lines: experimental data for Callovo Oxfordian claystone (COx) and illite/sand mixtures (80/20 and 60/40).

From Gimmi & Churakov (2019). Printed with permission from the publisher.

[8] The coefficient of variation is the standard deviation divided by the mean.

In the case of gaseous reactants, the existence of a connected gas phase in partially saturated porous media can accelerate reaction rates, particularly if the reactants can be transported in the gas phase. A prominent example is the atmospheric carbonation of cement materials. Carbonation fronts move faster at relative humidities in the range of about 50 – 70% than at the higher relative humidities present in most concrete materials (Russell et al. 2001, Šavija & Luković 2016, Winter 2009). At higher humidity, the CO_2 fluxes slow down as increasingly more pore space becomes water-filled, so that fast diffusion in gas-filled pores is replaced by slow diffusion in water-filled pores.

3.5.4 Inhibition of precipitation in very small pores

Even when larger pores (meso- to macro-pores, Fig. 3-2) are gas filled, some materials, notably clays, can retain significant amounts of water in micro-pores (< 2 nm). Godinho et al. (2019) investigated barite precipitation in shale using high resolution time-lapse X-ray tomography. On their short experimental timescale, they did not find any indication of porosity clogging in their "nano-porous" matrix, while transport in fractures and micrometre pores was significantly reduced.

There are several arguments for the inhibition of nucleation in micro-pores, which include the following (Tournassat & Appelo 2011, Stack 2015, Meldrum & O'Shaughnessy 2020):

- The limited availability of reactants/ions, which are needed to form nucleation clusters of critical sizes in smaller pores; in such pores, the transport of reactants, especially anions, can be strongly hindered due to the strong interaction of (polar) water molecules with charged pore surfaces.
- Interaction of reactants/ions with charged or uncharged pore walls is more probable, or occurs at a faster rate, in small pores, which might influence crystallisation. Stack (2015) assumes that the effect of overlapping diffuse layers (~ two times of Debye length) is significant in pore sizes up to 2 nm, for solutions with high ionic strength, and up to nearly 2 μm in pure water.
- Crystals with larger surface to volume ratios, which would be present to a greater extent in small pores, tend to have a higher solubility, which leads to pore-size controlled solubility, favouring crystal growth in larger pores.
- The growth of crystals by accumulation of nano-crystals might be retarded or even impossible in nano-pores. Nucleation theory predicts that the critical radius above which nuclei become stable, is about 1 to 1.5 nm, depending on the influence of the pore properties on the total surface energy of the nucleus (Stack 2015); see also Section 3.5.2.

3.5.5 Precipitation due to evaporation and water consumption

During the evaporation of water, i.e., the phase change of water from liquid to gaseous form, the concentrations of dissolved species in the liquid phase increase due to the loss of solvent, eventually leading to the precipitation of solid phases, mostly consisting of salts. Furthermore, in a porous medium, liquids and solutes are often continuously transported towards an evaporation zone by capillary forces. This can lead to the accumulation of significant amounts of precipitates and to a decrease in porosity (Rad 2014).

Nachshon et al. (2011) have summarised theories and observations on salt precipitation due to evaporation. Citing Wellman & Wilson (1965) and Zehnder & Arnold (1989), they note that thermodynamic theory for salt precipitation in porous media predicts that crystals will grow mainly in the larger pores, since growth in smaller pores requires a significant increase in surface area relative to a small increase in volume. However, *"that theory was developed for saturated*

conditions, where crystal formation responds only to interfacial energy of the solid matrix. In unsaturated media, crystals are limited to growing where liquid is present, and, as the medium dries, growth is restricted to smaller and smaller pores." They note contrasting observations of precipitates tending to accumulate in small pores, with large pores remaining open, and of precipitates tending to accumulate in large pores, with small pores remaining unaffected.

These authors also conducted their own long-term experimental studies on evaporation in heterogeneous porous media and performed CT imaging to elucidate the stages of salt precipitation. On the basis of these studies, they developed a conceptualisation of the mechanisms governing evaporation and salt precipitation, which is illustrated in Fig. 3-9. They found that there are different stages of evaporation, in each of which different chemical and physical processes dominate. At early stages, evaporation rates decrease slightly due to increasing osmotic potential (Stages B and C in Fig. 3-9). Later, salt crust formation and associated partial clogging of pore spaces lower evaporation rates more strongly (Stages D to E in Fig. 3-9). They found that precipitates preferentially fill and clog smaller pores (meso- to macro-pores, c.f., Fig. 3-2), with gas and vapour transport remaining possible in larger pores (macro-pores, cf., Fig. 3-2) (Stage F).

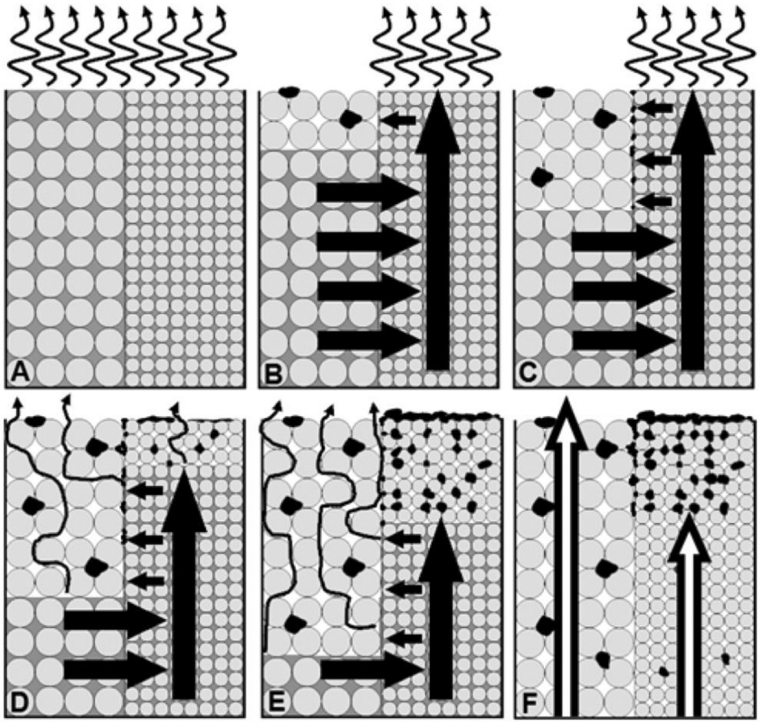

Fig. 3-9: Conceptual illustration of the mechanisms governing evaporation and salt precipitation in a two-layer heterogeneous porous medium in six consecutive stages, labelled A to F

Small and large light grey circles represent small and large solid grains, respectively. The dark grey and white background colours represent, respectively, liquid-filled and gas-filled interstitial spaces. Curved dark grey arrows represent diffusive vapour flow, and straight black arrows represent liquid flow driven by capillary forces toward the evaporation front. Black clusters represent precipitated salt. Most of the salt precipitates within the top of the section with small pores, with some precipitating along the vertical interface. The larger pores remain open for vapour and gas flow (white arrows).

From Nachshon et al. (2011)

3.6 Bio(-chemical) clogging

Microbiological processes in the repository environment have already been mentioned in Section 1.3 in the context of gas generation. Microbes will develop in places where sufficient space exists and where free water (Warthmann et al. 2013) and the nutrients needed for them to be active are available. Such places are available in porous and permeable materials, especially at interfaces. Microbes are known to exist underground in a range of geological media, where they can cause changes in porosity and transport properties (Gaol et al. 2021, Jeong et al. 2018, Yang et al. 2021). Such changes are encountered, and sometimes even utilised, in different applications, e.g., in groundwater aquifer storage and recovery systems (Jeong et al. 2018, Yang et al. 2021), during enhanced oil recovery (Youssef et al. 2009) and in underground gas storage (Dopffel et al. 2021). Porosity clogging related to hydrogen consumption by microbes is a recent focus of research in the framework of hydrogen underground storage (Eddaoui et al. 2021, Ennis-King et al. 2021, Gaol et al. 2021, Wagner 2019). Bio-clogging can be caused by the accumulation of biomass. In particular, partial or complete clogging of pores can be caused by the *in-situ* growth of immobile biomass and by the partial or complete detachment of cells in one location and their subsequent attachment to pore walls or accumulation at pore throats (a type of physical clogging) at another location. In addition, microbes can induce mineral precipitation, e.g., microbial induced carbonate precipitation associated with nitrate- and sulphate-reduction (Dopffel et al. 2021).

The Nagra sealing system employs sand-bentonite mixtures and microbial activity in such materials has therefore been specifically investigated. In particular, the formation of a microbial biofilm in a sand-bentonite mixture has been investigated in the Microbial Activity (MA) experiment at the Mont Terri rock laboratory; for details on the experimental set-up, see Burzan (2021). In this experiment, the injection of hydrogen gas, an efficient electron donor for microbial metabolism, stimulated microbial growth in bioreactors filled with a sand-bentonite mixture, which were fed with Opalinus Clay pore water. Mineralogical alterations were also observed in some of the bioreactors. It has been shown that hydrogen was consumed by sulphate-reduction and methanogenesis. Biofilm formation did not prevent gas transport across the sand-bentonite mixture. Burzan (2021) further observed that preferential flow paths for injected water were associated with wall effects and resulted in pore water only accessing a fraction of the pore space in the sand-bentonite filled reactors. Consistent with the view expressed in the conclusions of Warthmann et al. (2013) that microbes will develop in places with sufficient space and where free water is available, the experiments of Burzan (2021) support the thesis that microbial growth in sand-bentonite mixtures does not occur in the absence of a free water phase.

The sealing system also features so-called “transition layers” in the Nagra sealing system. As described in Section 2.2.3, these include volumes filled with material such as loose sand or gravel, which have relatively large pores that could be favourable to microbial activity. The potential for bio-clogging (and chemical clogging) in the transition layers is discussed in Section 6.3.

3.7 Main messages from this chapter

The focus of this chapter is on the possibility of pore clogging as a result of chemical reactions leading to the precipitation of solids. Physical pore clogging and bio(-chemical) clogging are also described. All chemical reactions considered in this report require water; if no water is available, such reactions do not occur. It follows that clogging by chemical reactions cannot occur in the absence of water. Some specific reactions can proceed solely with water as reactant and do not need reactants to be transported in gaseous or aqueous phases (c.f. iron corrosion Section 3.5.3).

For chemical reactions to proceed in partially saturated porous media, as will exist for a considerable period of time within the repository sealing system, then either:

- Liquid water needs to be present within pores or as water films on pore surfaces.
- This water needs to form connected pathways for the transport of reactants by diffusion and/or advection; an interruption of these pathways may decrease fluxes by several orders of magnitude.

or:

- Reactants (including water) need to be transported in a connected gas phase, e.g., humidity for iron corrosion (c.f. Section 3.5.3) or CO_2 for carbonation of cements.

Availability of free water, nutrients and space is also a prerequisite for microbial activity, which could potentially lead to porosity reduction by bio-clogging. In the absence of either water or nutrients, or with limited space available, microbial activity is limited or absent according to Warthmann et al. (2013). Sand-bentonite mixtures are used within the sealing system and provide a location where microbes could potentially impair the sealing system functionality. This issue has been addressed within the scope of the Microbial Activity (MA) experiment at the Mont Terri rock laboratory (Burzan 2021), where it was found that biofilm formation did not prevent gas transport across a sand-bentonite mixture. The potential for bio-clogging and chemical clogging in the coarse-grained material foreseen within the transition layers of the sealing system is discussed in Chapter 5.

A range of considerations, including nucleation theory, lead to the conclusion that precipitation happens more readily and faster in larger, water-filled pores in comparison with smaller pores under fully- and partially-saturated conditions. On the other hand, under partially-saturated conditions, it is the smaller pores that are more likely to be water-filled, due to the operation of capillary forces, In particular:

- upon desaturation, the largest pores will be desaturated first
- upon (re-)saturation, smaller pores will become water-filled

Hence, observations made, for example, in partially saturated soils, indicate that large, gas-filled pores stay open and only smaller, water-filled pores are filled with precipitates. On the other hand, in materials such as clays and cements, which contain a range of pore sizes, including very small nano-pores, precipitation in very small nano-pores will be inhibited, as discussed further in Chapter 5.

In summary, therefore, in partially saturated porous media, physical clogging of large pores by chemical precipitates requires that these pores are filled with liquid water, which will occur only when the medium as a whole nears full saturation. Precipitation will not occur in large, gas-filled pores; rather, it is smaller, water-filled capillary pores, though not the smallest nano-pores, that could potentially become blocked.

4 Precipitation and pore clogging at interfaces between clay- and cement-based materials

4.1 Precipitation at interfaces: modelling and experimental studies

Cement-clay interfaces are characterised by strong (geo-)chemical differences, which drive the transport of solutes from one material to another and lead to the formation of alteration fronts. Typically, dissolution of cement and clay phases are observed in combination with precipitation of secondary mineral phases at or near the material interface (see e.g., Fig. 3-5). Migration of hydroxyl ions and an associated increase of pore water pH in clay material is the main driving mechanism for mineral alteration. Alteration distances depend on the transport regime (diffusion vs. advection) and on the magnitude of the solute fluxes, as well as on changes in the porosity and transport properties of altered materials.

State-of-the-art information on chemical processes at cement-clay interfaces can be found in several recent reviews and studies related to radioactive waste disposal (Bildstein et al. 2019, Gaucher & Blanc 2006, Prasianakis et al. 2022, Savage & Cloet 2018, Seigneur et al. 2019, Wilson et al. 2021) and is summarised in the following sub-sections. Some of the experimental studies described below and nearly all reactive transport calculations dealing with cement/clay interactions show significant porosity changes due to precipitation/dissolution of minerals near the interfaces between these materials.

4.1.1 Reactive transport modelling

Reactive transport models used to simulate the evolution of cement-clay interfaces are commonly employed at a continuum scale, i.e., transport properties (porosity, diffusivity, permeability) and geochemical properties (mineralogy, water composition) are representative averaged properties of each sub-volume of the model.

Most modelling studies to date have investigated the geochemical evolution of interfaces in situations where diffusive transport dominates. They predict a strong porosity reduction and porosity clogging in narrow zones (Savage & Cloet 2018). The extent of these zones of perturbed mineral and fluid chemistry is controlled mainly by mass transport across the cement/clay interface. Inclusion of the effects of porosity change on mass transport in reactive transport models not only slows the progress of alteration fronts, but also changes the course of mineral evolution. Furthermore, the extent and rate of porosity change depends on rate of kinetic control of mineral precipitation/dissolution and is often dependent on the grid resolution of the model used in the simulations (Marty et al. 2009), as well as on the choice of secondary minerals that are allowed to precipitate (Savage & Cloet 2018). High dissolution rates for primary minerals accelerate mineralogical transformations and porosity changes, which limit the extent of alteration fronts due to the resulting reduction of mass transport (Wilson et al. 2021). In the context of a repository, the zone of perturbed minerals is expected to be narrow, in the range of centimetres up to tens of centimetres over a period in the order of 100'000 or more years, while the zone of changed fluid compositions may extend further (Savage & Cloet 2018, Wilson et al. 2021, Prasianakis et al. 2022). When comparing early studies and reviews with the most recent ones, it is obvious that different continuum-scale reactive transport modelling studies now give a consistent picture of evolution of clay/cement interfaces. Bildstein et al. (2019) specifically note that, in the last two decades, improvements in numerical codes and the accumulation of data feeding into thermodynamic and kinetic databases has greatly improved confidence in reactive transport calculations. "*Overall, these simulations provide a better understanding of physical and chemical change and how materials interact: they give more confidence in the prediction of the durability of materials by converging on the alteration extent that can be expected at the*

interfaces between different materials over long periods of time…this is not to say that we fully understand all the physical and chemical phenomena or that modelling is fully representative of all the processes occurring in such complex systems."

Bildstein et al. (2019) and Savage & Cloet (2018) have identified in their reviews that the role of charged (clay) mineral surfaces, especially their effects on pore space partitioning and transport in different pore space compartments, needs to be included in future reactive transport modelling studies. According to Savage & Cloet (2018) "*All modelling studies except one or two exceptions (Berner 1992, Jenni et al. 2017, Jenni & Mäder 2021) have assumed that the total porosity in clay and bentonite is available for geochemical interactions. The nature of porosity in clays is the subject of much current debate so that alternative models should be considered in future to scope all possible outcomes of the cement-clay interaction process.*"

4.1.2 Experimental observation of porosity reduction

Comparison of the predictions of reactive transport models with the results of field experiments carried out under repository-relevant transport conditions and with real materials is difficult, particularly for continuum scale models, where porosity change is partly dependent on spatial discretisation and needs to be calibrated using experimental data (Marty et al. 2009, Hayek et al. 2011, Hayek et al. 2012, Xie et al. 2015, Poonoosamy et al. 2015). Advective and diffusive fluxes in clay media are low and significant alteration of pore space due to cement/clay interactions is expected to occur only after relatively long times, possibly tens or hundreds of years. Nonetheless, there is some evidence for reduction of porosity (Wilson et al. 2021) from long-term observations of concrete/clay interfaces at the Tournemire industrial analogue (Gaboreau et al. 2011, Lalan et al. 2016, Soler 2013, Tinseau et al. 2006), from the Maqarin natural analogue (Pitty & Alexander 2014, Martin et al. 2016), from the Mont Terri cement interaction (CI) experiment (Jenni et al. 2014, Mäder et al. 2017, Yokoyama et al. 2021) and from the Grimsel FEBEX experiment (Gaboreau et al. 2020). Recent laboratory studies conducted at the University of Madrid (González-Santamaría et al. 2020b, González-Santamaría et al. 2020a) and at PSI (Luraschi et al. 2020, Shafizadeh et al. 2015, Shafizadeh et al. 2020) investigated small samples with cement paste and clay materials in contact with each other. Neutron imaging and X-ray tomography show that there were already significant changes in mineralogy and porosity near the material interface after 0.5 to 6 years (Fig. 4-1).

The studies are summarised in Prasianakis et al. (2022). Fig. 4-1 shows that, over the course of six years, a low-porosity zone in the montmorillonite developed that extended up to ~ 2 mm from the interface, with a pronounced porosity minimum occurring somewhere around 1 mm from the interface. This mainly developed during the first year. Thereafter, porosity within this zone continued to decrease slightly, but the zone itself barely expanded any further.

The porosity on the OPC side adjacent to the interface generally increased slightly, as inferred using neutron imaging. The increase was clearly related to the dissolution of portlandite. While the extent of this zone of higher porosity steadily increased with interaction time (up to ~ 2 mm in two years, and larger distances over 6 years), the porosity within the zone did not show a monotonic increase. Depending on position, it later also decreased and then partly increased again. This is likely to have been related to dynamic precipitation and possibly to re-dissolution of cement minerals.

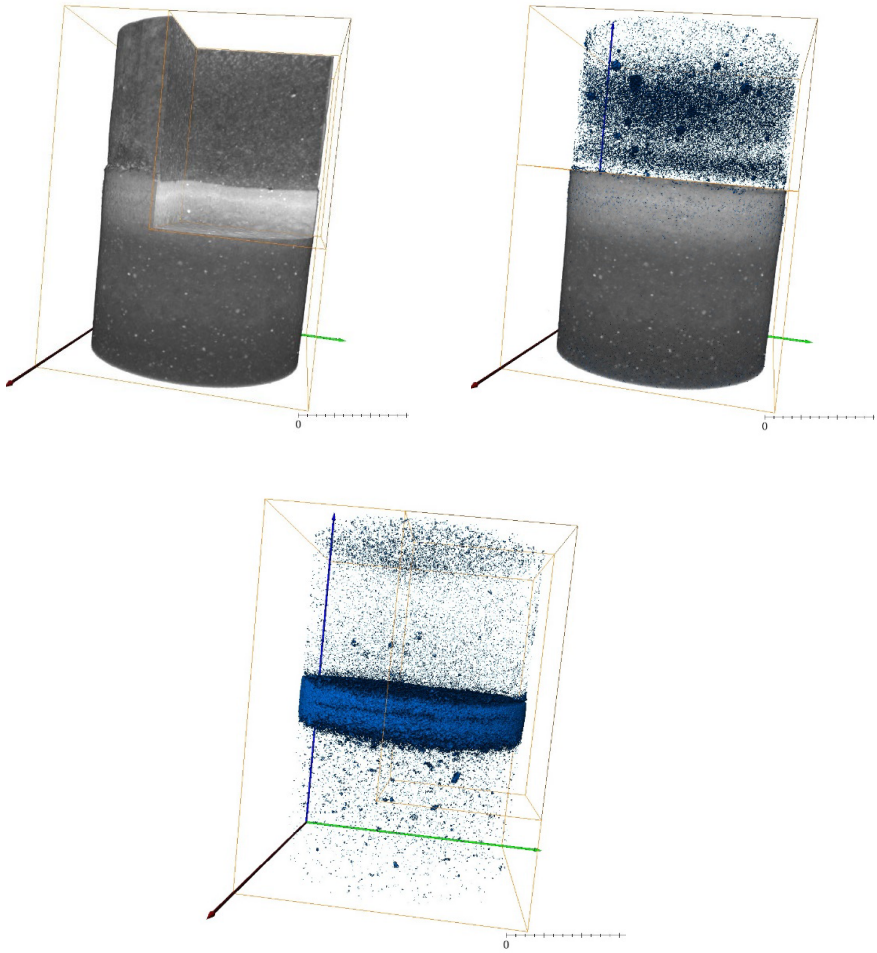

Fig. 4-1: Top left: tomogram of Ordinary Portland Cement (OPC)-Na montmorillonite sample C3 after about six years of interaction

Top right: (qualitative) porosity distribution on the cement side, derived from the tomogram, with dark blue areas representing pores. Bottom: (qualitative) visualisation of the high-density region, mainly in the Na montmorillonite part of the sample, represented by dark blue and blue areas. Manuscript available and in preparation for publication by Luraschi et al. (in prep.), Luraschi (in prep.) and Prasianakis et al. (2022)

Not all samples were found to contain a narrow, low-porosity region. In a few samples, the decrease in porosity was spread over nearly the entire 5 mm of the sample, while, in a few other samples, no clear patterns were detected. The reasons for the differences in behaviour between samples are not clear, but it could be related to small variations in properties between samples, especially at the interfaces. This would suggest that natural heterogeneities present at the repository scale may lead to non-uniform development of a low-porosity zone, possibly without any porosity alteration at some localities.

4.1.3 Influence of charged mineral surfaces on transport within porous media

Clay minerals and C-S-H phases in cements typically have a negatively charged surface (see e.g., Fig. 3-3 for clays, and Fig. 3-2, bottom part, for pore sizes). In contact with an aqueous solution, the charge is compensated by accumulation of positively charged counter ions (cations) near the surface, forming a so-called "electrical double layer" (EDL). The first layer of an EDL (the Stern layer) consists of cations attached to the charged mineral surface. Ions in the Stern layer are generally assumed to be immobile and only partially neutralise the naturally occurring negative surface charge. Gimmi & Kosakowski (2011) evaluated experimental data on cation diffusion in clays and could show that sorbed ions, including those in the Stern layer, are mobile. This finding is supported by various molecular modelling studies on the mobility of ions in presence of charged mineral surfaces (see e.g., Ma et al. 2019 and references therein). The second layer is also mostly composed of cations, which, however, are mobile and are found in high concentration. The extent of the EDL depends on the mineral surface charge and on the ionic strength of the aqueous solution. Depending on the pore size, EDLs of adjacent mineral surfaces may overlap (small nano-pores/inter-layers), in which case the pore solution composition is dominated by the presence of counter ions. The relatively small size of the pores and the negative charge of the mineral surfaces have a strong influence on the presence and transport of charged species. Neutral and positively charged chemical species are, in principle, able to diffuse through the entire pore space. Conversely, negatively charged anions are repelled by the negatively charged mineral surfaces and cannot enter the inter-layer or nanopores. Anion exclusion is thought to be one process that prevents mineral precipitation in nanopores, as strong dominance of ions in pore solution creates unfavourable conditions for nucleation (Stack 2015, c.f., Section 3.5.2). In addition, it has been found that the EDL has an influence on the adsorption of gases on mineral surface and thus influences the transport of dissolved gases in nano-pores (see e.g. Gadikota et al. 2017).

Diffusive transport parameters may change across material interfaces and will be affected by any porosity changes resulting from the dissolution and precipitation of minerals. The change in diffusive transport parameters across an evolving cement/clay interface was investigated as part of the small-scale laboratory experiments described in Section 4.1.2 by Shafizadeh et al. (2015, 2020) and by Luraschi et al. (2020). Diffusive transport across the interface was measured using neutral (HTO) and anionic (Cl) tracers (Figs. 4-2 and 4-3). It was found that diffusion of HTO across the sample was reduced by a factor of two due to the reduction of porosity on the clay side. The reduction of the diffusion coefficient for the anion Cl^- was much stronger than for the neutral HTO. As discussed further in Section 4.2, anions can only access the so-called free porosity (mainly larger capillary pores and meso-pores), whereas water, neutral and cationic species can access all pores, including inter-layer and similar nano-pores, which, as argued in Chapter 3, are not expected to be affected by precipitation.

This is in-line with recent experimental diffusion measurements across clay zones with reduced porosity caused by precipitates (Chagneau et al. 2015, Fukatsu et al. 2017, Luraschi et al. 2020, Wigger et al. 2018), as well as with observations by Martin et al. (2016), who investigated a sample from the Maqarin analogue and found that the alteration rim around a seemingly totally clogged vein still had a porosity of about 19%. Based on such observations and experiments, as well as on pore-scale modelling and arguments concerning precipitation in nano-pores (c.f., Section 3.5.4), Prasianakis et al. (2022) have concluded that complete clogging of porosity at clay/cement interfaces is unlikely, even in the long term.

Jenni et al. (2017) and Jenni & Mäder (2021) modelled the evolution of cement/Opalinus Clay interfaces with a dual-porosity approach, in which the porosity is split into two parts. One part is influenced by the negatively charged clay mineral surfaces and contains excess cations to compensate for the surface charge. This part of the pore space is not freely accessible to anions and other negatively charged species. The other part contains the remaining charge-neutral

solution and is freely accessible to all ions and solutes. For undisturbed Opalinus Clay, the total porosity is split roughly equally between the two types of pore space. Donnan equilibrium can be used to calculate the pore water composition in each part of the pore space (Jenni et al. 2017). Cation exchange reactions are not explicitly included in the model; rather, these reactions are intrinsically a part of the Donnan equilibrium approach. In addition, the Nernst-Planck equations have to be used to calculate the diffusive fluxes in the system. The model only gives rise to precipitation of minerals in the freely accessible pore space, which becomes completely clogged on the Opalinus Clay side of the interface.

The experimental evidence cited above, the modelling studies of Jenni et al. (2017) and Jenni & Mäder (2021), and the theoretical reasoning concerning precipitation in micro-pores presented in Section 3.5.4, provide a consistent picture in which precipitation in the clay takes place preferentially in the free porosity, i.e., in larger pores, which can become clogged. In smaller pores (i.e., inter-layer pores), diffusion of anions is strongly reduced or even prevented, whereas cations, HTO and other neutral species can circumvent blocked larger pores via inter-layers, such that diffusion of such species through the Na-montmorillonite still takes place, albeit at a slightly reduced rate.

A strong reduction in the anionic diffusion coefficient is expected, even if the zones responsible for this reduction are relatively thin, unless the partly reduced pore space is re-opened by other processes (e.g., mechanical cracking, dissolution).

The estimated solute diffusion coefficients of charged and neutral species for the “skin” zone with reduced porosity depend on the tracer-specific accessible porosity and are in-line with other measurements conducted in compacted bentonite (Fig. 4-3). These estimates, which make use of the relationship between porosity and effective diffusion coefficients implied by Archie’s law, can be included in numerical transport models and allow an estimation to be made of the effects of small zones of decreased porosity on large scale transport in the liquid phase.

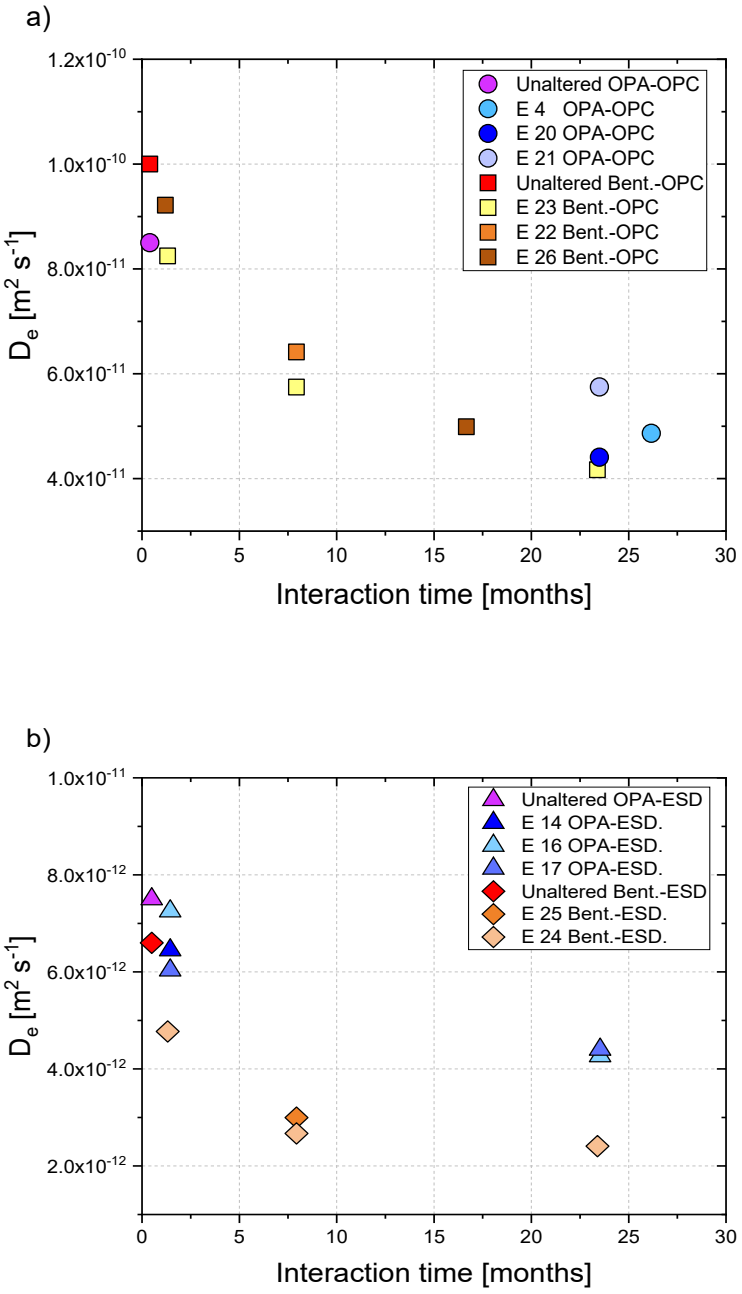

Fig. 4-2: Estimated evolution of the effective diffusion coefficient D_e of HTO in (a), OPC paste in contact with bentonite and Opalinus Clay and (b), ESDRED mortar in contact with bentonite and Opalinus Clay

Purple and red symbols represent theoretical (calculated) values for completely unreacted interfaces. The following values were used in these calculations: Opalinus Clay D_e for HTO = 5.4×10^{-11} m^2/s (Bossart et al. 2017), bentonite D_e for HTO = 6.1×10^{-11} m^2/s (Na-montmorillonite value from Luraschi et al., 2020), OPC paste D_e for HTO = 2.8×10^{-10} m^2/s (Tits et al., 2003), ESDRED mortar D_e for HTO = 4×10^{-12} m^2/s (estimate). (from Luraschi in prep., Luraschi et al., Prasianakis et al. 2022)

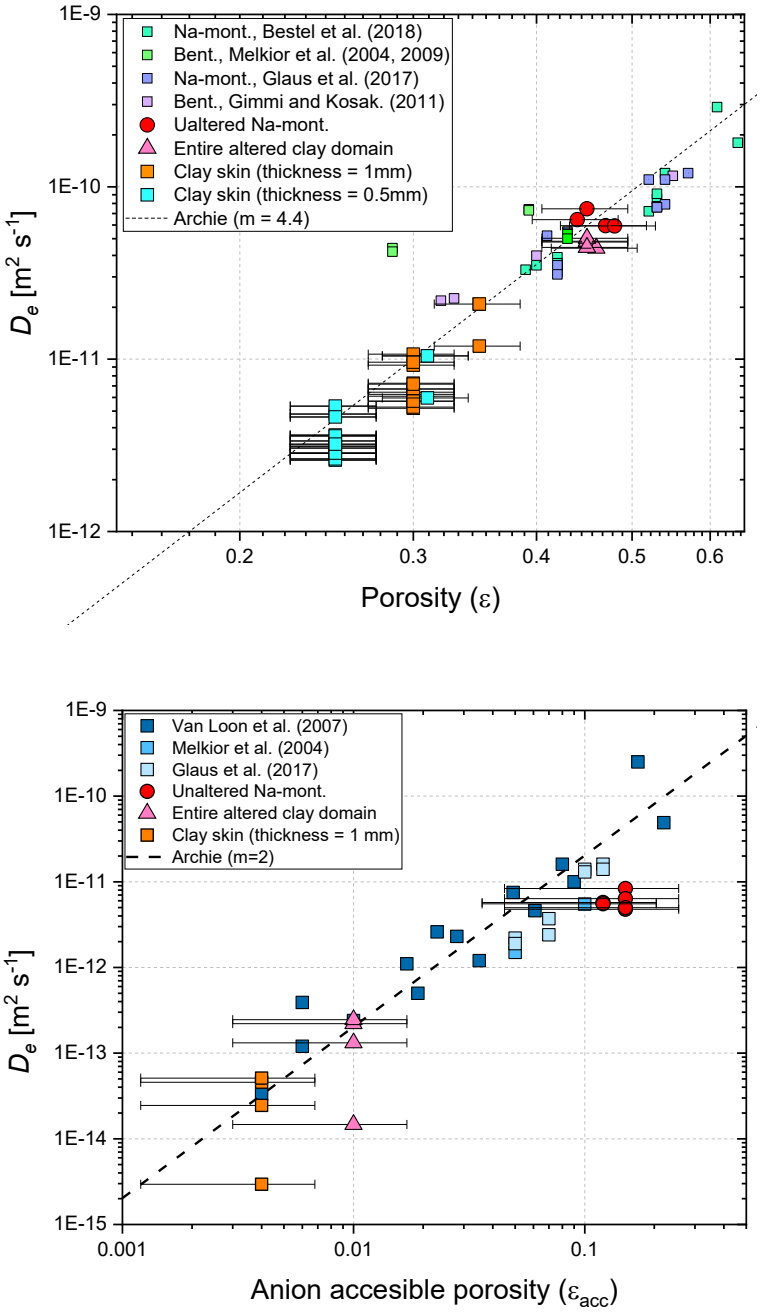

Fig. 4-3: Relationship between the effective diffusion coefficient of HTO (top) and of Cl-36 (bottom) and the diffusion accessible porosity for Na-montmorillonite and bentonite

The dashed line represents the classical Archie's relation with m = 4.4 for HTO and m = 2 for Cl^{-36}. HTO-accessible porosities for the skin regions (top) were derived from the data of Shafizadeh et al. (2020); the error in these porosities is estimated to be ± 10%. Cl^- accessible porosities (bottom) for the entire clay domain (pink symbols) and for the skin region (orange symbols) are rough estimates with large uncertainties. Figures from Luraschi et al. (2020).

4.2 Other factors and uncertainties related to the extent of precipitation and possible pore clogging

Modelling studies indicate that the reduction of the pore space that occurs over time leads to a strong reduction of advective and diffusive mass fluxes across a clay-cement interface, which essentially stops the geochemical alteration processes in the long term. Newer modelling and experimental studies indicate that anion and cation transport are differently affected by porosity change (Fukatsu et al. 2017, Jenni et al. 2017, Jenni & Mäder 2021, Luraschi et al. 2020). As noted in Section 4.1.3, anion transport across clogging cement/clay interfaces is typically significantly more strongly reduced than cation transport. The effect is related to a 'bottleneck effect', where diffusion of ions is limited by anion exclusion (Wigger et al. 2018). A diffusion pathway for cations can become blocked for anions by overlapping of electric double layers, typically in small pores or clay inter-layers, which cannot be filled with precipitates.

Other factors that may affect the extent of possible clogging at interfaces and its effect on transport include saturation (c.f., Section 3.5.3) and temperature. Wilson et al. (2021) remark that, in most modelling studies of cementitious barriers, the effects of temperature variation are not considered. Many models assume standard conditions, usually a temperature of 25 °C and a pressure of 1 bar (100 kPa), which are the default conditions for most common thermodynamic databases. Typically, diffusion coefficients increase with temperature. For example, van Loon et al. (2004b) found in experiments that the effective diffusion coefficient for HTO in Opalinus Clay increases by a factor of ~3 when temperature increases from 25 °C to 70 °C.

For repository conditions, the pressure dependence of thermodynamic data can be safely ignored (see e.g. Anderson 2005), except for the solubilities of gases, which deviate from ideal behaviour and need to be treated using an appropriate equation of state (e.g., the Peng-Robinson equation of state). In general, kinetic control of dissolution and precipitation shows a strong temperature dependence. For example, the dissolution rate of smectite increases by a factor of 20 to 30 when the temperature increases from 25 °C to 70 °C (Marty et al. 2015).

For Portland-cement-based materials, the stable phase assembly changes significantly only when temperatures rise above about 50 – 60 °C, i.e., ettringite is transformed into monocarbonate and monosulphate (Lothenbach et al. 2008). Many zeolite and clay minerals are metastable with respect to similar minerals at higher temperatures (Wilson et al. 2021). Note, however, that solubility data for most clay minerals at low temperatures are ambiguous (Jenni et al. 2019). Jenni et al. (2019) also reviewed available information on the stability of bentonite at elevated temperatures and concluded that, despite many uncertainties, thermally induced changes are not relevant at temperatures below 120 °C. Similarly, the influence of elevated temperatures on Opalinus Clay are expected to be minimal, as temperatures expected to arise in the Opalinus Clay around the repository are not expected to exceed the maximum temperatures of 80 – 90 °C that were reached during burial history of the rock (Leupin et al. 2016a).

The evolution of cement/clay interfaces is mainly driven by mass transport across the interfaces in combination with mineral dissolution under alkaline conditions. Under elevated temperatures, the combination of faster diffusion and higher kinetic rates will accelerate the evolution of the interfaces and also accelerate porosity changes. The limiting process will be the acceleration in diffusion, as this process also indirectly controls dissolution kinetics by advancing the alkaline front in the clay material.

Studies of the influence of water saturation on cement/clay interface processes are sparse and many aspects of the effects of liquid saturation on the evolution of cement/clay interfaces are largely unknown. Bildstein et al. (2019) note that "*Another aspect of unsaturated porous media that is not yet widely treated in RTM (Reactive Transport Models) relates to the dependence of chemical reactivity with regard to the water content, in particular looking at how the mineral and gas solubility and the aqueous speciation relate to capillary pressure at low water saturation*".

Nonetheless, from the general discussion of the influence of liquid saturation on precipitation given in Section 3.5.3, it can be stated that, in partially saturated media, larger pores (macro pores) are likely to be gas-filled and thus chemical reactions leading to precipitation will not occur in these pores, except potentially in thin water films on pore surfaces. Smaller pores (meso pores) are likely to remain water-filled due to the operation of capillary forces and might become filled with precipitates Precipitation in nano pores (micro pores) is expected to be inhibited for the reasons given earlier.

It should finally be noted that, under in-situ conditions within a tunnel in a geological repository in a clay host rock, mechanical forces will also act on the material interfaces e.g., due to tunnel convergence and the swelling of the host rock. As a result, microcracks in any layers of precipitates are likely to be formed, reducing clogging and allowing greater transport of solutes and gas.

Overall, it can be stated that, in clay- and cement-based materials and at the interfaces between them, whether partially or fully saturated, complete pore clogging is not expected to occur.

4.3 Main messages from this chapter

This chapter has reviewed experimental and modelling studies elucidating the precipitation and pore clogging that may occur at the interfaces between clay- and cement-based materials. The main points are as follows.

- As well as larger pores, clay and cement-based materials contain a large fraction of pores with apertures of less than a few nanometres, i.e., inter-layer pores in clays and in C-S-H-cement phases, as well as small “gel pores”.
- There is a reasonably good understanding of mineral changes that are observed and modelled at the contact between cement and clay materials.
- Migration of hydroxyl ions and the associated increase of pore water pH in clays is the main driving mechanism for mineral alteration and for precipitation.
- The zone of perturbed minerals is expected to be narrow, in the range of centimetres up to tens of centimetres over a period in 100'000 or more years. The zone of perturbed fluid composition might be more extensive.
- The porosity is expected to be reduced by precipitation, typically directly at such interfaces or on the clay side of the interfaces.
- Although there is significant uncertainty regarding the extent of precipitation and possible pore clogging under partially saturated conditions, there is evidence that it is not possible for complete clogging of the interfaces to occur, since the smallest, nano-pores will remain open; larger pores will also remain open as long as they remain unsaturated.
- Microcracks may form in modified material, e.g., due to tunnel convergence, which would enhance transport of gases and solutes.

Although nano-pores (i.e., inter-layer pores) are expected to remain free of precipitates, transport of gas through these pores is expected to be highly constrained. This is the topic of the following chapter.

5 Gas transfer and storage in clay- and cement-based materials: potential effects of clogging

5.1 Overview of transfer and storage processes

The gases produced in the backfilled repository can be transported by a variety of mechanisms. Gases generated in the repository near field will initially be fully dissolved in the pore water, but eventually, when the solubility limit is exceeded, a separate gas phase will form. At elevated gas pressures, the porous media in which the gas is present (host rock, buffer, backfill and sealing materials) could undergo mechanical deformation. Gas transport is thus controlled by the hydraulic and mechanical properties of the porous media (e.g., their intrinsic permeability, porosity and mechanical strength) as well as by the hydromechanical state (i.e., water saturation, gas and pore water pressure, stress state). Phenomenological considerations suggest the following subdivision of the basic transport mechanisms, as illustrated for the Opalinus Clay in Fig. 5-1 (see also Nagra 2008b):

1. advective-diffusive transport of gas dissolved in pore water
2. visco-capillary two-phase flow
3. dilatancy-controlled gas flow
4. gas transport along macroscopic tensile fractures (hydro- and gas-fracturing)

The transport mechanisms include complex hydromechanical processes that can be understood in terms of the coupling between the transport of immiscible fluids (Fig. 5-1b) and geomechanics (Fig. 5-1c). An overview of gas transport mechanisms is given in Sections 5.1.1 to 5.1.4; a more detailed description is provided in App. B.

5.1.1 Transport of gas dissolved in the pore water

Advective and diffusive transport of gas dissolved in pore water is characterised by three fundamental laws (Helmig 1998):

- Darcy's law, which describes advective groundwater flow under the influence of pressure and gravitational forces
- Fick's law, which represents the diffusion of dissolved gas (and other solutes) due to the concentration gradients in the pore water
- Henry's law, which describes the solubility of gas in pore water.

5.1.2 Visco-capillary two-phase flow

In visco-capillary (two-phase) flow, gas transport is controlled by the interaction between the visco-capillary forces, gravity/buoyancy, solubility and diffusion, and the connectivity and spatial variability of the pore network. Lenormand et al. (1988) identified three major flow regimes, namely viscous fingering, capillary fingering, and stable displacement. The capillary number *Ca*, defined as the ratio of viscous and capillary forces, and the viscous ratio *M*, defined as the ratio of the viscosities of the defending and invading fluid, determine the transition between these flow regimes (Lenormand et al. 1988). Additional two-phase flow phenomena, such as migration (buoyancy-controlled transport), fragmentation (competition between capillary and buoyancy effects), and coalescence (interaction with trapped gas) are described by a third dimensionless number, *K,* which is defined as the ratio between viscous and hydrostatic forces.

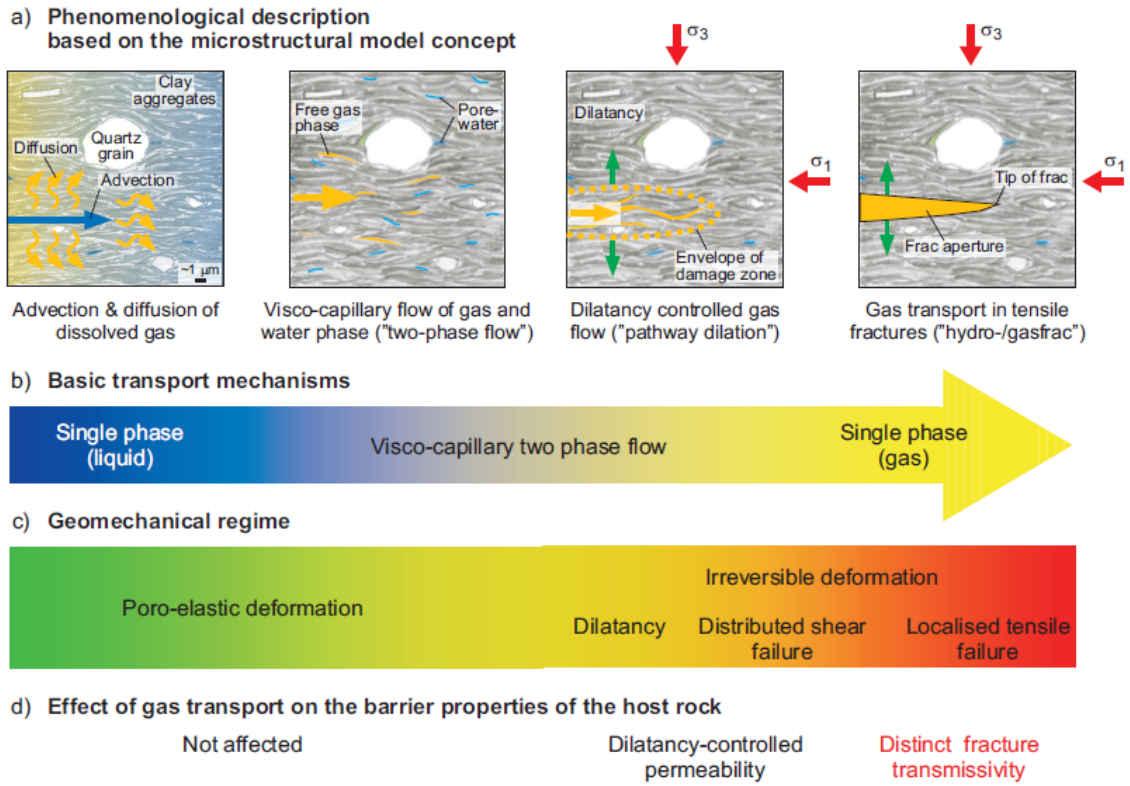

Fig. 5-1: Classification and analysis of gas transport processes in Opalinus Clay
From Nagra (2008a)

In a geomechanical sense, and for the purposes of modelling gas transport and storage, consolidated clay rocks, such as Opalinus Clay, can be assumed to behave as elastic porous medium, characterised by a porosity and a compressibility (additional considerations regarding phenomena occurring in bentonite and sand/bentonite mixture are given in Section 5.2.2). A controlling factor for two-phase flow in a porous medium is the gas entry pressure, also known as capillary threshold pressure and hereafter referred to as capillary strength, which represents the difference between gas pressure and water pressure needed to displace pore water from the medium when it is initially fully saturated. Considering the medium on a pore scale, the capillary strength corresponds to the capillary pressure of the smallest-radius pores that the gas pressure needs to overcome so that gas entry occurs in these pores. Once the capillary strength has been exceeded, gas flow is mostly controlled by the intrinsic permeability (k) of the medium, the permeability-saturation relationship (commonly known as relative permeability), and the relationship between the capillary pressure and the water saturation (also known as suction or water retention curve). The functional dependency between pore space saturation and the relative permeability or the capillary pressure is commonly described with parametric models, such as in the Van Genuchten approach (see App. B).

5.1.3 Dilatancy-controlled gas flow

Dilatancy-controlled flow (or "pathway dilation" after Horseman 1996) is a transport mechanism of special importance in clay media with low tensile strength. Such media cannot withstand long-term gas pressures with a magnitude greater than the minimum principal stress acting on the material. Due to the expected micro-scale variability of the geomechanical material properties, it is plausible that microfractures will form before yielding (ductile fracturing). The process of gas-driven micro-fracturing leads to an increase in the void space, which is accompanied by a detectable increase in intrinsic permeability and a change in the capillary pressure-saturation relationship. Porosity, permeability, and capillary strength are linked to rock deformation through empirical relationships. Gas flow is still controlled by visco-capillary forces – the main difference compared with the conventional two-phase flow described in Section 5.1.2 is that the transport properties of the solid phase can no longer be viewed as invariants, since they depend on the state of deformation of the material. A consequence of this conceptual framework is that a smooth transition is expected between conventional two-phase flow and dilatancy-controlled gas flow, when the geomechanical state of the porous medium changes from poro-elastic towards a plastic deformation. An important feature of the elasto-plastic material behaviour of these materials is their self-sealing capacity (e.g., Nagra 2002b). Permeability enhancement resulting from pathway dilation at elevated gas pressures tends not to be permanent; when the gas pressure is reduced the material reconsolidates and the hydraulic and mechanical properties of the porous medium approach the values characteristic of the undisturbed stress state (Nagra 2008a).

5.1.4 Gas transport along macroscopic tensile fractures (hydro- and gas-fracturing)

As a rule of thumb, a macroscopic tensile fracture (hydrofrac/gasfrac) develops when the gas pressure is larger than the sum of the minimal principal stress and the tensile strength of the rock (e.g., Valkó 2013). Fracturing is initiated quasi-instantaneously without precursory plastic deformation and the fracture propagates at about the velocity of a shear wave (e.g., Gross 2007). Gas flow in such a macroscopic tensile fracture can be seen as a single-phase process. The propagation comes to a halt when the gas pressure in the fracture becomes less than the value of the minimum principal stress (shut-in pressure). In a rock with low tensile strength, a macroscopic fracture develops only when the gas pressure build-up is rapid, i.e., when the combined effect of pore water displacement and formation of small-scale fractures (dilatancy) no longer counterbalances the gas production rate.

5.2 Gas transfer and storage processes in clay-based repository materials

Modelling of the fate of repository-generated gas, as will be presented in Chapter 6, shows that both the de-saturation of the Opalinus Clay host rock and advective transport in the rock are spatially and temporally limited. Diffusion of dissolved gases in pore water is the dominant large-scale transport process in the host rock surrounding the repository. This process is covered in Section 5.2.1.

Gas storage in engineered clay-based repository materials under fully saturated conditions will occur due to the dissolution of gas within the pore water. However, the above-mentioned modelling indicates that large parts of the repository near field and the sealing system will remain only partially-saturated for a long period of time, providing a much larger gas storage volume. Transport of the gas phase in the host rock surrounding the repository and in the repository itself will be addressed in Section 5.2.2.

5.2.1 Diffusion of gas in liquid phase across a fully saturated clay

Diffusive transport of dissolved gas through clay is the subject of the hydrogen transfer (HT) experiment, located at the Mont Terri Rock Laboratory (Vinsot et al. 2017, Vinsot et al. 2014). The experimental set-up consists of a gas-filled borehole drilled into fully saturated Opalinus Clay rock. The studies are focused on the long-term diffusion of gases, the estimation of gas fluxes between the injection reservoir and the surrounding rock, and the potential for microbial hydrogen consumption. The experiment provides an analogue for gas exchange between a partially water-saturated repository tunnel (or emplacement cavern), where a free gas phase exists, and the adjacent fully saturated host rock. It demonstrates the diffusion of gases across the tunnel/rock interface, as well as in the Opalinus Clay formation itself, and the possible influence of degassing of pre-existing dissolved gases in the Opalinus Clay pore water.

Damiani et al. (2022) presented a model of the HT experiment, which couples a reactive thermodynamic model describing the chemical conditions in the injection reservoir with a reactive transport model for diffusion of dissolved gases in the Opalinus Clay. In the modelling study, the assumption is made that gas fluxes across the borehole wall are due solely to the diffusive transport of dissolved gases in Opalinus Clay. This assumption is consistent with experimental observations for non-reactive gases. The gas phase composition and pressure in the borehole together control the gas concentrations in the water phase at the borehole wall in the injection interval. The concentration difference in the water phase between the borehole wall and Opalinus Clay is the driving force for the diffusive transport of gases between the borehole and Opalinus Clay, specifically, the transport of argon, neon and helium into the Opalinus Clay and the transport of nitrogen and methane, as well as other alkanes, from Opalinus Clay into the borehole. Advective transport of dissolved gases is of secondary importance, while water accumulation in the borehole increases the borehole gas pressure.

As shown in Fig. 5-2, the long-term evolution of gas composition could be reproduced well for major components, including argon, methane, and nitrogen. At the beginning of the experiment, after 560 days and after 780 days, the borehole was filled with argon, or argon-dominated gas mixtures, and the out-diffusion of argon and the in-diffusion of methane and nitrogen was observed. Borehole gas pressures were influenced by in-flow of formation water and several water extraction and leaking events. Fig. 5-2 shows only the evolution of argon, methane and nitrogen concentrations. Other gases show a more complex behaviour and are influenced by bio-chemical reactions in the borehole and by experimental artefacts. Details are provided in Damiani et al. (2022).

The model uses different effective diffusion coefficients for different gases. They are calculated based on a common Opalinus-Clay-specific geometry factor that is multiplied by gas-specific diffusion coefficients in water (D_w), taken from the literature. The effective diffusion coefficients for dissolved gases in Opalinus Clay were fitted by adjusting the geometry factor manually, as demonstrated in Fig. 5-2. Application of the reference geometry factor results in an effective diffusion coefficient for HTO (tritiated water tracer) of 3.1×10^{-11} m/s ($D_w = 2.24 \times 10^{-9}$, porosity = 0.16, temperature = 15.6 °C). This effective diffusion coefficient is slightly lower than values obtained in previous studies (van Loon et al. 2004a, van Loon et al. 2004b). A temperature corrected value of $(4.2 \pm 0.4) \times 10^{-11}$ m/s (porosity = 0.17, temperature = 14 °C) was measured for HTO in samples from Mont Terri in the laboratory (van Loon et al. 2004a) and the value of 4.0×10^{-11} m/s (porosity = 0.15, temperature = 14 ºC) was estimated from an *in-situ* migration experiment (van Loon et al. 2004b).

In addition to the reference geometry factor, Fig. 5-2 shows results using alternative factors that result in higher and lower effective diffusion coefficients for HTO of 4.4×10^{-11} m/s and 2.1×10^{-11} m/s, respectively. These effective diffusion coefficients yield results that envelope the concentrations in the gas phase measured experimentally in the HT experiment. In terms of gas

composition, the agreement using the lower effective diffusion coefficient seems better during the calibration phase, but, for this variant, calculated gas pressures in the borehole drop significantly below the measured values in the long term. Furthermore, the volume fractions and the in-diffusion of methane and nitrogen are underestimated in the long term.

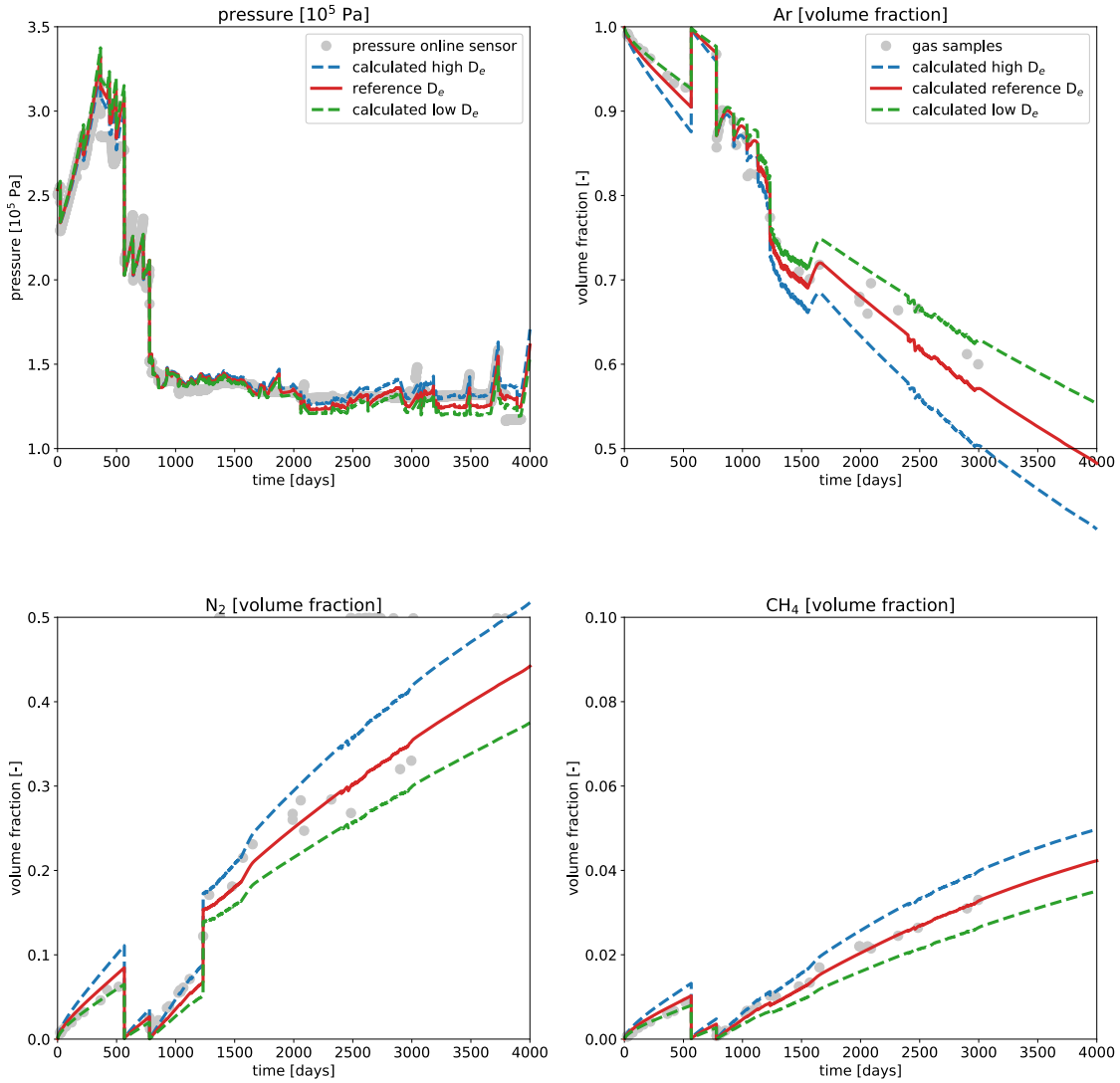

Fig. 5-2: Influence of effective gas diffusion coefficients on the predicted pressure and gas phase composition in the borehole of the HT experiment

From Damiani et al. (2022)

The experimental observations related to non-reactive gases in the HT experiment and the associated modelling study demonstrate that transport of dissolved gases in fully saturated Opalinus Clay follows the fundamental principles outlined in Section 5.1.1. Large-scale transport of these gases across the Opalinus Clay will be controlled by the pressure- and temperature-dependent solubility at the contact of the gas and water phases, by the large-scale concentration gradients in the Opalinus Clay pore water and by the diffusivity in the Opalinus Clay.

5.2.2 Transport of gases in partially liquid saturated clay media

As described in Chapter 2, the repository sealing system uses various materials as sealing elements, in abutments that transmit loads into the rock, in transition layers and as backfill for the remainder of the tunnels. The design concepts for the sealing elements, abutments, transition layers and backfill are described in Sections 2.2.1 to 2.2.4, respectively. As sealing materials, both clay/bentonite and sand/bentonite mixtures have the necessary long-term durability. Materials containing bentonite have properties favourable to slow transport and to the geochemical retention of most of the radionuclides that may be released from the repository disposal areas over time. Specifically, they are characterised by low hydraulic conductivity and they possess excellent sorption properties. Pure bentonites have a large swelling capacity and an extremely low permeability for both water and gas. In sealing elements where a certain permeability is required to enable the transport of repository-generated gas at reasonably low overpressures, sand/bentonite mixtures with relatively low bentonite content are suitable, because they simultaneously maintain favourable retention properties of bentonite and provide significant gas permeability.

Sand/bentonite mixtures

Comprehensive research studies have been conducted in the past decades to characterise gas transport in sand/bentonite mixtures (e.g. Graham et al. 1997, Nagra 2008b, Japan Nuclear Cycle Development Institute 1999, Tashiro et al. 1998). A mature understanding of the microstructure of such mixtures has been developed and the importance of this microstructure for gas transport behaviour has been investigated. It has been shown that sand/bentonite mixtures with a moderate bentonite content of 20 – 30% are characterised by a multi-modal pore size distribution; see Section 3.2.1. The form of the pore size distribution depends on a variety of factors, such as the degree of compaction and the water content of the sand/bentonite mixture (Fig. 5-3), enabling these materials to be tailored in such a way that they exhibit desired properties. In particular, through the application of appropriate techniques for their emplacement (compaction), their gas transport properties can be tailored to the performance and design requirements.

In the sand/bentonite mixtures with relatively low bentonite content that are intended for use in the sealing system, the sand grains form a “shielding skeleton” (Romero 2013) that carries the external stresses, while the bentonite (once saturated) can swell to effectively fill the pore space within this skeleton; Romero (2013) suggests filling fractions of ~ 98% for 80/20 sand/bentonite provided the swelling of the bentonite is not inhibited (the swelling pressure developed by the bentonite is a function of effective dry density and fluid chemistry).

As part of the Gas Migration Test (GMT) at the Grimsel Test Site, investigations of relatively low bentonite sand/bentonite mixtures were performed to characterise the dependency of the pore size distribution on the (i) emplacement density and (ii) the degree of saturation. Manca (2015) provides an analysis of the hydro-chemo mechanical (HCM) behaviour of an 80/20 sand/bentonite mixture, including the main mechanisms of liquid and gas transport under both saturated and unsaturated conditions. A comprehensive experimental database on sand/bentonite mixtures, including their hydro-mechanical and two-phase transport properties, has been compiled in the framework of the GAST experiment, also at the Grimsel Test Site (Lanyon et al. *planned*).

Fig. 5-3a shows that, with increasing mixture density, the macro-porosity, and hence the pore space available for water flow and solute transport, decreases significantly. If the material is saturated with water, the bentonite swells and fills the pore space of the sand matrix, thus resulting in a very pronounced decrease in the macro-pores, as shown in Fig. 5-3b and c. Laboratory tests on as-compacted sand/bentonite material (e.g., within the GMT Project) show that permeabilities to gas under fully desaturated conditions are significantly higher than the permeabilities to water in fully saturated conditions. Furthermore, a small desaturation of the material can be sufficient

to create a connected pore space available for gas flow and can result in a high gas permeability. The relevant gas flow mechanism is two-phase flow through the macro-porosity of the sand/bentonite associated with a very low capillary strength in the order of 10 kPa (Nagra 2008a, see also App. B). This macro-porosity exists between the sand grains and is available if the bentonite is not fully saturated and therefore does not entirely fill the porosity within the sand grain shielding skeleton.

As discussed in Section 3.2.1, under fully saturated conditions, particular features of the saturated 80/20 sand/bentonite are (i) bentonite particles and aggregates containing strongly bound water; (ii) inter-aggregate spaces containing weakly bound water; and (iii) macro-porosity containing free water (without bentonite aggregates). According to Lanyon et al. *planned*, gas entry into the saturated sand/bentonite occurs either into water-filled macro-porosity (controlled by the open pore size) or by consolidation/displacement of low-density bentonite aggregates. Consolidation can occur when the gas pressure is higher than the local swelling pressure plus the pore pressure. Gas entry is thus likely to preferentially occur in large pores in which the bentonite density is also low. Consolidation of the bentonite aggregates within the pore space will release water and locally increase the pore pressure in the surrounding pore volume. In addition, the swelling pressure of the compacted bentonite aggregate will increase locally. Over time, the swelling pressure plus pore pressure will equilibrate with the gas pressure and pore pressure gradients will slowly dissipate (due to the low water permeability of the sand/bentonite). The overall pore pressure increase will result in minor elastic dilation of the shielding skeleton, creating some small additional porosity for gas flow. Gas will then percolate into other connected pores via the same mechanisms of consolidation and water displacement. The gas flow path is likely to be along a tortuous network similar to that of fingering phenomena present in displacement flow of immiscible fluids in porous media. Locally, bentonite aggregates may become compacted and clog pore throats.

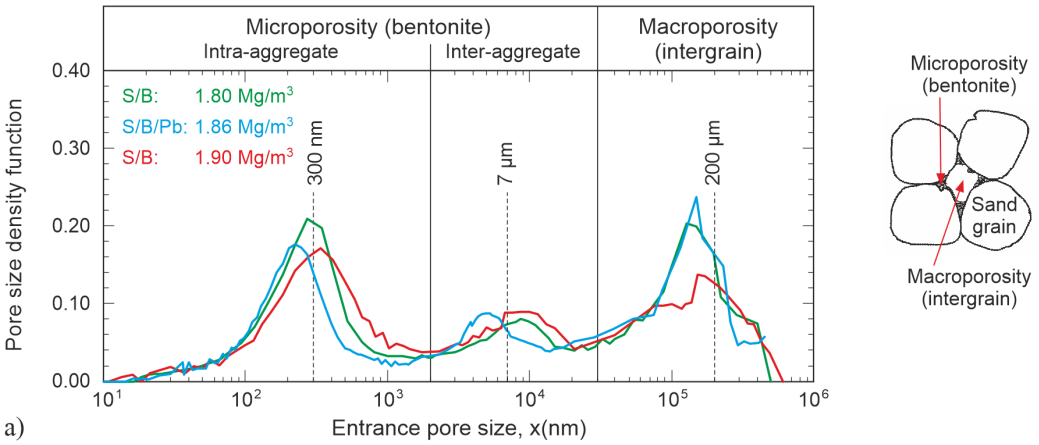

a)

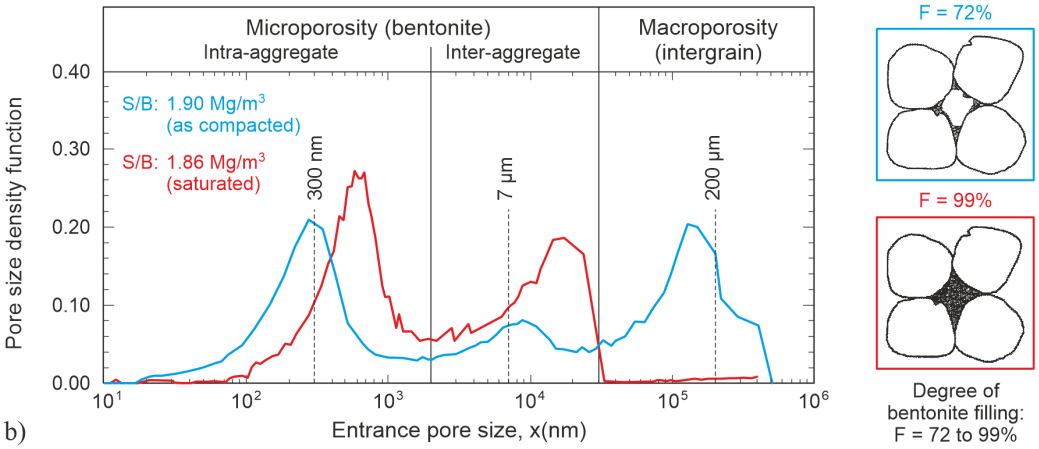

b)

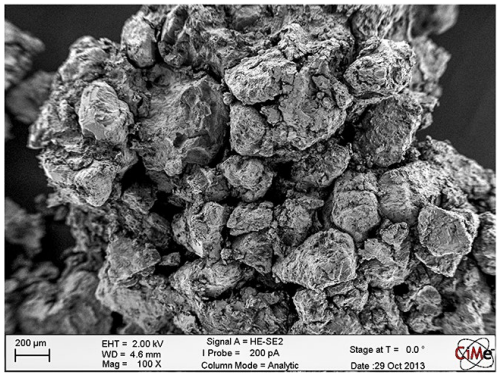

Aggregation of sand and bentonite.

c)

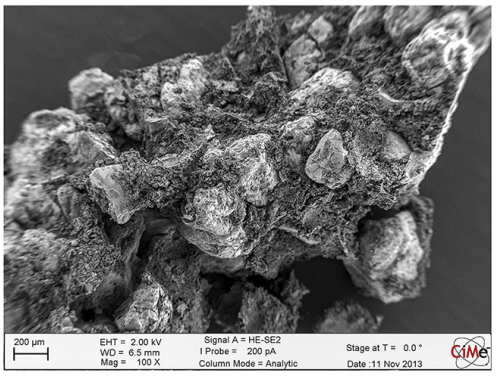

Aggregate of fully saturated 80/20 S/B bentonite.

d)

Fig. 5-3: Evolution of microstructure of sand/bentonite during wetting at nearly constant volume

(a) Pore size distribution of sand/bentonite mixtures (80/20) with various densities (Nagra 2008a). (b) Pore size distribution of a sand/bentonite mixture (80/20) with different degrees of saturation (Nagra 2008a). SEM image of 80/20 sand/bentonite as compacted (Manca 2015); SEM image of 80/20 sand/bentonite after saturation with distilled water (Manca 2016).

Pure (compacted) bentonite

Gas transport through pure (compacted) bentonite is relevant to the buffer around the SF/HLW canisters and to the sealing elements of the V1-HLW, V2-HLW and V3 seals, which are composed of compacted bentonite. Pure bentonite also exhibits a multi-modal pore-size distribution; see Section 3.2.1. This is particularly true if it has been compacted from an initially granular form. During saturation of compacted bentonites, the macro-porosity is slightly or even strongly reduced, depending on the saturation history. At the same time, micro- and meso-porosity increase slightly during hydration at the expense of the macro-pores (Romero & González-Blanco 2015). Important influencing factors are the duration of the saturation process and the stresses to which the material is subjected during saturation. A minimisation of the macro-porosity is expected when granular bentonite saturates to its maximum swelling capacity (bentonite slurry) through an unlimited supply of water and is subsequently compacted to the desired density. A bentonite sample treated with this type of procedure can be considered a bounding case for a saturation history in the evolution of a geological repository and leads to minimum water and gas permeability.

In a fully saturated and highly compacted bentonite, the porosity within the aggregates (micro- and meso-pores) may comprise 70 to 90% of the total porosity. This porosity is, however, characterised by a very high capillary strength. When the confining pressure (total pressure acting on the bentonite) is lower than the capillary strength, the porosity within aggregates is not at all accessible to gas. Sellin & Leupin (2013) indicate that no advective gas transport will take place until the applied gas pressure is equal to or above the total stress experienced by the clay. When a sufficiently high gas pressure is reached, a mechanical interaction will occur, which results in either (i) consolidation of the bentonite aggregates and water uptake by the micro- and meso-pores, with re-opening of macro-pores during gas entry, and/or (ii) formation of dilatant pathways. In the case of the former, a local increase in the swelling pressure of the bentonite develops to balance the gas pressure. As shown with oedometric tests on MX-80 samples reported in Romero & Gonzalez-Blanco (2017) and Romero & Gonzales-Blanco (2018), gas entry and the associated water uptake by the micro-pores results in expansion of the bentonite sample, whereas subsequent gas pressure decrease results in collapse of the macro-pores, disconnection of the gas pathways and compression of the sample. These experimental investigations have been additionally interpreted by numerical analyses using a double porosity approach to model the gas-accessible pathways through the macro-porosity (Senger et al. 2018).

The comprehensive experimental characterisation of the behaviour of granular bentonite (MX-80) accounting for thermo-hydromechanical processes, together with microstructural evolution, is described in detail in Seiphoori (2015) and in Romero & Gonzalez-Blanco (2017) and Romero & González-Blanco (2015). For repository modelling, work from the PEBS project (Gaus et al. 2014a, Gaus et al. 2014b) provides thermal, hydraulic and two-phase properties of the different bentonite materials.

Macroscopic fracture flow in the pure bentonite and sand-bentonite elements of a repository is not expected, since the repository is designed to avoid scenarios of rapid gas pressure build-up (Nagra 2008a).

Opalinus Clay

The Opalinus Clay is a moderately over-consolidated claystone that has been selected as the host rock for the disposal of radioactive waste in Switzerland (Nagra 2021a). The potential gas pathways through the Opalinus Clay include the microscopic pore space of the intact rock matrix and possible discrete tectonic structures (cracks, fractures, faults), as well as excavation-induced fractures in the vicinity of the backfilled underground structures. From the long-term safety point of view, gas release through the microscopic pore space is of particular significance, because this

release path always has the potential to exist, including in cases where other pathways, such as tectonic faults and the excavation damage zone (EDZ), can be considered to be gas impermeable (due to re-sealing) or when they do not exist at all. In the framework of gas-related studies for Nagra's Project "Entsorgungsnachweis" (Nagra 2002a, Nagra 2004), comprehensive databases have been compiled to describe gas transfer through Opalinus Clay phenomenologically, conceptually and quantitatively. Further studies on gas transport through Opalinus Clay were also later initiated as part of Nagra's RD&D programme. Important focal points of these investigations are the effect of spatial variability on gas propagation in the surroundings of a repository (scale dependency of the gas-related parameters) and an improved process understanding of the dependency of the transport capacity of Opalinus Clay on overburden depth (in-situ stress).

Gas transport in low-permeability formations is largely controlled by the microstructure of the rock. A balanced assessment of gas transport processes in the Opalinus Clay therefore requires careful consideration of both structure and texture. The mineralogical and structural features of the Opalinus Clay have been extensively investigated on various scales (Nagra 2008a). Petrophysical logs in investigation boreholes indicate moderate variability of clay content. Core inspection reveals a distinct anisotropy, made up of siderite concretions and silt and sandstone lenses, which are embedded in the clay-rich strata. Extensive analyses have been performed to characterise the pore space of the Opalinus Clay (adsorption/desorption isotherms, mercury porosimetry, TEM, FIB-nt); see also Nagra (2002b), Nagra (2008a), Keller et al. (2011), Keller et al., Keller et al. (2013a, 2013b). The anisotropy due to bedding is largely a result of microscopic heterogeneity, as seen in thin sections, where diagenetic cementation of the pore space has been observed in the silty and sandy layers. Scanning electron microscope (SEM) images reveal that the size of the mineralogical components (10^{-7} – 10^{-3} m) determines the microstructure of the rock. Quartz minerals may exhibit grain sizes in the range 0.01 – 1 mm, whereas the clay minerals form flake-like packages with typical sizes in the order of 100 nm – 10 μm. The pore space of the rock is thus formed by a network of micro/meso- and macro-pores, which dominate the flow and transport properties of the rock.

Water retention curves for the characterisation of viscous-capillary flow in the Opalinus Clay were determined through the desaturation and resaturation of core samples under controlled humidity (Schanz 2007, Muñoz et al. 2003, Ferrari et al. 2014, Favero et al. 2013, Nagra 2002b). In addition, the mobility of gas in the intact Opalinus Clay has been determined by water and gas testing in the laboratory and by in-situ gas injection tests in boreholes (Nagra 2002b, Marschall et al. 2005, Romero et al., Romero & Gómez 2013, Romero & González-Blanco 2015, Senger et al. 2013). Characteristic features of the Opalinus Clay based on these studies are its high capillary pressures, in the order of 10 MPa even at high water saturations > 90%, and low intrinsic permeability (Senger et al. 2014b). From a long-term safety perspective, these features result in diffusion-dominated gas transport for the range of pressure gradients expected in the vicinity of the geological repository (see also Chapter 7).

Pressure-dependent permeability approaches have been adopted to describe dilatant gas transport through the Opalinus Clay when gas pressure exceeds the threshold pressure for pathway dilation (see also Section 5.1.3). This has been successfully applied for the interpretation of gas injection tests in the HG-D experiment at Mont Terri (Marschall et al. 2013). Alternative approaches include embedded fracture models (e.g., Alonso and Olivella 2008) and fully coupled multi-phase hydromechanical models).

In the early post-closure period of the repository, the initial gas storage capacity has been shown to be sufficient to dampen the pressure build-up when high gas generation rates are expected (Nagra NTB 24-23 *in prep.*). At later times, the gas generation rates decrease and the gas transport capacity of the host rock and sealing system is sufficient to accommodate the generated gas (see also Chapter 7; Nagra NTB 24-23 *planned*). Therefore, hydro- and gas-fracs are not expected under the conditions relevant for the repository. Gas flow along macroscopic tensile fractures is expected to occur only within the EDZ of the geological repository.

5.3 Gas transfer and storage in cement-based repository materials

5.3.1 Gas storage in cement media

The storage capacity of gases in cement-based materials is connected to the porosity fraction that can be easily desaturated (Chapter 3.2). Cementitious material includes cement paste, which refers to hardened cement after it has reacted with water. If aggregates such as sand (grain size ≤ 2 mm) are added to the cement, the material is called a mortar or a grout. If, in addition, larger aggregates (grain size > 2 mm) are added to the cement, the material is called a concrete. The relationship between permeability and porosity in hardened cement pastes has been investigated in various studies, e.g., Schönlin & Hilsorf (1988), Powers et al. (1954), Nyame & Illston (1981). The porosity of such pastes ranges from 30 to 40 percent by volume (e.g. Young 1988). It includes both gel and capillary pores, which have respective diameters of about 2 nm and about 1'000 nm (Fig. 3-2). The smaller the pores, the more difficult they are to drain and the smallest may need an extreme low relative humidity before they desaturate. Mortars and concrete can also have larger air voids.

An example of how the formulation of cement-based materials can be adjusted to a certain extent to control their capacity to provide gas storage and to allow the transfer gas is the backfill mortar M1 used in the L/ILW emplacement caverns of the repository to fill the space between the inner shell tunnel support and the containers. This mortar, which is described in detail in Jacobs et al. (1994) & Martin et al. *planned* consists mainly of siliceous or alterantively calcareous aggregates with a single aggregate grain size fraction (i.e., monograin size fraction; e.g. 2/3 mm or 3.5/5.5 mm, see Martin et al. *planned*). The cement content of the mortar is so low that the cement paste, while coating the aggregates and fixing them together, preserves a large amount of pore space for gas storage - in the order of 20 vol.-% of the mortar. The pores themselves are large, up to mm in size, and thus easily drained. The intrinsic permeability of this mortar is also high – typically $> 10^{-11}$ m^2.

5.3.2 Transport of gases in partially liquid saturated cement media

Transport of gases into and across cementitious materials can take place by diffusion or by advection in either the gas phase or the liquid phase. A method that has been used to measure diffusion coefficients of gases (specifically that of oxygen) in cementitious material is described in Lawrence (1984), Buenfeld & Okundi (1998) and Villani et al. (2014). In this method, which is essentially a standard gas transport test, two reservoirs with the same gas pressures are separated by a cement core brought down to the moisture level of interrest before analysis (e.g. 65% RH at 20 °C). On one side, N_2 is circulated to provide a constant high concentration boundary condition for N_2. Similarly, O_2 is circulated on the other side to provide a high concentration boundary condition for O_2. At the same time, the circulating N_2 acts as “zero or concentration boundary condition” for O_2, and vice versa. Gas transport across the cement core is then dominated by diffusion in the gas phase at a humidity of 65% from the high concentration side to the zero-concentration side. O_2 diffusion coefficients are inferred from the O_2 concentration in nitrogen, which is measured until a steady-state is reached, as explained in Leemann et al. (2017). Measured

O_2 diffusion coefficients in pure CEM I and CEM II[9] blended with limestone powder, microsilica, portlandite and granulated blast furnace slag are in the range of 0.1 to 2.4 × 10^{-8} m^2/s (Leemann et al. 2017). This is similar to the range of 0.2 to 5.0 × 10^{-8} m^2/s measured for typical concretes, as summarised in Lea & Hewlett (2004). For carbonated samples, the diffusivity slightly decreases by a factor of about 1.37, as derived systematically in the study by Leemann et al. (2017) and Papafotiou & Senger (2016b).

Relative humidity within the partially saturated L/ILW disposal area of a repository will be rather high after repository closure. However, the cement-based construction elements will be desaturated in the early post-closure phase as a result of the ventilation during the operational period (Papafotiou & Senger 2016b). Gas diffusivity decreases as water saturation increases and, in fully saturated cement materials, gas will only be transported and stored as a solute dissolved in the liquid phase (c.f., Section 5.1.2). As described in Section 5.2.2, gas pathways form again once gas pressure increases and exceeds the capillary threshold pressure value of the material.

5.4 Potential effects of pore clogging at interfaces on gas transfer and storage

As discussed in the previous chapter, gas transfer and storage could potentially be affected by precipitation and pore clogging at interfaces between clay- and cement-based materials. There are a few recent studies (Chagneau et al. 2015, Fukatsu et al. 2017, Luraschi et al. 2020, Nakarai et al. 2021a, Nakarai et al. 2021b, Shafizadeh et al. 2015, Shafizadeh et al. 2020, Wigger et al. 2018) that deal with the changes in diffusivity caused by porosity changes at fully liquid saturated clay/cement interfaces or similar systems.

The alteration of the pore dimensions also has an impact on transport in the gas phase across such material interfaces. A few data on the changes in diffusion coefficients over evolving interfaces are presented in Fig. 4-2. There are, however, neither any experimental data on gas or water permeability for evolving fully saturated interfaces, nor any experimental data on transport parameters for evolving partially saturated interfaces. Some general considerations regarding the potential impact of clogging are, however, presented in Chapter 4. If the commonly observed clogging of pore throats with precipitates or colloids/particles is disregarded, the impact of precipitates on solute diffusion is expected to be similar to the impact of the filling of the corresponding porosity fraction with gas. Prasianakis et al. (2017) and Prasianakis et al. (2022) have investigated the influence of different modes of precipitation in fully saturated porous media with the help of nucleation theory, showing how homogeneous nucleation leads to preferential precipitation in larger pores (see Section 3.5.2 and, for further details, Bouissonnié et al. 2018, Putnis 2015, Putnis & Fernandez-Diaz 1990). Gas will also preferentially fill larger pores, reducing the aqueous phase diffusivity of the medium; see e.g., the simulations of diffusion by Tyagi et al. (2013) and Gimmi & Churakov (2019) discussed in Section 3.5.3. Thus, transport of dissolved gas and other solutes in the aqueous phase in partially clogged porous medium is qualitatively similar to solute transport in partial saturated media without clogging. In both cases, the largest pores are unavailable for the transport of solutes, since they are either precipitate-filled or gas filled. Transport of solutes (excluding gases that exchange with a gas phase) in both cases should be very similar, because the activity change of water in the porous media upon desaturation is an effect of pore size and pore surface, in which the water phase is contained (cf., Section 3.5.3). The activity change is similar for partially clogged media, if the water phase is contained in the

[9] CEM I and CEM II refers to the classification of cement material according to SN EN 197-1. CEM I contains > 95% of OPC-clinker, whereas, in CEM II, OPC clinker is reduced to 94 – 65 wt.-% and the cement blended with filler materials such as limestone powder, fly ash, granulated blast furnace slag, silicon dust, etc.

same pore size fraction. In addition, the solute composition (ionic strength) has an even larger impact on activity, but for diffusive transport the spatial activity gradient is important and not the absolute change in activity[10].

In general, transport in the gas phase near the interfaces could be hindered by the clogging of large pores. As discussed in Chapter 4, clogging of large pores would require that these are filled with water, which would only happen in the case of full saturation of the material. However, as discussed in Section 5.2.2, under saturated conditions, pure bentonite and sand/bentonite mixtures are characterised by very effective swelling of clay aggregates, which leads to collapse of the macro-pores and effectively reduces the pore space available for reactions leading to precipitation. Note that the mechanisms elaborated in Section 5.2.2 also allow the re-opening of macro-pores and entry of gas phase after full saturation. In the case of cement-based materials, clogging of large pores would result in higher capillary strength being required for gas to enter the material. However, the large pores will be the last to become water filled in the repository, which makes it unlikely that they become clogged while gas is still present.

It should also be noted that mechanical processes, related to the compaction of porous media and the formation of cracks due, e.g., to tunnel convergence, could affect gas storage and transfer. However, such processes are not the main focus of the present report.

5.5 Main messages from this chapter

Gas transfer and storage processes in clay-based materials and in cement-based materials are well understood for these materials in isolation.

For a fully saturated and highly compacted bentonite, the porosity within the aggregates may comprise 70 to 90% of the total porosity. This porosity is, however, characterised by a very high capillary strength. When the confining pressure (total pressure acting on the bentonite) is lower than the capillary strength, gas transport occurs only by diffusion of dissolved gas. If the confining pressure is exceeded, mechanical effects in the bentonite result in the formation of pathways for gas phase transport. Note that any permeability increase resulting from pathway formation at elevated gas pressures is not expected to be permanent due to the collapse and disconnection of the gas pathways once the gas pressure decreases.

The Opalinus Clay is a moderately over-consolidated claystone. Gas transport is expected to be largely controlled by the microstructure of the rock and therefore understanding gas transport in this material requires careful consideration of both structure, texture and clay mineral content and the resulting porosity distribution. The mobility of gas in the intact Opalinus Clay has been determined by water and gas testing in the laboratory and by in-situ gas injection tests in boreholes. Opalinus Clay is characterised by high capillary pressures, in the order of 10 MPa, even at high water saturations of > 90%, and very low intrinsic permeability. Therefore, from a repository perspective, these features result in gas transport being dominated by dissolution and diffusion for the range pressure gradients expected in the vicinity of the repository. Furthermore,

---

[10] Note that transport of gases in partially saturated media is dominated by transport in the gas phase and equilibrium concentrations (activity) of dissolved gases are controlled by the gas pressure, which is why the statement is based on solute transport for the partially saturated medium.

A special case that in which desaturation of a material is caused by evaporation or consumption of water by reactions (e.g., metal corrosion). This will cause a strong increase in ionic strength and might induce strong spatial activity gradients. The relationship between activity of water and solutes, pore size and pore surface properties, and how to implement those relationships in reactive transport codes, is an active area of research (see e.g., Tournassat & Steefel 2015, Tournassat & Steefel 2019). Further discussion of this topic is outside the scope of the report.

as in the case of compacted bentonite, even if dilatant pathways do form at elevated gas pressures, any permeability increase is not expected to be permanent due to the self-sealing capacity of the rock.

Sand/bentonite mixtures have a significantly lower capillary strength than either compacted bentonite or Opalinus Clay and even minor desaturation of the larger pores of the material can be sufficient to create connected pore space that is then available for gas flow, resulting in a high gas permeability. Such mixtures can also be tailored to meet the requirements of transport and storage of the gas phase. Cement-based materials also allow diffusion of dissolved gas in water-saturated conditions, and their ability to transfer gas as they desaturate can be adjusted by design (cf., Section 5.3.1).

Gas transfer and storage is less well understood where these different materials are in contact and interact, leading to precipitation and pore clogging. In general, transport in the gas phase could be most significantly hindered by the clogging of large pores, since, in the absence of clogging, the larger pores are the ones that tend to provide preferential gas pathways. In cement-based materials, clogging of larger pores would result in higher capillary strength required for gas to enter the smaller pores. In pure bentonite and sand/bentonite mixtures, the impact from clogging is expected to be less significant because of the swelling of clay aggregates that collapse the macro-pores but allow subsequent re-opening of gas pathways. Furthermore, in the context of a repository, it is the largest pores that will be the last to become water filled as the repository materials saturated, which reduces the likelihood that they become clogged while gas is still present.

Transport of dissolved gas and other solutes in the aqueous phase in a partially clogged porous medium is analogous to solute transport in partial saturated media without clogging. In both cases, the largest pores are unavailable for the transport of solutes, since they are either precipitate-filled or gas-filled. Laboratory experiments indicate that the impact of precipitation on the diffusion of neutral solutes, including dissolved gas, is not large, and leads to a reduction in the effective diffusion coefficient in the order of a factor of two.

In summary, the physical clogging of large pores by chemical precipitates requires that these pores first become water filled. If this were to occur, it could reduce the transport capacity of the medium, especially with respect to transport in the gas phase. However, as discussed further in Chapter 7, partial saturated conditions are expected to prevail, especially in the L/ILW emplacement caverns and in the repository sealing system, for the first few tens of thousands of years, which is the period during which gas is an issue. During this period, it is expected that larger pores will not become fully water saturated, meaning that clogging of these larger gas filled-pores, with its attendant reduction in gas-transport capacity, is unlikely to occur. Nonetheless, design measures can be taken to further ensure that this is the case, as discussed in the following chapter.

6 Implications for the design of repository seals

6.1 Cement-clay interfaces and their evolution

Partly because of the importance of avoiding or limiting chemical interactions that could hinder the passage of gas through the sealing system, transition layers are used as part of the seal design to separate the clay sealing elements from their adjacent concrete abutments, avoiding direct cement-clay interfaces within the seals. This design and role of the transition layers has been discussed in Section 2.2.3 and is discussed further in the later sections of this chapter. Cement or concrete are, however, in direct contact with clay at many interfaces throughout the repository, i.e., at the outer boundaries of the L/ILW emplacement caverns and of all other underground openings where cementitious rock support is employed. If chemical interactions at these interfaces lead to dissolution and precipitation, then their gas transfer characteristics and other transport properties will be affected.

The extent of the cement-clay interaction depends on the evolution of the water flow across the interfaces. As described further in Chapter 7, due to ventilation during tunnel construction and operation, the Opalinus Clay will partially desaturate. Thereafter, suction will pull water into this desaturated zone from the cementitious materials, as well as from the more saturated part of the rock. The influx of cementitious pore water to the partially saturated rock could lead to an alteration layer in the rock, near its interface with the liner. As the rock saturates, suction will decrease and there will be a phase of low water flow (see Section 6.2) from the rock towards the caverns and tunnels due to the inwardly-directly prevailing pressure gradient. As pressure increases in the L/ILW caverns and the adjacent tunnels due to gas generation, the water flow into the repository will be reduced such that near-stagnant conditions prevail.

In the long term, when gas production in the repository ceases and gas pressures drop, pore water from Opalinus Clay will flow into the tunnel backfill and L/ILW cavern backfill, as well as into any gaps at material interfaces. Above the zone of full saturation, a capillary zone with elevated water saturation will develop. However, it is unlikely that the caverns will reach full saturation within 100'000 years (see Chapter 7, Papafotiou & Senger 2016b).

Especially in the L/ILW caverns, the water phase will have an elevated pH and higher content of alkalis due to its equilibration with cementitious minerals (shotcrete, tunnel support, backfill, concrete containers, and waste conditioning cements). At the same time, the chlorine, sulphate and magnesium content of the Opalinus Clay water might cause minor additional alteration of the cementitious materials. The possible extent of reaction fronts due to the interaction of cement materials and Opalinus Clay waters under fully saturated conditions is discussed in Kosakowski & Berner (2013), Kosakowski et al. (2014).

As summarised in Sections 1.1 and 4.2, reactive transport modelling is a proven tool to predict qualitatively the evolution of interfaces between clay- and cement-based materials in terms of mineralogical changes that affect the porosity. The long-term degradation of the low-pH concrete tunnel liner around the SF/HLW emplacement drifts in contact with Opalinus Clay rock on one side and with bentonite on the other side was investigated by Bradbury et al. (2014) and by Berner et al. (2013). These authors used models that assume diffusive transport of solutes in fully liquid saturated materials and assume equilibrium chemical reactions, i.e., they do not kinetically constrain mineral precipitation and dissolution. Thus, the modelled temporal and spatial evolution of the mineralogy of materials is only controlled by diffusive transport and driven by chemical disequilibria between neighbouring clay and cement materials. Berner et al. (2013) state that, near both interfaces (bentonite-concrete liner and concrete liner-Opalinus Clay), precipitation of minerals causes a reduction in the porosity. The spatial extent of mineralogical changes in these clay materials is, however, limited to a few centimetres. The effect of porosity reduction is more pronounced and faster at the concrete liner-Opalinus Clay interface. Newer modelling studies on

short-term, low-pH cement/clay interaction that consider kinetic control of mineral dissolution and precipitation show a similar evolution (c.f., Section 4.1.3), although the spatial extent of dissolution/precipitation of clay minerals is not as pronounced as in models that use an equilibrium chemistry approach (Idiart et al. 2020, Jenni & Mäder 2021, Kosakowski et al. 2014).

Yokoyama et al. (2021) investigated the interaction of bentonite with high-pH and low-pH cement in the context of the CI-experiment at the Mont Terri rock laboratory. They observed a mm-thick alteration layer between cement and bentonite, which was generated within about the first 5 years. The alteration layer showed a very limited expansion in the following 5 years.

The limited growth of such alteration zones in the long term is supported by observations at the natural cement analogue at Maqarin, Jordan (e.g., Alexander et al. 1998, Alexander 1992, Martin et al. 2016). At Maqarin, pyrometamorphism of clay biomicrites and siliceous chalks, caused by in-situ combustion of organic matter, produced various clinker minerals, similar to some extent to those in cements used in engineering. The interaction of infiltrating groundwater with these clinker phases resulted in a portlandite-buffered hyperalkaline leachate plume. The hyperalkaline water flowed along fractures and veins. From the open fluid pathways, the solutes diffused into the adjacent biomicrite host rock and triggered the precipitation of hydrated cement minerals, such as C-S-H, ettringite, AFm, thaumasite. The alteration zones surrounding the fluid pathways were typically smaller than 4 mm and reached maximal distance of 25 mm. The limited extent of such alteration zones, even under such conditions, confirms that early porosity reduction reduces transport across the interfaces and limits the development of such alteration layers.

As discussed in Chapter 4, pore clogging at cement-clay interfaces could reduce but not eliminate the transport capacity across the interfaces (c.f., Section 4.1), especially with respect to transport in the gas phase. Nanopores will remain open (cf. Prasianakis et al. 2022), and processes exist whereby new microfractures can form.

6.2 Transition layers in an example seal design

The transition layers in the sealing system are used to physically separate clay- and cement-based materials and thus avoid or minimise chemical interactions, especially those of the type described in Chapter 5 that could lead to precipitation and pore clogging.

Kosakowski & Smith (2014) have assessed the long-term evolution of generic seals with various transition layer materials with a view to determining whether significant detrimental chemical changes could occur over a 100'000-year time frame. The focus was on mineralogical evolution and the potential for pore clogging. These authors first considered an example design (i.e., the reference design in Fig. 6-1) in which limestone gravel, represented as calcite in their models, was used to fill a 10-m long transition layer between sand/bentonite on one side and concrete on the other. The choice of limestone gravel was motivated by the fact that bentonite, cement and Opalinus Clay all contain small amounts of calcite, and are in thermodynamic equilibrium with it. This limits the availability of solutes necessary to build precipitates. In addition, limestone in the form of calcite was assumed as the aggregate used in the concrete. In the models, cementitious materials were represented as a generic concrete of average composition.

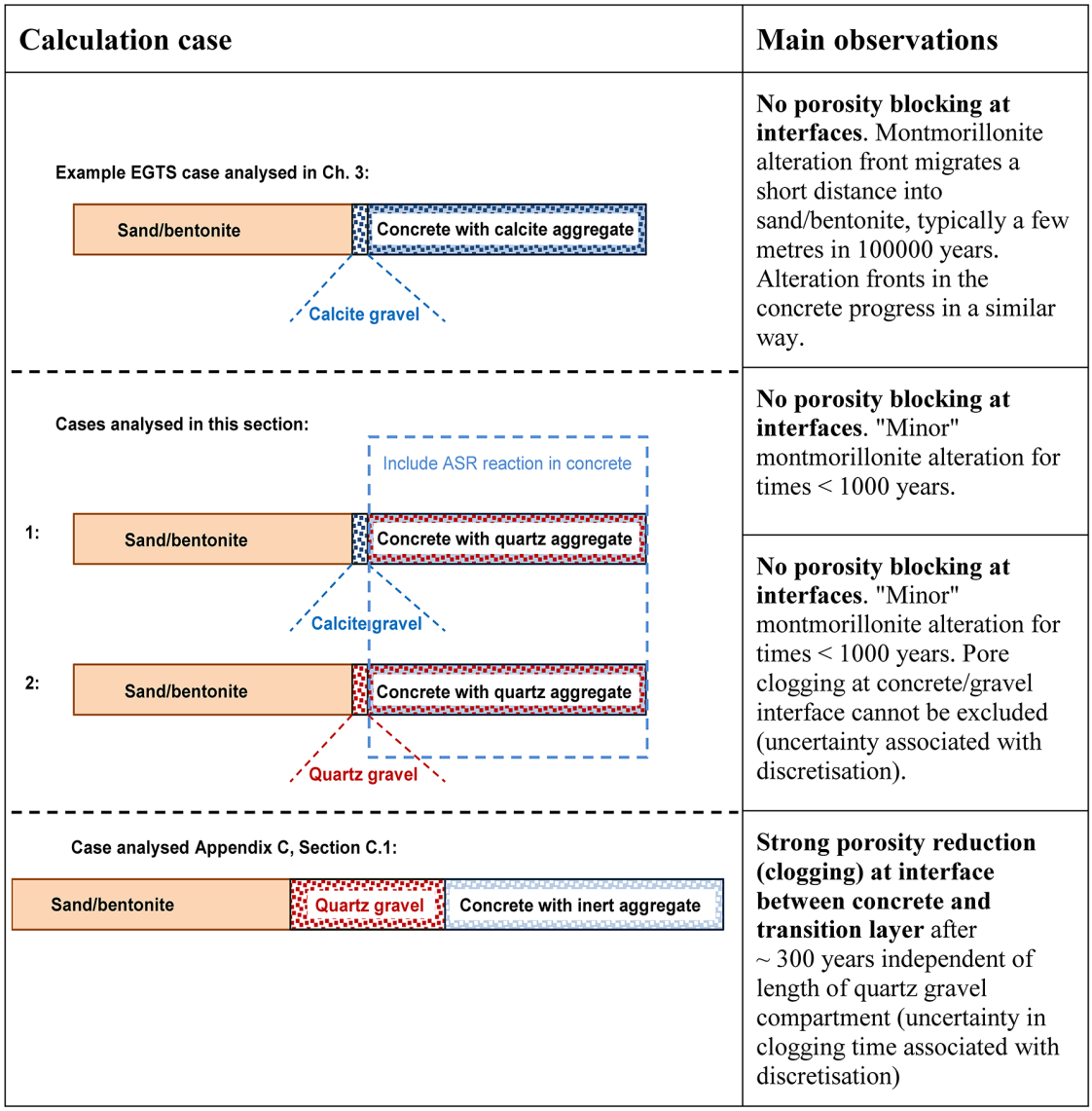

Fig. 6-1: Overview of the calculation cases analysed and comparison of main observations with other model variants included in Kosakowski & Smith (2014)

Chapters referenced in the figure refer to chapters in that report.

Even in this design, geochemical gradients between concrete and other backfill materials cannot be avoided and their impacts were analysed in 1-D and 2-D calculations. The chemical evolution of this system is governed primarily by mineral dissolution and by the diffusion of solutes across the interfaces. Fig. 6-2 summarises the main processes.

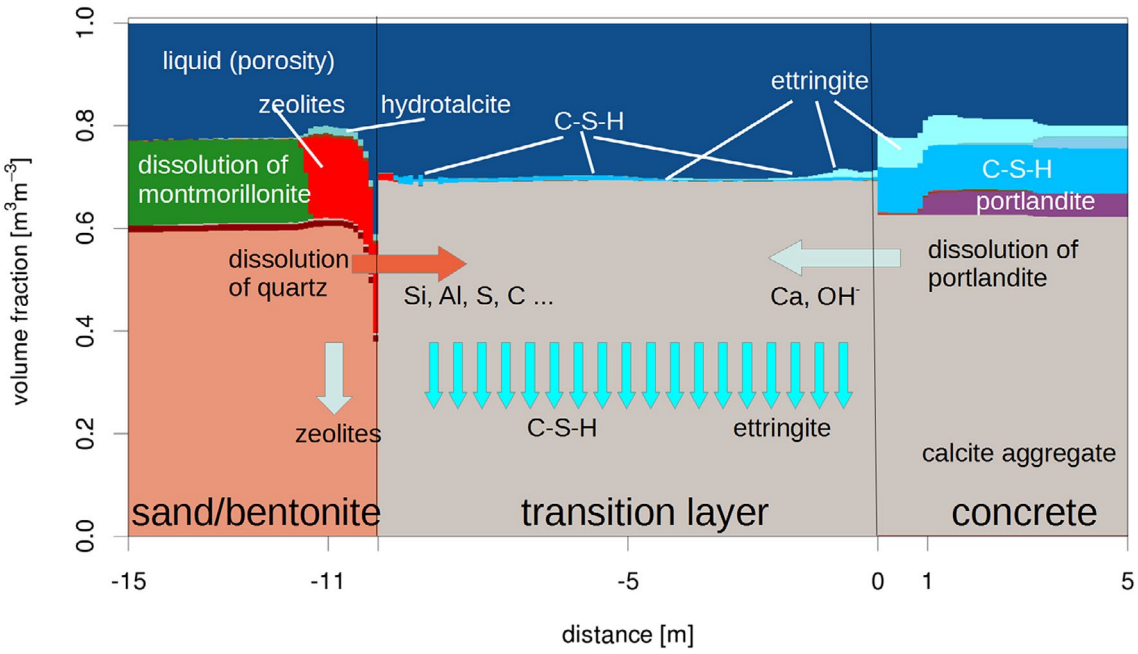

Fig. 6-2: Schematic illustration of major processes in a seal after 100'000 years of evolution, where a sand/ bentonite sealing element and concrete abutment are separated by a 10 m transition layer of calcite gravel

It is assumed that the system is fully liquid saturated

From Kosakowski & Smith (2014)

Solutes from sand/bentonite and from the concrete interact and mix within the transition layer. Several reaction fronts caused by solutes migrating from one zone into another are formed and gradually migrate. The fronts move with decreasing speed, as expected since diffusion is the rate-controlling process. Progress x with time t follows the relation $x \sim (Dt)^{1/2}$, where D is an apparent diffusion coefficient, which will vary as minerals are dissolved and precipitated.

Fig. 6-2 shows that, in the concrete, monocarbonate and portlandite progressively dissolve and some ettringite and small amounts of calcite are formed. This is triggered by the in-diffusion of SO_4^{2-} from the transition- and sand/bentonite layers saturated with host-rock pore water, resulting in a small decrease in porosity between the dissolving monocarbonate front and the dissolving portlandite front. The decrease in porosity is, however, a transient feature that migrates and does not build up over time, so there is no risk of clogging. The progress of similar dissolution fronts in the case of direct contact between clay- and cement-based materials has been evaluated in Kosakowski & Smith (2014) and shown to be typically in the order of a few meters in 100'000 years, provided porosity clogging does not occur. In calculations that include a transition layer, progress of dissolution fronts is slower, as large-scale concentration gradients between clay and cement materials are reduced.

Accessory minerals, such as montmorillonite and quartz, are quickly dissolved in the transition layer. They provide Si, which reacts with Ca from portlandite in the concrete to form C-S-H between the dissolution fronts in the transition layer and the portlandite dissolution front in the concrete. Montmorillonite and quartz are present in the transition layer in much lower quantities than portlandite in concrete. Dissolution fronts in the transition layer thus move much faster than

in concrete, which also induces a rapid displacement of the location where C-S-H precipitation occurs. C-S-H precipitation is thus not highly localised, but is distributed across the whole transition layer, reducing its impact on porosity.

Some ettringite precipitation is also observed in the transition layer near the interface with the concrete. This occurs during early stages due to the sulphate inventory in the initial pore water present in the layer. At later stages, further minor ettringite precipitation is also observed elsewhere within the transition layer.

Montmorillonite and silica in the quartz sand of the sand/bentonite are progressively dissolved due to the influence of the high-pH conditions, diffusing through the transition layer, and are replaced by phillipsite (included as a proxy mineral for the zeolite group in the model setup), along with minor amounts of hydro-magnetite and hydrotalcite. The montmorillonite contains some amount of Fe both structurally and in the inter-layer. This is taken up to form hydromagnetite, which is also initially present in the bentonite. Excess Al and Mg cause the formation of hydrotalcite. The thermodynamic model setup does not contain any magnesium silicate hydrates (M-S-H phases). There are experimental indications from the Mont Terri CI experiment that, in reality, M-S-H phases might form instead of hydrotalcite (Jenni et al. 2014, Mäder et al. 2017). Note also that the model variant does not include the additional pH buffering capacity provided by surface complexation in the sand/bentonite, as described in Berner et al. (2013).

The reference evolution shows limited changes in porosity related to the occurrence of reaction fronts. At such fronts, one mineral is typically dissolved and is replaced by another with a different molar volume. In the modelled system, such volume changes cause only relatively small porosity changes.

A high pH is maintained throughout the concrete because the system does not contain any mineral phases that can take up hydroxide ions. In order to reach the portlandite-buffered pH of about 12.5, the hydroxyl ion concentration in the concrete pore water would have to be lowered significantly by out-diffusion towards the transition layer. The increase of pH in the sand/bentonite, although sufficient to promote some montmorillonite and silica dissolution, remains moderate, since the pH is buffered by the dissolution and transformation of clay and zeolite minerals.

Calcite gravel in water at neutral pH shows a concentration of Ca similar to that of concrete (see Appendix A, Tab. A-2 in Kosakowski & Smith 2014), but the partial pressure of CO_2 is much higher. The transport of dissolved CO_2 from the gravel compartment towards the adjacent concrete could cause dissolution of calcite gravel and carbonation of concrete. This process is overridden by diffusion of OH^- from concrete towards the gravel, which causes an increase in the pH. The molar solubility of calcite decreases strongly with increasing pH and increases again above pH 11. The increase in pH to a value above 11 in the gravel compartment therefore prevents the redistribution of calcite.

Overall, the 1-D calculations for the example seal design indicate that porosity changes are relatively minor and caused either by the replacement of mineral phases with phases that have a different molar volume, or by distributed precipitation of minerals due to diffusive mixing of solutes originating from different materials. The porosity changes are far less than would be required for clogging to occur.

The example seal design, with calcite representing limestone as transition layer material and as concrete aggregate, is chosen such that neighbouring materials do not impose strong geochemical gradients across the interfaces. In particular, the pore waters of the sand/bentonite tunnel backfill (quartz, montmorillonite and small amounts of calcite) and the calcite transition layer (calcite, with minor amounts of quartz and montmorillonite) are nearly identical, each having the same pH and similar pore water compositions. Not surprisingly, there are no reaction fronts originating

from the interface between these materials. Stronger gradients exist across the interface between the calcite transition layer and the concrete backfill. In particular, concrete pore water has a much higher pH than that initially present in the transition layer and has a substantially different initial composition. C-S-H is precipitated in the transition layer. This reaction is driven by the availability of Si provided by the montmorillonite/quartz dissolution, primarily in the sand/ bentonite backfill, and Ca originating from portlandite dissolution in the concrete. C-S-H precipitation is not, however, highly localised, but distributed across the whole transition layer, reducing its impact on porosity and the possibility of clogging.

6.3 Influence of saturation evolution

An illustrative 2D model was set up in Kosakowski & Smith (2014) to test the influence of saturation on the mineralogical evolution of the sealing elements. It consists of a simplified cross-section through concrete and sand/bentonite, separated by a calcite gravel transition layer. It considers full saturation at the bottom of the model and a partially saturated layer above. The model addresses a hypothetical scenario in which 30 kg of water flows per year in a tunnel with a cross-section area of 20.5 m^2 through the transition layer from the bentonite/sand region to the cavern filled with cement-based backfill. Although water flow was found to be effectively restricted to the lower, fully saturated parts of the model, the flow rate was low enough that diffusive transport strongly influenced the evolution of the system. Note that the simulation results for the repository cavern models of Senger & Ewing (2009) and Papafotiou & Senger (2016a) provide no indication that such amounts of water will flow through the sealing system towards the emplacement caverns (c.f., Chapter 7). The model implemented an extreme and purely hypothetical case, and aimed only at demonstrating the effects of long-term advective and diffusive transport in a partially saturated setup for up to 100'000 years.

The findings were essentially that chemical interactions in the saturated material at the bottom of the modelled system occur in a similar manner to the fully saturated 1-D calculations described in Section 6.4. In particular, the calculated mineralogical and porosity changes are similar in both model approaches, as illustrated in Fig. 6-3. Concrete degradation advanced more rapidly in the 2-D model, as inflow of water caused much higher fluxes of S and Mg into the concrete. However, the 2-D model demonstrates that the extent and magnitude of mineralogical and porosity changes at material interfaces strongly depends on the effect of saturation on diffusive and advective transport. Thus, changes towards the de-saturated top of the modelled system are much more limited than towards the fully liquid saturated bottom.

Even though the model used to generate the results shown in Fig. 6-3 represent a rather hypothetical case, it is nonetheless consistent with the expectation that full saturation of the transition layer in the L/ILW sealing elements with the fluxes provided from the Opalinus Clay (see Chapter 7) will not occur within the period of 100'000 years.

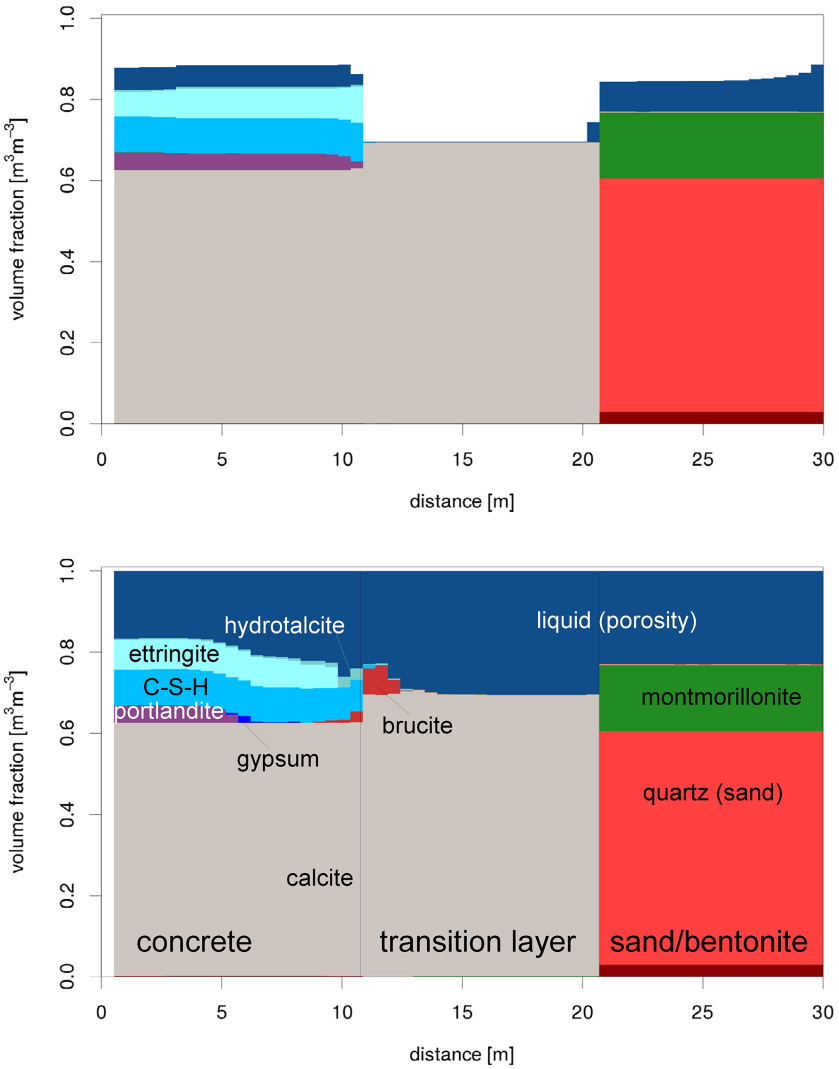

Fig. 6-3: Mineralogical profiles along the top (upper picture) and the bottom (lower picture) of the 2-D model domain after 100'000 years

Compared with the 1-D diffusion only model results in Fig. 6-2, the reaction fronts in concrete and transition layer show a longer lateral extension due to the advective transport towards the concrete.

From Kosakowski & Smith (2014)

The degree of saturation of a porous material is controlled by capillary suction, which is in turn controlled by the pore size distribution of the material. According to Jurin's law, capillary forces are small for loose materials, such as the calcium carbonate sand or aggregate provisionally envisaged for the transition layers, which have pore sizes in the hundred µm to mm-range. This means that water rise will be in the range of decimetres to centimetres (c.f., Fig. 6-4) and hence not far above the fully saturated water level. This has the following implications on reactions at interfaces, formation of biofilms, colloid transport and gas transport pathways:

- Chemical interactions occur only where a connected water phase is present. As a result, chemical reactions within, and adjacent to, the transition layers will be restricted by the limited saturation of the materials.

- Microbial activity will be limited to the highly water saturated regions in the lower parts of the partially saturated transition layers.
- Transport and sedimentation of dispersed particles (colloids) within the transition layers, which could lead to the physical blockage of the pores, will also be limited to the highly water saturated, lower parts of the transition layers.

From this, it can be concluded that pores in the upper parts of the transition layers will not be blocked by physical precipitates, colloid particles or biofilms, as long the transition layers are not fully saturated with water. Water will rise further within the sealing elements themselves, due to the smaller pore sizes, but processes with the potential to clog pores will be confined to the lower parts of the sealing elements that are in direct contact with the fully saturated parts of the transition layers. In the upper sections of the partial saturated sealing elements, the capacity for gas transport pathways will always be maintained.

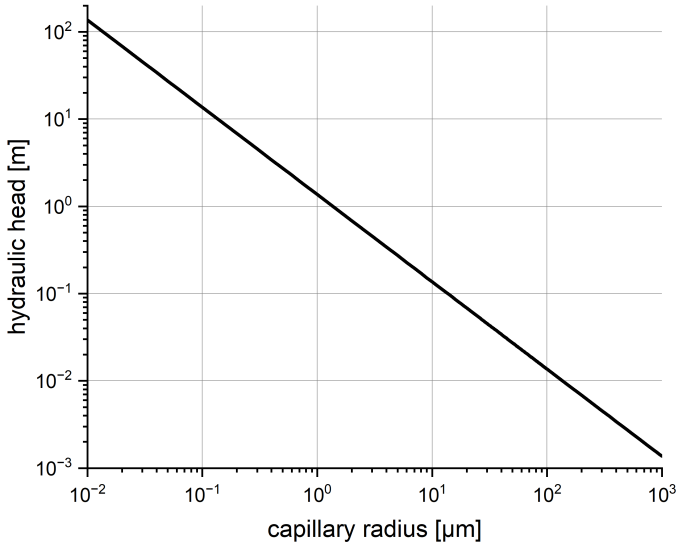

Fig. 6-4: Capillary head for water as wetting fluid and dry air as nonwetting fluid at 20 °C as a function of capillary radius according to Jurin's law

Calculated by the equation presented in Rodríguez-Valverde & Tirado Miranda (2011)

6.4 Design variants and implications

1-D calculations reported in Chapter 3 of Kosakowski & Smith (2014) show that the choice of aggregate in concrete might strongly influence the evolution of the seals. A concrete aggregate composed of quartz would be in thermodynamic disequilibrium with the initial cement minerals. The subsequent equilibration of the cement phases with quartz and other alumino-silicate aggregates would be kinetically controlled. Reaction rates depend on the type of mineral; they increase with increasing pH and are larger for smaller aggregate grains due to their higher specific surface area. The modelling indicates that these cement-aggregate reactions are complete after a few thousand years (Kosakowski et al. 2020). After cement phases are equilibrated with quartz aggregate, the pH drops to values close to 10. In addition, the pH in the transition layer and in concrete will equilibrate and differences in the solubility of SiO_2 will diminish. At this stage, the

geochemical difference between concrete and materials in the transition layer will be small and the long-term evolution of the system is then governed by the transport of solutes from the sand/bentonite into the concrete.

The long-term evolution of the reference sealing element in Chapter 3 of Kosakowski & Smith (2014) (i.e., the example seal design in Section 2.2 of the present report) was characterised by dissolution/precipitation fronts that slowly migrated into sand/bentonite and into the concrete. These reactions are driven by the strong geochemical differences between sand/bentonite and (non-degraded) concrete. Model variants with reactive aggregates show much less pronounced effects, as the geochemical gradients between sand/bentonite and concrete are lowered due to aggregate-cement reactions in concrete (Fig. 6-1). Replacement of montmorillonite by zeolites in sand/bentonite is only visible at early times (< 1'000 years), i.e., when the pH is still high. Development of long-term dissolution fronts affecting the main constituents of sand/bentonite or concrete are not observed in cases 1 and 2 in Fig. 6-1.

No strong reduction of porosity at the interface between the concrete and the transition layer was observed in cases 1 and 2, where the aggregate-cement reaction occurs in the bulk of the concrete due to the interplay between pozzolanic and distributed precipitation of C-S-H in the transition layer. Especially for case 2, with quartz gravel as transition layer material, accumulation of C-S-H in a very fine layer near the transition layer/concrete interface at early simulation times cannot be ruled out by modelling studies. However, for real media with large pores (e.g., media composed of gravel or stones) it seems questionable if precipitation zones which are much smaller than an average pore size can completely clog the pore space and reduce gas and liquid transport significantly.

As discussed in Kosakowski et al. (2020) and in Section 6.3 of the present report, aggregate cement reactions causing concrete to degrade are limited by the availability of water under strongly de-saturated conditions. Even under saturated conditions, aggregate cement reactions are kinetically controlled, strongly depend on aggregate size (reactive surface area) and probably need thousands to tens of thousands of years to reach thermodynamic equilibrium (Kosakowski et al. 2020).

6.5 Main messages from this chapter

Chemical reactions within the sealing system that could lead to mineral precipitation and to the clogging of larger pores need to be minimised or avoided, as they could detrimentally affect the capacity of the sealing system for gas transfer and storage. It has been shown in this chapter, using qualitative reasoning and quantitative illustrative analyses, that, for an appropriately chosen design, significant pore clogging is not expected to occur, even if the system is pessimistically assumed to be fully saturated at all times. The expected evolution is that much of the sealing system will remain only partially saturated for a substantial period of time (c.f. Chapter 7), reducing the possibility of pore clogging still further. This is because, in the parts of a seal that remain mostly unsaturated, transport in the liquid phase will be very small and this restricts further mineral reactions that cause porosity changes. In addition, with an appropriately chosen design, chemical changes that induce the formation of colloids, which could become mobilised and also lead to the physical blockage of pores and pore throats, are also to be minimised or avoided.

The design measures focus on avoiding, or limiting the use of, materials that can chemically interact strongly and on avoiding direct contact between potentially interacting materials by providing physical separation between them. Specific possible design measures for the seals include:

- use of low pH cement (OPC blended with pozzolanic material) for the construction of the abutments adjacent to the sealing sections, which lowers, but does not entirely avoid, the potential for chemical reactions (c.f., Section 6.1)

- separating these cement-based abutments from the sealing sections (sand-bentonite mixture, bentonite) by transition layers consisting of suitable material that is initially highly unsaturated, which slows the transport of reactive species and particles/colloids migrating from the abutments and/or sealing sections (c.f. Sections 6.2 – 6-4)

The most favourable design options for the seals are those that minimise chemical gradients across the transition layer, through the choice of transition layer material and length. Materials that are in thermodynamic disequilibrium should be physically separated by a transition layer in order to avoid any detrimental porosity changes associated with ion transport and precipitation. In particular, the choice of limestone (with calcite as the key component) as a filling material for the transition layer is an attractive option, since bentonite, cement and Opalinus Clay all contain this mineral, and are in thermodynamic equilibrium with it. With this option, the precipitation of C-S-H minerals at the interface between the transition layer and concrete, and the potential for pore clogging, are much reduced.

The chemical reactions that do occur with these design options could still lead to a degree of pore clogging, but, as long as the upper parts of the seals remain unsaturated, which is favoured by the weak capillary suction forces within the coarse-grained transition layer material, this will not greatly inhibit the transport of gas across the seals.

The analyses also show that progress of dissolution fronts in concrete and in clay-based materials, separated by a transition layer, depends on the length of the transition layer, but porosity changes remain small across the range of transition layer lengths considered within the modelled time period. The design of the transition layers still needs to be optimised. Guiding principles are that:

- the axial length of the transition layers needs to be optimised, with larger lengths being favourable with respect to reducing the chemical/diffusion gradients driving the migration of reactants and thus minimising the potential for pore clogging
- the pore sizes within the layers should be such that suction by capillary forces is minimised, thus delaying saturation (and the transport of reactants), minimising the potential for pore clogging and favouring the transport and storage of gas

A low capillary rise within the transition layer has the following implications:

- Chemical interactions occur only where a connected water phase is present. As a result, chemical reactions within, and adjacent to, the transition layers will be restricted by the limited saturation of the materials.
- Microbial activity will be limited to the highly water saturated regions in the lower part of the partially saturated transition layers.
- Transport and sedimentation of dispersed particles (colloids) within the transition layers, which could lead to the physical blockage of the pores, will also be limited to the highly water saturated, lower regions of the transition layers.

A low capillary rise thus contributes in various ways to maintaining a continuous gas pathway in the upper part of the transition layers.

It should be noted that the discussions of interface and material evolution in this chapter are based on rather generic cement and clay materials, as the exact material specifications will be available only in later phases of the repository project. It is likely, however, that the general findings are largely valid, at least in a qualitative sense, for a range of detailed material options.

In summary, design measures are available to reduce the potential for pore clogging within and around the seals for as long as a gas phase is present and the seals are not fully saturated. During this period, the seals will allow the passage of gas and, as discussed further in the following chapter, minimise the danger of development of potentially damaging gas pressures.

7 Implications for the fate of repository-generated gas

This chapter presents quantitative analyses that test whether the sealing system described in Chapter 2 is likely to perform its role of providing for gas transport and storage adequately, and thus preventing the build-up of potentially detrimental gas pressures in the disposal areas (cf. Rodríguez-Valverde & Tirado Miranda 2011, Nagra NTB 24-23 *planned*). The multiple coupled processes that control the fate of gas in the repository are illustrated in Fig. 7-1.

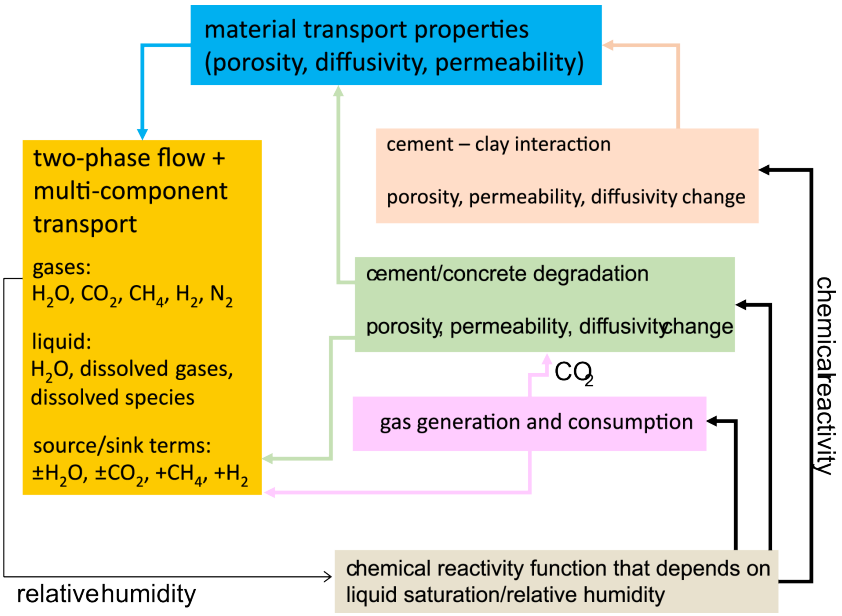

Fig. 7-1: Simplified coupled processes that control the fate of gas in a combined repository

The analyses are based largely on an equivalent porous medium conceptual model for the transport of fluids in gaseous and liquid phases, which is in turn based on the classical mixing theory of the continuum mechanics of fluids (e.g. Coussy 2004). In this concept, the three phases (solid, wetting fluid, non-wetting fluid) are assumed to be simultaneously present at any given location within the porous medium. Basic physical principles, such as mass and momentum balance and the laws of thermodynamics, apply to each phase and for all types of energy transformation in the system. The phases are described in terms of continuous density functions, implying that a representative elementary volume exists that is relevant at the macroscopic scale for all the physical phenomena involved in the intended application.

7.1 Evolution during pre-closure period: impact of excavation, ventilation and cooling

Even prior to the emplacement of waste, processes may occur that affect the later performance of the repository, including the rate of repository gas generation. The excavation and ventilation of the open tunnels will result in the gradual de-saturation and de-pressurisation of the surrounding rock (Leupin et al. 2016a), resulting in the creation of desiccation cracks in the unlined tunnel sections. Precipitation of salts may occur in these cracks due to evaporation of pore water and also increase the salinity of the pore fluid, as was observed in the ventilation (VE) experiment at Mt. Terri (Mayor et al. 2007).

The atmospheric CO_2, which will be present due to ventilation, will cause carbonation of cement-based materials, such as example tunnel support. Carbonation depths will be small, in the order of millimetres to a few centimetres after 50 years according to Trotignon et al. (2011). As a result of the carbonation process, a significant change in pore size distribution of the cement-based surface layer can occur. Typically, the distribution is shifted towards larger pore diameters (see e.g., Auroy et al. 2018), due to the transformation of C-S-H and other cement minerals to carbonates. In the carbonated part of the cement, the nano- (C-S-H inter-layer) and meso-pores ('gel porosity') connected to C-S-H are absent and capillary pores are generated which will change two-phase flow parameters (notably the relationship between capillary pressure and saturation). This may affect the corrosion passivation of the steel reinforcement within the concrete exposed to carbonation if the amount of cement overlying the rebars is too thin.

The cement-based tunnel support may also become partially desaturated at the surface as a result of the ventilation and capillary suction from the de-saturated rock. In addition, some water loss from the shotcrete grout to the in-situ concrete elements and the EDZ is expected. These processes may result in the partial desaturation of the shotcrete on the tunnel wall, potentially resulting in a concrete that is sensitive to carbonation due to the generated micro-cracks.

7.2 Post-closure evolution, saturation and the fate of gas

At the time of repository closure, the underground structures and the immediately surrounding rock will be only partly saturated.

Fig. 7-2 summarises the expected evolution of the L/ILW emplacement caverns. Gas and water re-distribution in the system is controlled by chemical- and transport source/sink terms for gas and water, as well as by capillary, buoyancy, and viscous forces acting in the different materials. As will be discussed in Section 7.3, gas is mainly produced by (bio-)chemical reactions (degradation of organic wastes and metal corrosion). It is then distributed in emplacement caverns and other underground openings and will enter the Opalinus Clay rock, where it will be dissolved in pore water and diffuse away from the repository. A small part of the hydrogen gas will be consumed by microbial reactions in the tunnel system.

As described in the previous chapters, gas and water transport, as well as kinetic and equilibrium chemical reactions that change porosity in concrete and clay media, are influenced by liquid saturation. In addition, gas source terms are heavily influenced by liquid-saturation-dependent degradation of cement materials used for waste conditioning (Huang et al. 2021). Most chemical reactions consume significant amounts of water and might cause significant change in liquid saturation in a locally closed system (waste packages).

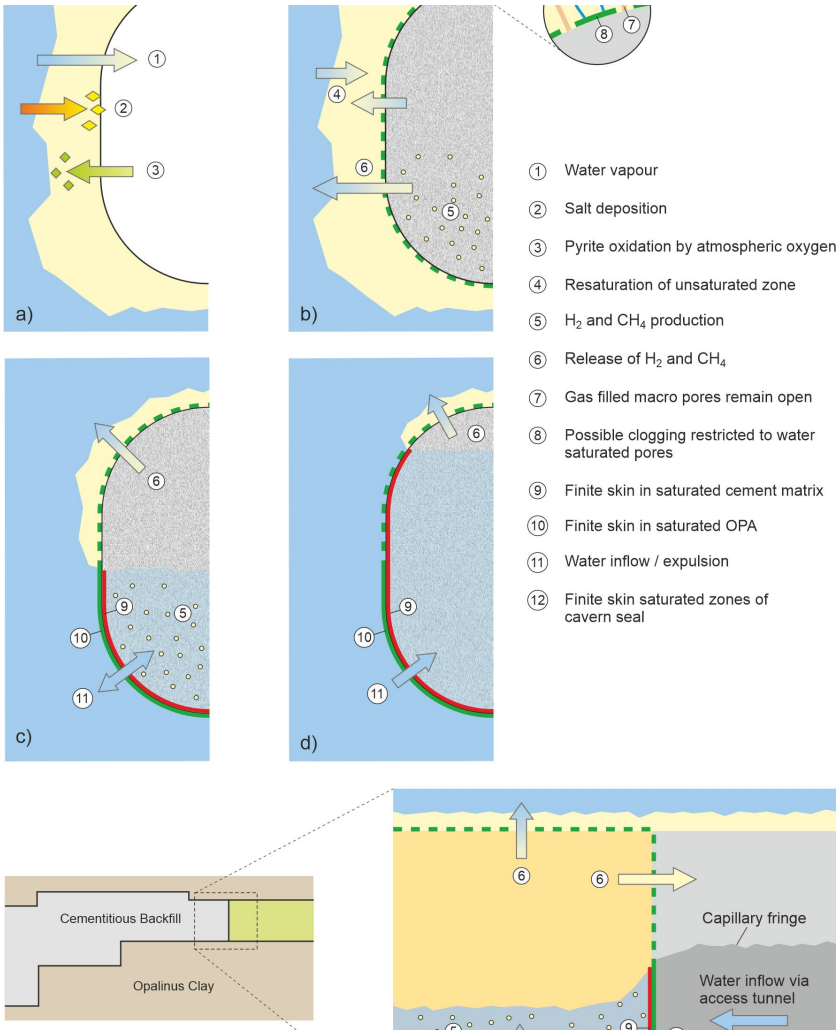

Fig. 7-2: Schematic illustration of the evolution of an L/ILW emplacement cavern and its immediate surroundings during the operational phase and after closure

a) Development of an unsaturated zone during the operational phase. b) – d) mass transfer processes at early time, mid time and late time after closure. e) mass transfer processes around the V1-L/ILW seal after closure

From Nagra (2008a)

Extensive modelling has been carried out at different spatial scales to elucidate the saturation of the repository and the fate of repository-generated gas, including:

- repository-scale assessments for semi-generic, separate HLW and L/ILW repositories, with sections of the repository represented as homogenised materials (seals, caverns, etc.)
- component-scale assessments, with more detailed representations of individual sections of the repository
- repository-scale assessments for a combined repository, using site-specific repository configurations and geoscientific data

Numerous variant cases have been analysed in the repository-scale assessments of both separate repositories and the combined repository, using different assumed seal permeabilities, including cases of malfunctioning seals and seals with very low permeability (which could be taken to represent the consequences of pore clogging), see e.g., Papafotiou & Senger (2016b), Papafotiou & Senger (2016a), Senger & Ewing (2009).

The description of post-closure evolution in the following sections is based largely on the findings of these modelling studies, which are themselves based on the modelling assumptions detailed in Nagra (2008a). Model abstractions are further summarised in Nagra NTB 24-22 *planned*.

7.2.1 Re-saturation of the near-field rock

Following backfilling of the underground openings, partially saturated regions of the near-field rock will slowly re-saturate due to flow from the rock and pore pressures will equilibrate. Re-saturation of the near-field rock will be driven by movement of water from the undisturbed host rock, which is controlled by the host rock permeability, capillary forces and pore compressibility. Re-saturation of the EDZ will be associated with swelling and self-sealing of EDZ features (Lanyon & Senger 2011, Lanyon 2019, Alcolea et al. 2014). At the same time, the EDZ may develop further, as ongoing failure is driven by pore pressure recovery/equilibration with increasing pore pressure and possible ongoing compaction and crack growth.

7.2.2 Saturation of the V3 seals

The V3 seals will be placed in the access shafts up to the top of the Opalinus Clay to seal the repository from the surface environment. These seals are expected to saturate relatively rapidly, within a few hundred years (Fig. 7-3), due to the high suction of their compacted bentonite sealing elements and the availability of water from more permeable rock formations above the repository, which will flow down the shafts and into the seals. Once saturated, the V3 sealing elements are designed to have a very low permeability to both water and gas (permeability to water of 10^{-19} to 10^{-18} m^2; see Tab. 2-1). This will largely prevent further water flow down the shafts into the unsaturated underground structures of the repository. It will also largely prevent the migration of repository-generated gas from the underground structures of the repository towards the surface environment. This is relevant to radiological safety, as repository-generated gas may convey gaseous and volatile radioactive species, such as ^{14}C in the form of methane.

Because the saturated seal is, in any case, designed to have very low permeability, pore clogging of the V3 seal at the interface between the sealing element and the over-lying concrete abutment (App. A, Fig. A-4), if it were to occur, would have no impact on post-closure evolution that would be detrimental to repository performance and safety.

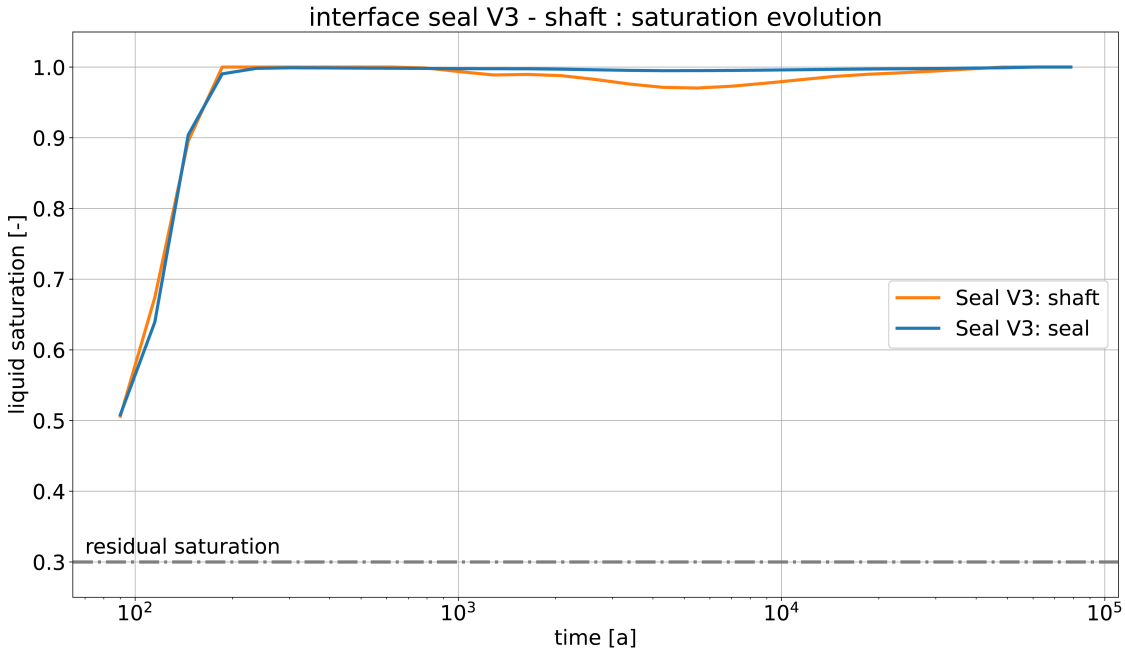

Fig. 7-3: Temporal evolution of liquid fluxes across the seal (top) and liquid saturation (bottom) for seal V3 and upper shaft backfill material

From base case model in Papafotiou & Senger (2016b)

7.2.3 Saturation of the V1-HLW and V2-HLW seals and SF/HLW emplacement drifts

The sealing elements of the V1-HLW and V2-HLW seals are also composed of compacted bentonite (see App. A.1). Due mainly to the significant initial water content and high capillary pressure (suction) exerted by this partially saturated material, in combination with the small tunnel diameter, the V1-HLW sealing elements will also saturate relatively quickly after emplacement. The V2-HLW sealing elements may take somewhat longer to re-saturate because of their larger diameters. In both cases, the rate of the re-saturation process will be mostly limited by the low permeability of the rock.

In a similar fashion, the bentonite buffer surrounding the SF/HLW canisters is expected to become fully saturated with pore water a couple of hundred years after emplacement, when the effects of heat from the SF/HLW waste forms on buffer temperature have decreased. Gas generated by corrosion of the SF/HLW canisters will initially dissolve in the pore water of the saturated bentonite buffer surrounding the canisters. Prior to breaching of the steel canisters, gas generated by steel corrosion will result in small gas saturations next to the canister (ca. 1 – 2%) that, depending on the near-field conditions, may dissolve entirely in the pore water of the bentonite (Senger et al. 2014a). After canister breaching (expected at least several thousands of years after emplacement), gas generation increases due to corrosion of the internal surfaces of the canister, resulting in a slight increase of gas saturation in the bentonite. In general, gas saturations in the bentonite buffer are expected to remain low throughout the post-closure phase of the repository due to the high capillary suction of the material (e.g., Senger et al. 2013, Senger et al. 2014a). Combined with the low permeability of the bentonite, this will lead to gas release from the drifts taking place predominantly through dissolution and diffusion in the Opalinus Clay pore water (see Sections 4.1.3 and 5.2.1). A concrete liner will be present between the bentonite buffer and

Opalinus Clay. As summarised in Chapter 4, cement/clay interaction might clog part of the pore space, although nanopores are not expected to be filled with precipitates. Furthermore, tunnel convergence and the resulting fracturing after degradation and mechanical failure of the liner might result in the opening up of new gas and solute transport paths. Transport of charged species in regions affected by cement/clay interaction will be affected by anion-exclusion. Transport of dissolved gas will still be possible, although at reduced rates (Prasianakis et al. 2022). Although some gas may be transported along the emplacement drifts and surrounding EDZ towards the seals, the V1 and V2 seals in the HLW disposal area are essentially not required to provide gas transport capacity. As a consequence, pore clogging of these seals is not relevant to the gas issue.

7.2.4 Saturation of the L/ILW disposal section and the remainder of the repository

Most of the gas generation within the repository occurs within the L/ILW emplacement caverns. To provide greater gas permeability and a lower capillary strength (see Tab. 2-1), and hence to favour gas transport and storage, the V1-L/ILW and V2-L/ILW sealing elements are composed of a sand/bentonite mixture. The design goal is to achieve gas pressure equilibration between emplacement caverns and the sealing system of the L/ILW disposal section[11], limiting the maximum gas pressures that will be reached. This means that, even when largely saturated, the seals should allow the passage of repository-generated gas. This requires that significant pore clogging must be avoided; as described in Chapter 6, design measures are available that are expected to limit pore clogging within and around the seals and pore clogging is, in any case, not expected in those parts of the seals that remain unsaturated.

L/ILW caverns

In the early phase of the evolution of the repository, i.e., after waste emplacement and the sealing of the L/ILW caverns and prior to repository closure, water from the host rock will start moving towards the caverns due to the hydraulic pressure gradient. At the same time, pore water that was present in the near-field materials at emplacement will start to re-distribute due to their different capillary suctions (i.e., shotcrete, concrete of inner-shell tunnel support, backfill-mortar, concrete of the disposal containers). The partially saturated adjacent rock will begin to re-saturate (Fig. 7-4). As the saturation of this rock increases, some water from the rock will move into the caverns and accumulate under gravity, particularly in the lower part above the cavern floor between the shotcrete and clay (Fig. 7-2c). Accumulation of water in the lower parts of the caverns may impact the evolution of underlying EDZ, which will re-saturate and thus seal faster than other parts of the EDZ (Fig. 7-2c).

By the time of repository closure (i.e., tens of years after L/ILW emplacement in the caverns), it is expected that the L/ILW emplacement caverns will have a high relative humidity, whereas the availability of free water will depend on the chosen emplacement saturation of the cavern materials. The gases present will be a mix of trapped air and repository-generated gases. Anaerobic conditions will develop quickly during this phase, due to the consumption of O_2 in the trapped air by aerobic corrosion, oxygen sorption on clay materials and other processes.

Gas generated by the anaerobic corrosion and degradation of materials in the L/ILW caverns will first dissolve in pore water and then, once the solubility limit is reached, form an additional gas phase. Pressure in the cavern will begin to increase due to gas accumulation and, temporarily,

[11] A disposal section is taken to include the main disposal area for a waste type and also the pilot facility for the same waste type.

pore water inflow from the surrounding rock will decrease or cease altogether. Model calculations indicate that the net water flow between the cavern and the surrounding rock in the early post-closure phase is very low (i.e., below 1 dl/m^2/a based on repository scale simulations from Papafotiou & Senger 2016a).

Water exchange between the caverns and the surrounding rock during this period may take place in both directions, depending on the interplay of capillary, viscous, and gravity forces at different elevations of the cavern wall. At later times during the post-closure phase (ca. 1'000 to 10'000 years), the increase of gas pressure in the cavern will result in water expulsion into the surrounding rock. Thereafter, in the late post-closure phase (after ca. 40'000 years) when gas pressures decrease and the rock becomes fully re-saturated, the flow direction will once again reverse and it will be directed from the surrounding rock into the cavern. However, water fluxes during this long re-saturation phase remain low (i.e., below 0.1 dl/m^2/a based on Papafotiou & Senger 2016a). Water accumulation in the caverns will happen very slowly after 40'000 years and will be confined to the bottom parts of the caverns, while highly de-saturated conditions, with pore space occupied by remaining waste-generated gas, will persist in the upper parts for several tens of thousands to hundreds of thousands of years (Fig. 7-4).

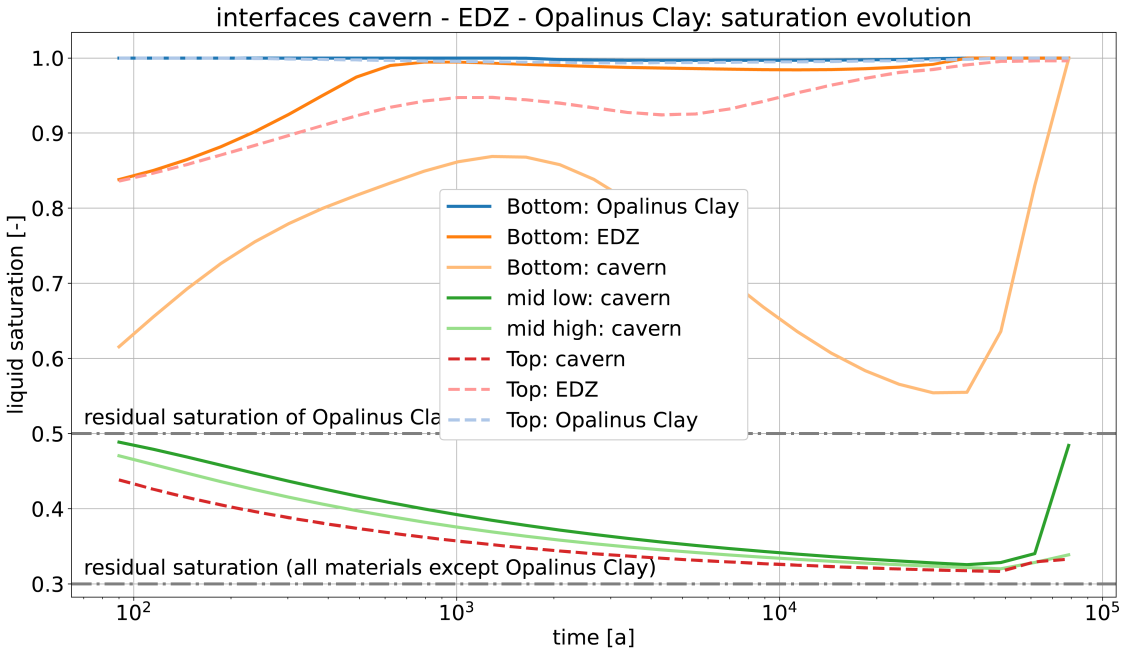

Fig. 7-4: Temporal evolution of liquid saturation of an L/ILW cavern and neighbouring materials

Extracted from base case model in Papafotiou & Senger (2016a)

The saturation evolution of the V1-L/ILW seal is tied to that of the emplacement cavern. During the early post-closure phase, water will be displaced from the cavern into the V1-L/ILW seal, due to the pressure build-up in the cavern. The direction of water transport between the cavern and the V1-L/ILW seal will change over time depending on the pressure gradients (i.e., when gas pressures dissipate in the repository). More details on the saturation evolution of the V1-L/ILW seal are given in the following.

V1-L/ILW seals and VF1 backfill

In a similar way to the emplacement caverns, pore water initially present in the V1-L/ILW seals will begin to re-distribute within the seals through the interaction of capillary and buoyancy forces (Fig. 7-5), while some water mass will be drawn into the surrounding unsaturated EDZ (Fig. 7-6). The gradual increase of gas and liquid pressures in the L/ILW emplacement caverns will result in water expulsion from the caverns into the V1-L/ILW seals (and subsequently into the VF1 backfill). Saturation in the lower part of the less permeable sealing elements will increase slightly until pressure in the L/ILW emplacement caverns exceeds hydrostatic (corresponding to the peak liquid saturation in Fig. 7-5, at cavern top, ca. 2'000 years) and water displacement to the surrounding rock increases. The upper part will remain unsaturated for several tens of thousands of years, forming the predominant pathway for gas release from the L/ILW caverns to the VF1 backfill (Fig. 7-5). The transport of gas through the upper part of the seal above the capillary fringe will sustain a continuous gas pathway for as long as gas phase is supplied by the emplacement caverns across the seal to the backfill VF1.

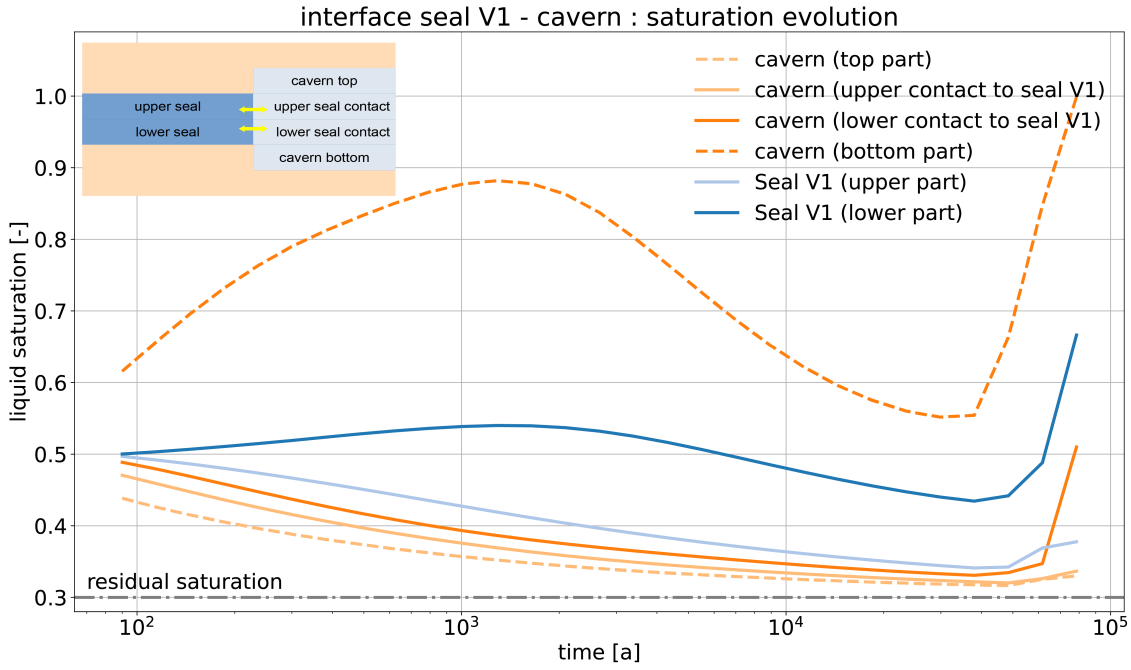

Fig. 7-5: Temporal evolution of liquid saturation for a V1-L/ILW seal and adjacent cavern

Extracted from base case model in (Papafotiou & Senger 2016a)

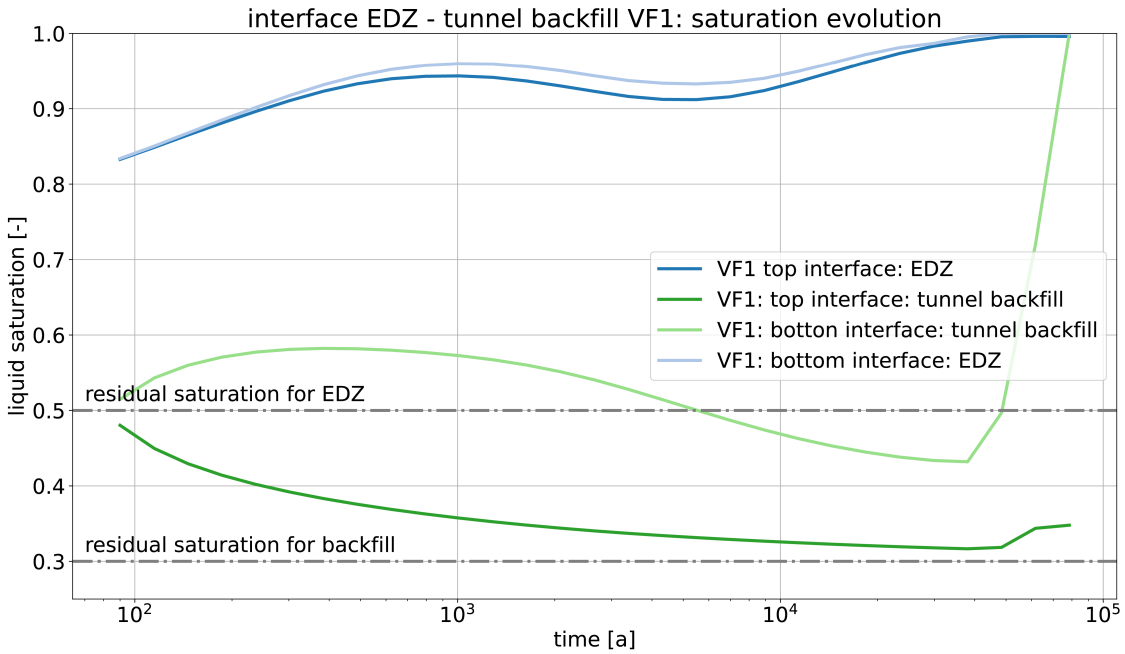

Fig. 7-6: Temporal evolution of liquid saturation at the top and bottom interface between tunnel backfill/EDZ halfway between the V1-L/ILW seals and the V2 seals

Extracted from base case model in (Papafotiou & Senger 2016a)

In the late post-closure phase (> 50'000 years), gas generation in the L/ILW caverns will decrease significantly and the V1-L/ILW seals and the lower part of the VF1 backfill will begin to saturate with pore water from the surrounding rock. However, the volume for gas storage will still be maintained in the upper part of the caverns and the VF1 backfill for a period > 100'000 years, as shown in Figs. 7-5 and 7-6 (data from Papafotiou & Senger 2016b). The VF1 backfill next to the V1-HLW seals will re-saturate earlier, as the V1-HLW seals are not required to provide gas transport to the VF1 (Section 7.2.3), however this is not relevant to the gas issue.

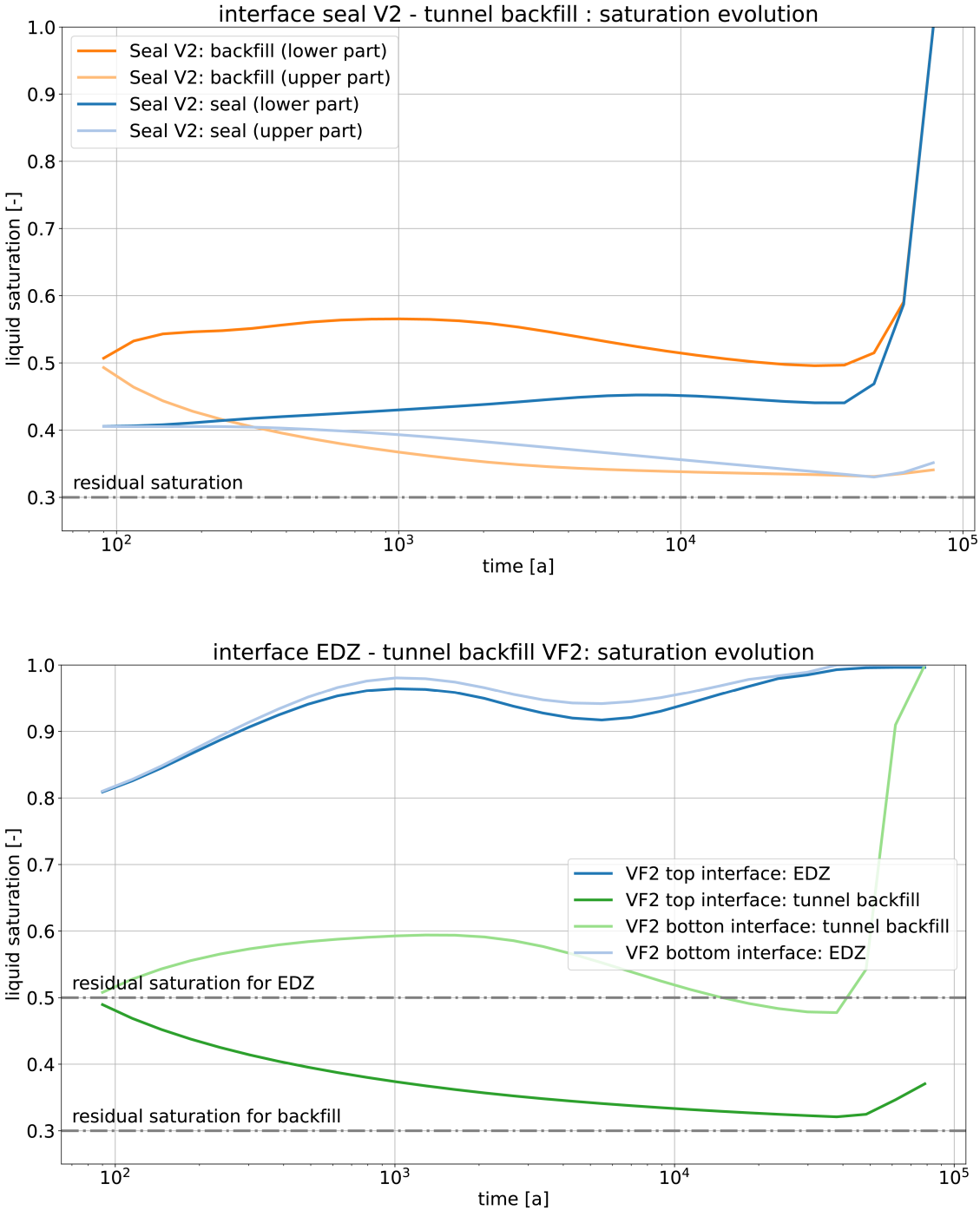

Fig. 7-7: Top: Temporal evolution of liquid saturation for a V2-L/ILW seal and adjacent backfill material

Bottom: Temporal evolution of liquid saturation at the top and bottom interface halfway between the V2 and V3 seals

Extracted from base case model in (Papafotiou & Senger 2016a)

V2-L/ILW seals and VF2 backfill

Saturation in the V2-L/ILW seals will evolve in a similar way to that of the V1-L/ILW seals, albeit with a somewhat lower magnitude of saturation changes over time, as shown in Fig. 7-7. Saturation in the lower parts of the V2-L/ILW seals will slowly increase, whereas gas coming from the VF1 backfill of the L/ILW disposal area will result in lower saturations in the upper parts. Saturation of the VF2 backfill (Fig. 7-7 bottom) will occur, overall, in a very similar manner to VF1 in the L/ILW disposal area, providing a continuous pathway for gas over tens of thousands of years.

Overall, transport of repository-generated gas through the sand-bentonite V1-L/ILW and V2-L/ILW sealing elements will tend to maintain a gas pathway in sand-bentonite mixture above the capillary fringe, thus further supporting the maintenance of a continuous gas storage volume. As discussed in earlier chapters, as long as there is a connected gas phase along the underground openings, pore clogging will be limited and continuous gas transport will remain unperturbed, as assumed in the model calculations.

7.3 Gas generation and sinks for gas in the repository

As indicated in Section 7.2, it is expected that a free gas phase will be present over tens of thousands of years in the L/ILW disposal area. The fate of gases in time and space is controlled by a complex feedback system (Fig. 7-1) between gas and water transport processes in the repository system, and gas generation processes and rates, as well as by gas consumption processes (cf. Nagra NTB 24-23 *planned*), which will be discussed in the following paragraphs.

7.3.1 Gas production and consumption in L/ILW caverns

Gases will be produced in the closed combined repository, once oxygen is consumed, by the anaerobic corrosion of metals, which produces H_2 (Diomidis et al. *in prep.*), by microbial and chemical degradation of organic matter, which may produce gaseous compounds such as CO_2 and CH_4, and, to a lesser degree, by radiolysis (Guillemot et al. 2023). In comparison with the HLW disposal area, the volumetric gas generation rates per cavern within the L/ILW disposal area are much higher and the gas is generated much faster, whereas, in the HLW disposal area, gas generation is distributed over a larger volume and over a longer period (Nagra NTB 24-23 *planned*). A large portion of the gas generated in a combined repository will therefore occur in the L/ILW emplacement caverns and is strongly influenced by the chemical conditions, which are dependent on the cementitious pore water composition (Kosakowski et al. 2023).

Gas production rates in the L/ILW emplacement caverns will be reduced by the alkalinity of the chemical environment, e.g., due to the passivation of steel, which occurs at pH > 10.5 (Diomidis et al. in prep., Diomidis et al. 2016), as well as the limitation of microbial activity (Small 2019). Nonetheless, gases will still be produced by anoxic metal corrosion and by the abiotic and/or biotic degradation of organic matter, provided conditions are locally favourable. Specifically, if not limited by availability of water, the fast corrosion of reactive metals (e.g., aluminium) will result in high production rates of hydrogen shortly after closure of the repository. CO_2 produced in the L/ILW emplacement caverns by the microbial degradation of organic matter will be dissolved in the adjacent pore solution, resulting in the carbonation of cement surfaces and a lowering of the local pH of the pore waters towards neutral values to a degree that will depend on the amount of CO_2 generated. By contrast, other gases that will be produced, mainly H_2 and CH_4, are not expected to interact with cementitious materials. The formation of these gases will increase the gas pressure in the near field, and delay the re-saturation of the emplacement caverns, backfill and sealing system.

Due to ongoing carbonation and to the interaction of siliceous compounds within the concrete with the alkaline pore solution via the pozzolanic reaction, portlandite will, over time, become decomposed and the C-S-H initially present will become congruently converted to C-S-H with a lower Ca/Si-ratio (Nagra 2023). At the stage during which the pH is above 12, low gas generation rates for metal corrosion can be assumed. However, as the degradation of cement progresses, the pH will continuously decrease towards 10.5, or even lower (due to carbonation if sufficient CO_2 is locally generated), and corrosion rates will then increase (Nagra 2023). As indicated above, corrosion is dependent on the availability of water. As water is consumed, and provided the relative humidity in the gas phase inside the material is very low, the reaction will come to a halt and corrosion will not progress further until the steel surfaces are again covered with water films (cf. Section 3.5.3, Kosakowski et al. 2023).

Overall, the amount of gas generated as a function of time depends on the inventories of relevant materials (steel, organic matter) and on the gas generation rates, which depend on the local conditions of cement and other materials in a highly heterogeneous near field, as well as on the above-mentioned availability of water.

7.3.2 Gas production in HLW emplacement drifts

In the HLW emplacement drifts, the main source for gas is the corrosion of the metal canisters and of the reinforcement within the tunnel support material, which generates hydrogen. In general, gas generation in the HLW drifts takes place at lower rates compared with the L/ILW caverns, but continues over a longer period of time (Nagra NTB 24-23 *planned*). Moreover, the large total tunnel length and correspondingly large interface area with the adjacent Opalinus Clay allows a higher degree of gas dissolution in the pore water around the HLW repository. In contrast with the L/ILW disposal area, due to the smaller disposal drift diameter and the strong capillary suction of the bentonite in the HLW drifts, fully or almost fully saturated conditions will prevail, and H_2 production will proceed uninterrupted, except during a short period of a couple of hundreds of years in the early phase after emplacement, when the bentonite around the canister is dried due to the high temperatures at the steel surface.

7.3.3 Influence of gas production rates and gas consumption rates on saturation evolution

Extensive modelling has been carried out at different spatial scales to elucidate the saturation of the repository and the fate of repository-generated gas (see Senger & Ewing 2009, Papafotiou & Senger 2016a, Diomidis et al. 2016). Papafotiou & Senger (2016a) investigated systematically the influence of processes and material parameters on re-saturation of a L/ILW repository. This includes scenarios that investigate the influence of sealing system layout, two-phase flow properties of EDZ and Opalinus Clay, the gas generation rates and consideration of microbial consumption of hydrogen in tunnels.

Gas pressures and re-saturation of the repository were shown to depend strongly on gas generation rates. Higher gas generation rates cause higher peak pressures that prevent early re-saturation of the repository. On the other hand, assuming a fixed inventory of gas-generating materials, gas generation rates in such scenarios decrease faster and gas pressures decrease to hydrostatic pressure earlier, after a few tens of thousands of years, allowing inflow of formation water into the repository. Nonetheless, it was shown that complete re-saturation of the L/ILW repository takes more than 100’000 years for all investigated model cases (Papafotiou & Senger 2016a). Very low gas generation rates result in water inflow in the first ten thousand years, causing a partial re-saturation of the repository. Gas pressures only slightly exceeded hydrostatic pressure after about 10’000 years and remained close to hydrostatic for a long period. Nonetheless, despite

the early partial re-saturation of the repository, it was shown that these partially water saturated conditions would prevail for at least 100'000 years, similar to the base case scenario (Papafotiou & Senger 2016a).

The consideration of hydrogen consumption by microbially-mediated sulphate reduction in operation, ventilation and access tunnels – discussed further in Section 7.3.4 – could contribute to a reduction of peak gas pressures, but has a relatively small influence on overall saturation times (Papafotiou & Senger 2016a). In general, the availability of sulphate in pore water is a limiting factor for sustainable hydrogen consumption. As a design measure, additional sulphate can be provided by a suitable choice of sulphate rich tunnel backfill, if deemed desirable or necessary for the cultivation of microbes.

The sensitivity analyses showed that the design and the permeability of the seals and tunnel backfill significantly influence gas pressure build-up in the repository. For low permeability seals and tunnel backfill, peak gas pressures are increased but remain at all times below values that could compromise the functionality of the repository barriers (Nagra NTB 24-23 *planned.,* Diomidis et al. 2016; Sections 3.4.4 and 3.5). None of the model variants investigated in the analysis resulted in full liquid saturation of the repository after 100'000 years.

In general, the model variants show a clear correlation between pressure build-up and the gas release via different gas pathways. Two gas release pathways are of major importance: the release from the emplacement caverns directly to the rock surrounding them, and the release to the host rock via the sealing system. The latter pathway generally dominates, especially after few hundreds of years, and is more effective for a more gas-permeable sealing system: as the front of waste-generated gas propagates and spreads throughout the repository tunnel system, the interface area to the surrounding rock increases, thus also increasing the amount of gas dissolved in pore water.

In summary, the different scenarios calculated by Papafotiou & Senger (2016b), which take into account a broad range of design variants, gas generation rates and material properties, show that full liquid saturation of the repository is unlikely to take place in less than around 100'000 years. Furthermore, the correlation between pressure build-up, gas release pathways and the gas-permeability of the sealing system indicates that the hydraulic evolution of the repository can be tailored using the repository design measures.

7.3.4 Gas consumption in the emplacement caverns and drifts and in the sealing system

Microbial activity can lead to gas generation (see Section 7.3.3) but can also provide sinks for gas. The maximum amount of hydrogen that can be consumed by chemical reactions (biotic or abiotic) is related to (Kosakowski et al. 2023):

- the initial amounts of oxidised components present in repository materials
- access to these components (transport and contact with aqueous solutions)
- the significance of the reaction rates for the time scale under consideration

Microbial activity in the small pores of intact Opalinus Clay is limited. In proximity to a deep geological repository, however, the existence of increased space in the engineered barriers and tunnel system will allow additional microbial activity to take place (Cloet et al. 2017). The salt concentration found in the pore water of the Opalinus Clay is tolerated by many microorganisms. If, however, the water activity is reduced, the activity of the microorganisms decreases and the cells die. Motamedi (1996) have experimentally demonstrated that, in compacted bentonite, where water activity drops to values of < 0.96, anaerobic sulphate-reducing bacteria die rapidly, as also discussed in Jenni et al. (2019). Microbial activity is therefore not expected in the HLW emplacement drifts, except potentially around their outer perimeters.

Throughout the L/ILW disposal section, the high pH of cement pore water, the water availability in de-saturated parts of repository (see Section 7.2) and the limited availability of nutrients will all act to reduce the potential for microbial activity (Small 2019, Warthmann et al. 2013, Leupin et al. 2016b). On the other hand, due to the heterogeneous nature of the L/ILW near-field, microbial activity in some parts of the L/ILW disposal area cannot be excluded (Kosakowski et al. 2023). The most likely place within the L/ILW disposal section for hydrogen consumption due to sulphate reducing microbial activity is in saturated niches and along the backfilled tunnels.

7.4 Main messages from this chapter

At the time of repository closure, the underground repository structures and the immediately surrounding rock will be only partly saturated. Ingress of water from the upper geological units will lead to a relatively fast saturation of the V3 seals (according to model predictions within few hundred years); the saturated V3 seals are highly impermeable, largely preventing further ingress of water from the upper geological units as well as the escape of repository-generated gas to these units and to the surface environment.

The majority of gas generated in the HLW emplacement drifts will be H_2 due to metal corrosion, whereas, in the L/ILW emplacement caverns, material heterogeneities are higher and, in addition to the H_2 generated by the corrosion of metals, CH_4 and CO_2 will be generated by microbial and chemical degradation of organic matter. CO_2 will be consumed by carbonation reactions as it dissolves and contacts cement materials. This will lower the alkalinity of the cement pore solution and accelerate corrosion reactions in carbonated materials.

Corrosion is, in principle, constrained by water availability in both disposal sections. In the HLW disposal section, however, water availability is practically unlimited and therefore complete and almost uninterrupted corrosion of the metallic materials within the repository will occur in the long-term (Nagra NAB 24-20 *planned*). In the L/ILW disposal section, abiotic and biotic degradation reactions are controlled by alkaline conditions and by water availability, which in turn depends on pore water exchange between the emplacement caverns and the surrounding rock. In the early post-closure phase, the hydraulic gradient will generally be directed from the rock towards the caverns, and the rock around the caverns will re-saturate with pore water. As a result of the presence of water, gas generation by both corrosion and microbial processes will occur, although these will be constrained by the limited availability of water.

The consumption of water from corrosion and the increasing presence of gas may lead to a temporary reduction in the corrosion and gas generation rates in the L/ILW emplacement caverns, until larger amounts of pore water again become available. As fluid pressure in the caverns increases, the general direction of the hydraulic gradient will change and will be directed from the cavern to the rock. Analyses indicate that the L/ILW disposal section will remain partially saturated for at least 100’000 years, with gas pressures that are insufficient to cause damage to the rock.

In the rest of the repository (except for the HLW disposal area), the saturation evolution will be similar. Ingress of water from the saturated parts of the rock will be very slow, due to the low permeability of the rock at repository depth, in combination with the increasing gas pressure in the L/ILW caverns and sealing system. Model calculations indicate that the pore space of the VF1 and VF2 backfill material in the upper parts of the underground openings outside the HLW disposal area will not become water-filled for at least several tens of thousands and possibly much longer. As long as there is a connected gas phase along the underground openings, pore clogging will be limited, and continuous gas transport and a continuous storage volume for gas will be maintained. Transport of repository-generated gas through the sand-bentonite V1-L/ILW and

V2-L/ILW sealing elements will tend to maintain partial saturation of the sand-bentonite mixture above the capillary fringe, thus further supporting the maintenance of a continuous gas storage volume.

In summary, a continuous gas pathway and associated storage volume within the underground structures of the repository outside the HLW disposal area is expected to be maintained throughout the period during which gas is expected to be generated within the repository, preventing significant pore clogging at interfaces and equalising and limiting gas pressures.

8 Summary and conclusions

Chemical reactions leading to dissolution of, and precipitation on, pore surfaces may potentially occur within the disposal sections and sealing system of a repository, especially near the interfaces between clay- and cement-based materials. Precipitation is a particular concern because it may affect the function of the sealing elements, especially with respect to gas transfer and storage. This report has reviewed and summarised the current understanding of the chemical processes that could lead to precipitation in relevant porous media and their implications for the design and performance of the sealing system.

Chemical reactions in a repository environment require water; if no water is available, chemical reactions do not occur. This implies that no clogging by chemical reactions can occur in the absence of water. For chemical reactions to proceed in partially saturated porous media, as will exist for a considerable period of time within the repository sealing system:

- water needs to be present within pores or as water films on pore surfaces
- water needs to form connected pathways for the transport of reactants by diffusion and/or advection; an interruption of these pathways may decrease fluxes substantially

A range of considerations, including nucleation theory, lead to the conclusion that precipitation happens more readily and faster in larger, water-filled pores in comparison with smaller pores under fully- and partially saturated conditions. On the other hand, under partially saturated conditions, it is the smaller pores that are more likely to be water-filled, due to the effect of capillary forces. In particular:

- upon desaturation, the largest pores will be desaturated first
- upon (re-)saturation, smaller pores will become water-filled

Hence, observations made, for example, in partially saturated soils, indicate that large, gas-filled pores stay open and only smaller, water-filled pores are filled with precipitates. On the other hand, clay and cement-based materials contain a large fraction of pores with apertures of less than a few nanometres, i.e., inter-layer pores in clays and in C-S-H-cement phases. In these very small nano-pores, precipitation will also be inhibited.

Numerous experimental and modelling studies have elucidated the precipitation and pore clogging that may occur at the interfaces between clay- and cement-based materials. The main points of interest from these studies are as follows.

- There is a reasonably good understanding of mineral changes that are observed and modelled at the contact between cement and clay materials.
- Migration of hydroxyl ions and the associated increase of pore water pH in clays and decrease of pore water pH in cements is the main driving mechanism for mineral alteration and precipitation.
- The zone of perturbed minerals and fluid composition in clay materials is expected to be narrow, in the range of centimetres up to tens of centimetres over a period in 100'000 or more years. In cement-based materials, these zones might be more widespread, due to the generally higher reactivity of cement minerals compared to clays.
- The porosity is expected to be reduced at the clay/cement interface by precipitation.
- Although there is significant uncertainty regarding the extent of precipitation and possible pore clogging under partially saturated conditions, it is probably not possible for complete clogging of the interface to occur, since, as noted above, the smallest, nano-pores will remain open; larger pores will also remain open as long as they remain unsaturated.

Gas transfer and storage processes in clay- and cement-based materials is well understood for these materials in isolation, but less well understood where these materials interact, leading to precipitation and pore clogging. It is likely, however, that, although nano-pores will remain open, transport of dissolved gases through these pores will be constrained by gas adsorption at clay surfaces, depending on size and shape of the gas molecules and water structure at clay surfaces.

Transport of dissolved gas and other solutes in the aqueous phase in partially clogged porous media is analogous to solute transport in partial saturated media without clogging. In both cases, the largest pores are unavailable for the transport of solutes, since they are either precipitate-filled or gas-filled. Laboratory experiments in clay media indicate that the impact on the diffusion of neutral solutes, including dissolved gas, might be significant, leading to a reduction of the effective diffusion coefficient by one up to two orders of magnitude if the transport-relevant water filled porosity is reduced by factor 2.

In general, transport in the gas phase could be more significantly hindered by the clogging of large pores. In the absence of clogging, the larger pores are the ones that tend to provide preferential gas pathways. In pure bentonite and in sand/bentonite mixtures, the impact of clogging is expected to be less significant because of the swelling of clay aggregates that collapses the macro-pores, where clogging would otherwise most likely to occur, but allows subsequent re-opening of gas pathways. In cement-based materials, clogging of larger pores would result in a higher capillary strength being required for gas to enter the smaller pores. On the other hand, in the context of a repository, it is the largest pores that will be the last to become water filled as the repository material is saturated, which reduces the likelihood that they become clogged while gas is still present.

The sealing system is designed such that chemical reactions within the sealing system that could, under fully saturated conditions, lead to mineral precipitation and the pore clogging of larger pores, are minimised or avoided, as they could otherwise detrimentally affect the capacity of the sealing system for gas transfer and storage. In addition, chemical changes that could induce the formation of colloids, which could become mobilised, also leading to the physical blockage of pores and pore throats, are also minimised or avoided. The focus of design measures to avoid such reactions and changes is on the interfaces between the clay-based sealing elements and the cement-based abutments. Unremoved cement-based tunnel support around the sealing elements may induce local scale chemical changes, but, especially under partially saturated conditions, disturbance will be limited.

The design measures focus on avoiding, or limiting the use of, materials that can interact strongly and on avoiding direct contact between potentially interacting materials by providing physical separation between them. Specific measures design measures for the seals could include:

- use of low pH cement (OPC blended with pozzolanic material) for the construction of the abutments adjacent to the sealing sections, which lowers, but does not entirely avoid, the potential for chemical reactions,
- separating these cement-based abutments from the sealing sections (sand-bentonite mixture, bentonite) by transition layers consisting of inert material that is initially highly unsaturated, which slows the transport of reactive species and particles/colloids migrating from the abutments and/or sealing sections

Potentially suitable inert materials for the transition layers have been proposed, e.g., pure limestone aggregates/sand consisting of relatively pure $CaCO_3$.

The design of the transition layers could be optimised if required based on the following guiding principles:

- The axial length of the transition layers should be optimised, with larger lengths being favourable with respect to reducing the chemical/diffusion gradients driving the migration of reactants and thus minimising the potential for pore clogging.
- The pore sizes within the layers should be such that suction by capillary forces is minimised, thus delaying saturation (and the transport of reactants), minimising the potential for pore clogging and favouring the transport and storage of gas.

A low capillary rise within the transition layer has the following implications:

- Because relevant chemical reactions occur only where water is present, chemical reactions within, and adjacent to, the transition layers will be restricted by the limited saturation of the materials in the upper parts of the transition layers.
- Microbial activity will be limited to the highly water saturated regions in the lower part of the partially saturated transition layers.
- Transport and sedimentation of dispersed particles (colloids) within the transition layers, which could lead to the physical blockage of the pores, will also be limited to the highly water saturated, lower regions of the transition layers.

A low capillary rise thus contributes in various ways to maintaining a continuous gas pathway in the upper part of the transition layers.

The saturation behaviour of the repository and the fate of repository-generated gas has been investigated in modelling studies. Ingress of water from the upper geological units will lead to a relatively fast saturation of the V3 seals (according to model predictions within few hundred years); the saturated V3 seals are highly impermeable, largely preventing further ingress of water from the upper geological units and limiting or preventing the escape of repository-generated gas. Ingress of water from the saturated parts of the rock to the remainder of the repository will be slow, due to the low permeability of the rock at repository depth and, increasingly over time, due to gas generation. Gas generation will occur due to corrosion and microbial processes, although it will be partly constrained by the limited availability of water. Gas generated by corrosion in the HLW emplacement drifts is expected to dissolve and diffuse mainly into the host rock. In the case of L/ILW, the model calculations confirm that a continuous gas pathway and associated storage volume within the underground structures of the repository is expected to be maintained throughout the period during which the gas generation is relevant to the evolution of the repository, limiting the resulting gas pressures.

The present study has been conducted based on a preliminary generic design and layout of the repository, including its sealing system (Nagra 2021c). The layout of the repository, its dimensions, selected materials, construction technologies, as well as waste emplacement strategies and procedures for repository operation, will be further developed and optimised in forthcoming years. Part of this optimisation procedure will be related to the optimisation of the components of the sealing system, including, e.g., the selection of the bentonite type to be used, the detailed design of the transition layers, their partitioning walls and the adjoining abutments, selection of the backfill materials. Optimisation will be an iterative process, guided by further assessments of key issues, including repository saturation and gas transport and storage in the sealing system.

The information provided in this report with related to pore clogging by chemical processes, as well as the insights gained in the course of the experimental and modelling studies performed over many years as part of Nagra's RD&D programme, indicates that the chemical interactions and other processes that could lead to porosity alteration are generally well understood. This

understanding supports the development of design measures to further guard against the adverse effects of pore clogging by, e.g., avoiding, or limiting the use of, materials that can interact strongly, and on avoiding direct contact between potentially interacting materials by providing physical separation between them.

To conclude, this report has discussed how clogging of pores by precipitation at cement-clay interfaces will not affect the functioning of a well-designed sealing system. Physical clogging of large pores by chemical precipitates requires that these pores are liquid filled (fully saturated medium), which model calculations indicate will only happen in the lower parts of the seals. Precipitation will not occur in the large, gas-filled pores in the upper parts of the seals; rather, it is smaller, water-filled capillary pores, though not the smallest nano-pores/inter-layer pores, that could potentially become blocked. Furthermore, the design measures outlined above and discussed at greater length in the main body of this report are available that would further reduce the extent of precipitation and the possibility of pore clogging in the sealing sections. There is thus good evidence that the sealing system can perform its function of limiting the development of potentially damaging gas pressures within the repository.

9 References

Ahlström, J. (2015): Corrosion of steel in concrete at various moisture and chloride levels. Report 2015:133. Energiforsk.

Alcolea, A., Kuhlmann, U., Lanyon, G.W. & Marschall, P. (2014): Hydraulic conductance of the EDZ around underground structures of a geological repository for radioactive waste – A sensitivity study for the candidate host rocks in the proposed siting regions in Northern Switzerland. Nagra Arbeitsbericht NAB 13-94.

Alexander, W.R., McKinley, I.G., Linklater, C.M., Tweed, C.J., Casas, I., Börjesson, S. & Selin, P.: Testing the limits of applicability of thermodynamic databases. - In: Linklater, C. M. (ed.) (1998). A natural analog study of cement-buffered hyperalkaline groundwaters and their interaction with a repository hostrock: Phase II. Harwell, UK: Nirex, 242-277.

Alonso, E.E., Gens, A. & Hight, D.W. (1987): Special Problem Soils, General Report. Proceedings of the 9th European Conference on Soil Mechanics and Foundation Engineering, Dublin. 31 August-3 September, 1087-1146.

Anderson, G.M. (2005): Thermodynamics of natural systems. 2. ed. Cambridge Univ. Press.

Argiz, C. & Saniuan, M.A. (2017): Full factorial design to assess the concrete gas permeability. AFINIDAD LXXIV 2017/July - September, 169-175.

Auroy, M., Poyet, S., Le Bescop, P., Torrenti, J.-M., Charpentier, T., Moskura, M. & Bourbon, X. (2018): Comparison between natural and accelerated carbonation (3% CO2): Impact on mineralogy, microstructure, water retention and cracking. Cement and Concrete Research 109, 64-80. DOI: 10.1016/j.cemconres.2018.04.012.

Bear, J. (1972): Dynamics of Fluids in Porous Media. Soil Science/120(2), 162-163.

Berner, U., Kulik, D.A. & Kosakowski, G. (2013): Geochemical impact of a low-pH cement liner on the near field of a repository for spent fuel and high-level radioactive waste. Physics and Chemistry of the Earth, Parts A/B/C 64, 46-56. DOI: 10.1016/j.pce.2013.03.007.

Berner, U.R. (1992): Evolution of pore water chemistry during degradation of cement in a radioactive waste repository environment. Waste Management 12/2–3, 201-219. DOI: 10.1016/0956-053X(92)90049-O.

BFE (2008): Sachplan Geologische Tiefenlager: Konzeptteil. BFE 2. April 2008 (Revision vom 30. November 2011). Departement für Umwelt, Verkehr, Energie und Kommunikation UVEK, Bern.

Bildstein, O., Claret, F. & Frugier, P. (2019): RTM for Waste Repositories. Reviews in Mineralogy and Geochemistry 85/1, 419-457. DOI: 10.2138/rmg.2019.85.14.

Botes, A., James, C. & Sheridan, C.M. (2018): Assessing the clogging and permeability of degrading packed bed reactors. Water SA 44/1, 20-26. DOI: 10.4314/wsa.v44i1.03.

Bouissonnié, A., Daval, D., Marinoni, M. & Ackerer, P. (2018): From mixed flow reactor to column experiments and modeling: Upscaling of calcite dissolution rate. Chemical Geology 487/April, 63-75. DOI: 10.1016/j.chemgeo.2018.04.017.

Bradbury, M.H., Berner, U., Curti, E., Hummel, W., Kosakowski, G. & Thoenen, T. (2014): Geochemical near-field evolution of a deep geological repository for spent fuel and high-level radioactive waste. Nagra Technical Report NTB 12-01.

Buenfeld, N. & Okundi, E. (1998): Effect of cement content on transport in concrete. Magazine of Conrete Research 50/4, 339-351, available online at https://doi.org/10.1680/macr.1998.50.4.339.

Burzan, N. (2021): Growth and viability of microorganisms in bentonite and their potential activity in deep geological repository environments. École Polytechnique Fédérale de Lausanne EPFL, available online at http://infoscience.epfl.ch/record/283941.

Chagneau, A., Claret, F., Enzmann, F., Kersten, M., Heck, S., Mad, B. & Schaefer, T. (2015): Mineral precipitation-induced porosity reduction and its effect on transport parameters in diffusion-controlled porous media. Geochemical Transactions 16/1, p. 13. DOI: 10.1186/s12932-015-0027-z.

Claveau-Mallet, D. & Comeau, Y. (2020): Chemical clogging and evolution of head losses in steel slag filters used for phosphorus removal. Water (Switzerland) 12/6. DOI: 10.3390/W12061517.

Cloet, V., Pekala, M., Smith, P., Wersin, P. & Diomidis, N. (2017): An Evaluation of sulphide fluxes in the near field of a HLW repository. Nagra Technischer Bericht NTB 17-04.

Collins, K. & McGown, A.T. (1974): The form and function of microfabric features in a variety of natural soils. Geotechnique 24, 223-254.

Coussy, O. (2004): Poromechanics. 2nd ed., Chichester. Wiley.

Damiani, L.H., Kosakowski, G., Vinsot, A. & Churakov, S.V. (2022): Hydrogen gas transfer between a borehole and claystone: experiment and geochemical model. Environmental Geotechnics, 1-14. DOI: 10.1680/jenge.21.00061.

Deinert, M.R. & Parlange, J.Y. (2009): Effect of pore structure on capillary condensation in a porous medium. Physical Review E - Statistical, Nonlinear, and Soft Matter Physics 79/2, p. 21202. DOI: 10.1103/PhysRevE.79.021202.

Diomidis, N., Cloet, V., Leupin, O.X., Marschall, P., Poller, A. & Stein, M. (2016): Production, consumption and transport of gases in deep geological repositories according to the Swiss disposal concept. Nagra Technischer Bericht NTB 16-03.

Diomidis, N., Guillemot, T. & King, F. (in prep.): Definition of reference corrosion rates for performance and safety assessments in the framework of the general Licence Application. Nagra Arbeitsbericht NAB 23-22.

Dopffel, N., Jansen, S. & Gerritse, J. (2021): Microbial side effects of underground hydrogen storage – Knowledge gaps, risks and opportunities for successful implementation. International Journal of Hydrogen Energy 46/12, 8594-8606. DOI: 10.1016/j.ijhydene.2020.12.058.

Eddaoui, N., Panfilov, M., Ganzer, L. & Hagemann, B. (2021): Impact of Pore Clogging by Bacteria on Underground Hydrogen Storage. Transport in Porous Media 139/1, 89-108. DOI: 10.1007/s11242-021-01647-6.

Ennis-King, J., Michael, K., Strand, J., Sander, R. & Green, C. (2021): Underground storage of hydrogen: mapping out the options for Australia, Wollongong Australia.

Favero, V., Ferrari, A. & Laloui, L. (ed.) (2013): An insight into the water retention behaviour of shales. International Workshop on Geomechanics and Energy, EAGE. Lausanne, Switzerland, 26-28 November 2013.

Feldman, R.F. & Sereda, P.J. (1968): A model for hydrated Portland cement paste as deduced from sorption-length change and mechanical properties. Matériaux et Constructions 1/6, 509-520. DOI: 10.1007/BF02473639.

Ferrari, A., Favero, V. & Laloui, L. (2014): Experimental analysis of the water retention behaviour of shales. International Journal of Rock Mechanics and Mining Sciences (2014, available online at DOI:10.1016/J.IJRMMS.2014.08.011.

Fukatsu, Y., van Loon, L.R., Shafizadeh, A., Grolimund, D., Ikeda, Y. & Tsukahara, T. (2017): Effect of Celestite Precipitation in Compacted Illite on the Diffusion of HTO 36Cl- and 22Na+. *In:* Energy Procedia, vol. 131: Elsevier Ltd, 133-139.

Gaboreau, S., Prêt, D., Tinseau, E., Claret, F., Pellegrini, D. & Stammose, D. (2011): 15 years of in situ cement–argillite interaction from Tournemire URL: Characterisation of the multi-scale spatial heterogeneities of pore space evolution. Applied Geochemistry 26/12, 2159-2171. DOI: 10.1016/j.apgeochem.2011.07.013.

Gaboreau, S., Rodríguez-Cañas, E., Maeder, U., Jenni, A., Turrero, M.J. & Cuevas, J. (2020): Concrete perturbation in a 13-year in situ concrete/bentonite interaction from FEBEX experiments. New insight of 2:1 Mg phyllosilicate precipitation at the interface. Applied Geochemistry 118/March, p. 104624. DOI: 10.1016/j.apgeochem.2020.104624.

Gadikota, G., Dazas, B., Rother, G., Cheshire, M.C. & Bourg, I.C. (2017): Hydrophobic Solvation of Gases (CO 2, CH 4, H 2, Noble Gases) in Clay Interlayer Nanopores. J. Phys. Chem. C 121/47, 26539-26550. DOI: 10.1021/acs.jpcc.7b09768.

Gaol, C.L., Ganzer, L., Mukherjee, S. & Alkan, H. (2021): Investigation of clogging in porous media induced by microorganisms using a microfluidic application. Environmental Science: Water Research and Technology 7/2, 441-454. DOI: 10.1039/d0ew00766h.

Gaucher, E.C. & Blanc, P. (2006): Cement/clay interactions - a review: experiments natural analogues and modeling. Waste Management 26/7, 776-788. DOI: 10.1016/j.wasman.2006.01.027.

Gaus, I., Garitte, B., Senger, R.K., Gens, A., Vasconcelos, R., García-Siñeriz, M.J.-L., Trick, T., Wieczorek, K., Czaikowski, O., Schuster, K., Mayor, J.C., Velasco, M., Kuhlmann, U. & Villar, M.V. (2014a): The HE-E Experiment: Lay-out, interpretation and THM modelling. Nagra Arbeitsbericht NAB 14-53.

Gaus, I., Wieczorek, K., Schuster, K., Garitte, B., Senger, R., Vasconcelos, R. & Mayor, J.-C. (2014b): EBS behaviour immediately after repository closure in a clay host rock: HE-E experiment (Mont Terri URL). Clays in Natural and Engineered Barriers for Radioactive Waste Confinement, 5th international meeting, Montpellier, October 22-25, 2012, Geological Society, London, Special Publications 400, 71-91.

Gens, A. & Alonso, E.E. (1992): A framework for the behaviour of unsaturated expansive clays. Can. Geotech. J. 29/6, 1013-1032. DOI: 10.1139/t92-120.

Gimmi, T. & Churakov, S.V. (2019): Water retention and diffusion in unsaturated clays: Connecting atomistic and pore scale simulations. Applied Clay Science 175/December 2018, 169-183. DOI: 10.1016/j.clay.2019.03.035.

Gimmi, T. & Kosakowski, G. (2011): How Mobile Are Sorbed Cations in Clays and Clay Rocks? Environmental science & technology 45/4, 1443-1449. DOI: 10.1021/es1027794.

González-Santamaría, D.E., Fernández, R., Ruiz, A.I., Ortega, A. & Cuevas, J. (2020a): Bentonite/CEM-II cement mortar INTERFACE EXPERIMENTS: A proxy to in situ deep geological repository engineered barrier system surface reactivity. Applied Geochemistry 117/August 2019, p. 104599. DOI: 10.1016/j.apgeochem.2020.104599.

González-Santamaría, D.E., Fernández, R., Ruiz, A.I., Ortega, A. & Cuevas, J. (2020b): High-pH/low pH ordinary Portland cement mortars impacts on compacted bentonite surfaces: Application to clay barriers performance. Applied Clay Science 193. DOI: 10.1016/j.clay.2020.105672.

Graham, J., Chandler, N., Dixon, D., Roach, P., To, T. & Wan, A.W. (1997): The buffer/container experiment: results, synthesis, issues. Atomic Energy of Canada limited report/AECL-11746, COG-97-46-1, available online at https://www.semanticscholar.org/paper/The-buffer%2Fcontainer-experiment%3A-results%2C-issues-Graham-Chandler/6f7335d546d1fdf84c66ae17ec5e5600e517210f.

Gross, D. (2007): Bruchmechanik. Mit einer Einführung in die Mikromechanik. 4., bearb. Aufl. 2007, Berlin, Heidelberg. Springer Berlin Heidelberg, available online at http://nbn-resolving.org/urn:nbn:de:bsz:31-epflicht-1551365.

Guillemot, T., Wieland, E. & Moosberger, L. & Warthmann R. (2023): Degradation of organic materials in a L/ILW repository. Nagra Arbeitsbericht NAB 23-11.

Hansen, J., Doudou, S., Palmu, M. & White, M. (2016): DOPAS Work Package: Deliverable D6.4: DOPAS Project Final Summary Report. European Commssion, Euratom 7th Framework Programme Project, Brussels.

Harrison, A.L., Dipple, G.M., Song, W., Power, I.M., Mayer, K.U., Beinlich, A. & Sinton, D. (2017): Changes in mineral reactivity driven by pore fluid mobility in partially wetted porous media. Chemical Geology 463, 1-11. DOI: 10.1016/j.chemgeo.2017.05.003.

Hartley, F.R., Burgess, C. & Alcock, R. (1980): Solution equilibria. Edited by Ellis Horwood Ltd. Publishers, Chichester, UK.

Hayek, M., Kosakowski, G. & Churakov, S. (2011): Exact analytical solutions for a diffusion problem coupled with a precipitation-dissolution reaction and feedback of porosity change. Water Resources Research 47/7. DOI: 10.1029/2010WR010321.

Hayek, M., Kosakowski, G., Jakob, A. & Churakov, S.V. (2012): A class of analytical solutions for multidimensional multispecies diffusive transport coupled with precipitation-dissolution reactions and porosity changes. Water Resources Research 48/3. DOI: 10.1029/2011WR011663.

Helmig, R. (1998): Multiphase flow and transport processes in the subsurface. A contribution to the modeling of hydrosystems. Journal of the Marine Biological Association of the United Kingdom 78/1, 349-350. DOI: 10.1017/S0025315400040170.

Hill, R. (1963): Elastic properties of reinforced solids: Some theoretical principles. Journal of the Mechanics and Physics of Solids 11/5, 357-372. DOI: 10.1016/0022-5096(63)90036-X.

Hoffmann, C., Alonso, E.E. & Romero, E. (2007): Hydro-mechanical behaviour of bentonite pellet mixtures. Physics and Chemistry of the Earth Parts A/B/C 32/8-14, 832-849. DOI: 10.1016/j.pce.2006.04.037.

Hommel, J., Coltman, E. & Class, H. (2018): Porosity–Permeability Relations for Evolving Pore Space: A Review with a Focus on (Bio-)geochemically Altered Porous Media. Transport in Porous Media 124/2, 589-629. DOI: 10.1007/s11242-018-1086-2.

Horseman, S.T. (Nuclear Energy Agency) (1996): Water, gas and solute movement through argillaceous media. OECD publications, 79325, Paris. OECD.

Huang, Y., Shao, H., Wieland, E., Kolditz, O. & Kosakowski, G. (2021): Two-phase transport in a cemented waste package considering spatio-temporal evolution of chemical conditions. npj Materials Degradation 5/1, p. 4. DOI: 10.1038/s41529-021-00150-z.

IAEA (2022): IAEA Safety Glossary. Terminology used in nuclear safety and radiation protection 2018 Edition. International Atomic Energy Agency (IAEA), Vienna.

Idiart, A., Laviña, M., Kosakowski, G., Cochepin, B., Meeussen, H., Samper, J., Mon, A., Montoya, V., Munier, I., Poonoosamy, J., Montenegro, L., Deissmann, G., Rohmen, S., Damiani, L., Coene, E. & Naves, A. (2020): Reactive transport modelling of a low-pH concrete / clay interface. Applied Geochemistry 115, p. 104562, available online at https://www.semanticscholar.org/paper/Reactive-transport-modelling-of-a-low-pH-concrete-%2F-Idiart-Lavi%C3%B1a/97fd9c9011ded71467f67c0ca49e0e81f3f1c347.

Indraratna, B., Medawela, S., Rowe, R.K., Thamwattana, N. & Heitor, A. (2020): Biogeochemical Clogging of Permeable Reactive Barriers in Acid-Sulfate Soil Floodplain. Journal of Geotechnical and Geoenvironmental Engineering 146/5, p. 4020015. DOI: 10.1061/(asce)gt.1943-5606.0002231.

Jacobs, F., Mayer, G. & Wittmann, F.H. (1994): Hochpermeable, zementgebundene Verfüllmörtel für SMA Endlager. Nagra Technischer Bericht NTB 92-11.

Japan Nuclear Cycle Development Institute (1999): H12 project to establish technical basis for HLW Disposal in Japan : Project overview report : The draft second progress report on research and development for the geological disposal of HLW in Japan. JNC, Tokyo.

Jenni, A., Gimmi, T., Alt-Epping, P., Mäder, U. & Cloet, V. (2017): Interaction of ordinary Portland cement and Opalinus Clay: Dual porosity modelling compared to experimental data. Physics and Chemistry of the Earth, Parts A/B/C 99, 22-37. DOI: 10.1016/j.pce.2017.01.004.

Jenni, A. & Mäder, U. (2021): Reactive Transport Simulation of Low-pH Cement Interacting with Opalinus Clay Using a Dual Porosity Electrostatic Model. Minerals 11/7, p. 664. DOI: 10.3390/min11070664.

Jenni, A., Mäder, U., Lerouge, C., Gaboreau, S. & Schwyn, B. (2014): In situ interaction between different concretes and Opalinus Clay. Physics and Chemistry of the Earth, Parts A/B/C 70–71, 71-83. DOI: 10.1016/j.pce.2013.11.004.

Jenni, A., Wersin, P., Thoenen, T., Baeyens, B., Ferrari, A., Gimmi, T., Mäder, U.K., Marschall, P., Hummel, W. & Leupin, O.X. (2019): Benotnite backfill performance in a high-level waste repository: a geochemical perspective. Nagra Technical Report NTB 19-03.

Jennings, H.M., Bullard, J.W., Thomas, J.J., Andrade, J.E., Chen, J.J. & Scherer, G.W. (2008): Characterization and Modeling of Pores and Surfaces in Cement Paste. Journal of Advanced Concrete Technology 6/1, 5-29. DOI: 10.3151/jact.6.5.

Jennings, H.M., Thomas, J.J., Rothstein, D. & Chen, J.J. (2002): Cements as Porous Materials. *In:* Handbook of Porous Solids. Weinheim Germany: Wiley-VCH Verlag GmbH, 2971-3028, available online at http://doi.wiley.com/10.1002/9783527618286.ch40.

Jeong, H.Y., Jun, S.-C., Cheon, J.-Y. & Park, M. (2018): A review on clogging mechanisms and managements in aquifer storage and recovery (ASR) applications. Geosciences Journal 22/4, 667-679. DOI: 10.1007/s12303-017-0073-x.

Kaufmann, J., Loser, R. & Leemann, A. (2009): Analysis of cement-bonded materials by multi-cycle mercury intrusion and nitrogen sorption. Journal of colloid and interface science 336/2, 730-737. DOI: 10.1016/j.jcis.2009.05.029.

KEG (2003): Kernenergiegesetz (KEG) vom 21. März 2003, Stand am 1. Januar 2021. Systematische Sammlung des Bundesrechts SR 732.1, Schweiz.

Keller, L.M., Holzer, L., Schuetz, P. & Gasser, P. (2013a): Pore space relevant for gas permeability in Opalinus clay: Statistical analysis of homogeneity, percolation, and representative volume element. Journal of Geophysical Research: Solid Earth 118, 2799-2812.

Keller, L.M., Holzer, L., Wepf, R. & Gasser, P. (2011): 3D geometry and topology of pore pathways in Opalinus clay: Implications for mass transport. Applied Clay Science 52/43862, 85-95.

Keller, L.M., Schuetz. P., Erni, R., Rossell, M.D., Lucas, F., Gasser, P. & Holzer, L. (2013b): Characterization of multi-scale microstructural features in Opalinus Clay. Microporous and Mesoporous Materials 170, 83-94. DOI: 10.1016/j.micromeso.2012.11.029.

Kia, A., Wong, H.S. & Cheeseman, C.R. (2017): Clogging in permeable concrete: A review. Journal of Environmental Management 193, 221-233.
DOI: 10.1016/j.jenvman.2017.02.018.

Kosakowski, G. & Berner, U. (2013): The evolution of clay rock/cement interfaces in a cementitious repository for low- and intermediate level radioactive waste. Physics and Chemistry of the Earth, Parts A/B/C 64, 65-86. DOI: 10.1016/j.pce.2013.01.003.

Kosakowski, G., Berner, U., Wieland, E., Glaus, M.A. & Degueldre, C. (2014): Geochemical evolution of the L/ILW near-field. Nagra Technical Report NTB 14-11.

Kosakowski, G., Churakov, S., Glaus, M., Guillemot, T., Kulik, D.A., Ma, B., Martin, L., Miron, G.D. & & Prasianakis, N. (2023): Geochemical evolution of the L/ILW near field. Nagra Technischer Bericht NTB 23-03.

Kosakowski, G., Huang, Y. & Wieland, E. (2020): Influence of material heterogeneities, process couplings and aggregate reactivity on the geochemical evolution of the L/ILW repository. Nagra Arbeitsberichte NAB 20-11.

Kosakowski, G. & Smith, P. (2014): Long-term evolution of the Engineered Gas Transport System. Nagra Arbeitsbericht NAB 14-16.

Kuila, U. & Prasad, M. (2013): Specific surface area and pore-size distribution in clays and shales. Geophysical Prospecting 61/2, 341-362. DOI: 10.1111/1365-2478.12028.

Kurganskaya, I. & Rohlfs, R.D. (2020): Atomistic to meso-scale modeling of mineral dissolution: Methods challenges and prospects. American Journal of Science 320/1, 1-26. DOI: 10.2475/01.2020.02.

Lalan, P., Dauzères, A., Windt, L. de, Bartier, D., Sammaljärvi, J., Barnichon, J.-D., Techer, I. & Detilleux, V. (2016): Impact of a 70 °C temperature on an ordinary Portland cement paste/claystone interface: An in situ experiment. Cement and Concrete Research 83, 164-178. DOI: 10.1016/j.cemconres.2016.02.001.

Lanyon, B., Reinicke, A., Papafotiou, A., Finsterle, S. & Romero, E. (*planned*): GAST: Strategy and risk report. Nagra Arbeitsbericht NAB 22-20.

Lanyon, G.W. (2019): Update of synopsis regarding EDZ development and evolution at the Mont Terri Rock Laboratory. Nagra Arbeitsbericht NAB 18-45.

Lanyon, G.W. & Senger, R. (2011): A Structured Approach to the Derivation of Effective Properties for Combined Water and Gas Flow in the EDZ. Transp Porous Med 90/1, 95-112. DOI: 10.1007/s11242-011-9716-y.

Lawrence, C.D. (1984): Transport of oxygen through concrete. British Ceramic Proceedings/35, 277-293, available online at https://jglobal.jst.go.jp/en/detail?JGLOBAL_ID=200902012787171311.

Lea, F.M. & Hewlett, P.C. (eds.) (2004): Lea's chemistry of cement and concrete. 4. ed., Amsterdam, Heidelberg, New York, NY. Elsevier; Elsevier Engineering Information Online-Anbieter, available online at http://www.sciencedirect.com/science/book/9780750662567.

Leemann, A., Loser, R. & Münch, B. (2010): Influence of cement type on ITZ porosity and chloride resistance of self-compacting concrete. Cement and Concrete Composites 32/2, 116-120. DOI: 10.1016/j.cemconcomp.2009.11.007.

Leemann, A., Loser, R., Münch, B. & Lura, P. (2017): Steady-state O2 and CO2 diffusion in carbonated mortars produced with blended cements. Mater Struct 50/6. DOI: 10.1617/s11527-017-1118-3.

Lenormand, R., Touboul, E. & Zarcone, C. (1988): Numerical models and experiments on immiscible displacements in porous media. J. Fluid Mech. 189, 165-187. DOI: 10.1017/S0022112088000953.

Leupin, O.X., Smith, P., Marschall, P., Johnson, L., Savage, D., Cloet, V., Schneider, J. & Senger, R. (2016a): Low- and intermediate-level waste repository-induced effects. Nagra Technical Report NTB 14-14.

Leupin, O.X., Smith, P., Marschall, P., Johnson, L., Savage, D., Cloet, V., Schneider, J. & Senger, R.K. (2016b): High-level waste repository-induced effects. Nagra Technischer Bericht NTB 14-13.

Levasseur, S., Collin, F., Daniels, K., Dymitrowska, M., Harrington, J., Jacops, E., Kolditz, O., Marschall, P., Norris, S., Sillen, X., Talandier, J., Truche, L. & Wendling, J. (2020): Initial State of the Art on Gas Transport in Clayey Materials. Edited by Deliverable D6.1 of the HORIZON 2020 project EURAD, Work Package Gas. EC Grant agreement no: 847593.

Liu, M., Starchenko, V., Anovitz, L.M. & Stack, A.G. (2020): Grain detachment and transport clogging during mineral dissolution in carbonate rocks with permeable grain boundaries. Geochimica et Cosmochimica Acta 280, 202-220. DOI: 10.1016/j.gca.2020.04.022.

Lothenbach, B., Matschei, T., Möschner, G. & Glasser, F.P. (2008): Thermodynamic modelling of the effect of temperature on the hydration and porosity of Portland cement. Cement and Concrete Research 38/1, 1-18. DOI: 10.1016/j.cemconres.2007.08.017.

Luraschi et al., P.: In preparation for publication.

Luraschi, P., Gimmi, T., van Loon, L.R., Shafizadeh, A. & Churakov, S.V. (2020): Evolution of HTO and 36Cl− diffusion through a reacting cement-clay interface (OPC paste-Na montmorillonite) over a time of six years. Applied Geochemistry, p. 104581. DOI: 10.1016/j.apgeochem.2020.104581.

Luraschi, P. (in prep.): Interactions of cement and clay components studied experimentally at small scale. PhD Thesis. University of Berne.

Ma, Z., Pathegama Gamage, R., Rathnaweera, T. & Kong, L. (2019): Review of application of molecular dynamic simulations in geological high-level radioactive waste disposal. Applied Clay Science 168, 436-449. DOI: 10.1016/j.clay.2018.11.018.

Mäder, U., Jenni, A., Lerouge, C., Gaboreau, S., Miyoshi, S., Kimura, Y., Cloet, V., Fukaya, M., Claret, F., Otake, T., Shibata, M. & Lothenbach, B. (2017): 5-year chemico-physical evolution of concrete–claystone interfaces Mont Terri rock laboratory (Switzerland). Swiss Journal of Geosciences 110/1, 307-327. DOI: 10.1007/s00015-016-0240-5.

Manca, D. (2015): Hydro-chemo-mechanical characterisation of sand/bentonite mixtures, with a focus on the water and gas transport properties, Thèse No. 6790. École polytechnique fédérale de Lausanne EPFL, Lausanne.

Marschall, P., Horseman, S. & Gimmi, T. (2005): Characterisation of Gas Transport Properties of the Opalinus Clay, a Potential Host Rock Formation for Radioactive Waste Disposal. Oil & Gas Science and Technology - Rev. IFP 60/1, 121-139. DOI: 10.2516/ogst:2005008.

Martin, L., Jacobs, F., Loser, R., Lothenbach, B., Leemann, A. & Winnefeld, F. (*planned*): Using calcareous aggregates in the backfill mortar M1: A suitability assessment. Nagra Arbeitsbericht NAB 22-44.

Martin, L.H., Leemann, A., Milodowski, A.E., Mäder, U.K., Münch, B. & Giroud, N. (2016): A natural cement analogue study to understand the long-term behaviour of cements in nuclear waste repositories: Maqarin (Jordan). Applied Geochemistry 71, 20-34. DOI: 10.1016/j.apgeochem.2016.05.009.

Marty, N.C.M., Claret, F., Lassin, A., Tremosa, J., Blanc, P., Madé, B., Giffaut, E., Cochepin, B. & Tournassat, C. (2015): A database of dissolution and precipitation rates for clay-rocks minerals. Applied Geochemistry 55, 108-118. DOI: 10.1016/j.apgeochem.2014.10.012.

Marty, N.C.M., Tournassat, C., Burnol, A., Giffaut, E. & Gaucher, E.C. (2009): Influence of reaction kinetics and mesh refinement on the numerical modelling of concrete/clay interactions. Journal of Hydrology 364/1–2, 58-72. DOI: 10.1016/j.jhydrol.2008.10.013.

Mayer, K.U., Blowes, D.W. & Frind, E.O. (2001): Reactive transport modeling of an in situ reactive barrier for the treatment of hexavalent chromium and trichloroethylene in groundwater. Water Resources Research 37/12, 3091-3103. DOI: 10.1029/2001WR000234.

Mayor, J.-C., Velasco, M. & García-Siñeriz, J.-L. (2007): Ventilation experiment in the Mont Terri underground laboratory. Physics and Chemistry of the Earth Parts A/B/C 32/8-14, 616-628. DOI: 10.1016/j.pce.2006.04.030.

Meldrum, F.C. & O'Shaughnessy, C. (2020): Crystallization in Confinement. Advanced Materials 32/31, p. 2001068. DOI: 10.1002/adma.202001068.

Motamedi, M. (1996): Survival of sulfate reducing bacteria at different water activities in compacted bentonite. FEMS Microbiology Letters 141/1, 83-87. DOI: 10.1016/0378-1097(96)00213-3.

Muñoz, J.J., Lloret, A. & Alonso, E. (2003): VE Experiment. Laboratory Report: Characterization of hydraulic rock properties under saturated and non saturated conditions. Project Deliverable D4. Edited by EC Contract FIKW-CT2001-00126. CIMNEUPC, Barcelona.

Nachshon, U., Weisbrod, N., Dragila, M.I. & Grader, A. (2011): Combined evaporation and salt precipitation in homogeneous and heterogeneous porous media. Water Resources Research 47/3. DOI: 10.1029/2010WR009677.

Nagra (2002a): Project Opalinus Clay: Safety report: Demonstration of disposal feasibility for spent fuel, vitrified high-level waste and long-lived intermediate-level waste (Entsorgungsnachweis). Nagra Technischer Bericht NTB 02-05.

Nagra (2002b): Projekt Opalinuston: Synthese der geowissenschaftlichen Untersuchungs-ergebnisse: Entsorgungsnachweis für abgebrannte Brennelemente, verglaste hochaktive sowie langlebige mittelaktive Abfälle. Nagra Technischer Bericht NTB 02-03.

Nagra (2004): Effects of post-disposal gas generation for spent fuel, high level waste and long lived Intermediate level waste sited in Opalinus Clay. Nagra Technischer Bericht NTB 04-06.

Nagra (2008a): Effects of post-disposal gas generation in a repository for low- and intermediate-level waste sited in the Opalinus Clay of Northern Switzerland. Nagra Technischer Bericht NTB 08-07.

Nagra (2008b): Vorschlag geologischer Standortgebiete für ein SMA- und ein HAA-Lager: Begründung der Abfallzuteilung, der Barrierensysteme und der Anforderungen an die Geologie (Bericht zur Sicherheit und Machbarkeit). Nagra Technischer Bericht NTB 08-05.

Nagra (2021a): Entsorgungsprogramm 2021 der Entsorgungspflichtigen. Nagra Technischer Bericht NTB 21-01.

Nagra (2021b): The Nagra Research, Development and Demonstration (RD&D) Plan for the Disposal of Radioactive Waste in Switzerland. Nagra Technical Report NTB 21-02.

Nagra (2021c): Verschlusskonzept für ein geologisches Tiefenlager. Nagra Arbeitsbericht NAB 21-12.

Nagra (2022): Ableitung Anforderungen an Lagerauslegung aus Sicht Langzeitsicherheit. Nagra Arbeitsbericht NAB 21-02.

Nagra (2023): Chemical Criteria for Waste Group Classification: a Model Approach. Nagra Arbeitsbericht NAB 23-28.

Nagra NAB 24-20 (*planned*): Phenomenological Description of the Evolution of a Combined Geological Repository for Radioactive Waste at Nörlich Lägern in Opalinus Clay. Nagra Arbeitsbericht NAB 24-20.

Nagra NTB 24-22 (*planned*): Synthesis of the Performance Assessment for a Combined Repository at the Nördlich Lägern Site. Nagra Technical Report NTB 24-22.

Nagra NTB 24-23 (*planned*): Production, consumption and transport of gases in a deep geological repository for combined disposal in Switzerland. Nagra Technical Report NTB 24-23.

Nakarai, K., Shibata, M., Sakamoto, H., Owada, H. & Kosakowski, G. (2021a): Calcite Precipitation at Cement–Bentonite Interface. Part 1: Effect of Carbonate Admixture in Bentonite. Journal of Advanced Concrete Technology 19/5, 433-446. DOI: 10.3151/jact.19.433.

Nakarai, K., Watanabe, M., Koibuchi, K. & Kosakowski, G. (2021b): Calcite Precipitation at Cement–Bentonite Interface. Part 2: Accelera-tion of Transport by an Electrical Gradient. Journal of Advanced Concrete Technology 19/5, 447-461. DOI: 10.3151/jact.19.447.

Nishiyama, N. & Yokoyama, T. (2013): Does the reactive surface area of sandstone depend on water saturation?-The role of reactive-transport in water film. Geochimica et Cosmochimica Acta 122, 153-169. DOI: 10.1016/j.gca.2013.08.024.

Nishiyama, N. & Yokoyama, T. (2021): Water Film Thickness in Unsaturated Porous Media: Effect of Pore Size Pore Solution Chemistry and Mineral Type. Water Resources Research 57/6, e2020WR029257. DOI: 10.1029/2020WR029257.

Noiriel, C. & Daval, D. (2017): Pore-Scale Geochemical Reactivity Associated with CO2 Storage: New Frontiers at the Fluid-Solid Interface. Accounts of Chemical Research 50/4, 759-768. DOI: 10.1021/acs.accounts.7b00019.

Nyame, B.K. & Illston, J.M. (1981): Relationships between permeability and pore structure of hardened cement paste. Magazine of Concrete Research 33/116, 139-146. DOI: 10.1680/macr.1981.33.116.139.

Olsen, H.W. (1969): Simultaneous Fluxes of Liquid and Charge in Saturated Kaolinite. Soil Science Society of America Journal 33/3, 338-344. DOI: 10.2136/sssaj1969.03615995003300030006x.

Papafotiou, A. & Senger, R.K. (2016a): Sensitivity analyses of gas release from a L/ILW repository in the Opalinus Clay including the microbial consumption of hydrogen. Nagra Arbeitsbericht NAB 16-07.

Papafotiou, A. & Senger, R.K. (2016b): Sensitivity analyses of gas release from a SF/HLW repository in the Opalinus Clay. Nagra Arbeitsbericht NAB 16-08.

Pinson, M.B., Masoero, E., Bonnaud, P.A., Manzano, H., Ji, Q., Yip, S., Thomas, J.J., Bazant, M.Z., van Vliet, K.J. & Jennings, H.M. (2015): Hysteresis from Multiscale Porosity: Modeling Water Sorption and Shrinkage in Cement Paste. Physical Review Applied 3/6, p. 64009. DOI: 10.1103/PhysRevApplied.3.064009.

Pitty, A.F. & Alexander, W.R. (Bedrock Geosciences) (2014): A natural analogue study of cement buffered, hyperalkaline groundwaters and their interaction with a repository host rock IV : an examination of the Khushaym Matruk (central Jordan) and Maqarin (norhtern Jordan) sites. 2, Auenstein Switzerland.

Poonoosamy, J., Kosakowski, G., van Loon, L.R. & Mäder, U. (2015): Dissolution–precipitation processes in tank experiments for testing numerical models for reactive transport calculations: Experiments and modelling. Journal of Contaminant Hydrology 177–178, 1-17. DOI: 10.1016/j.jconhyd.2015.02.007.

Powers, T., Copeland, L.E., Hayes, J.C. & Mann, H.M. (1954): Permeablity of Portland Cement Paste. undefined, available online at https://www.semanticscholar.org/paper/Permeablity-of-Portland-Cement-Paste-Powers-Copeland/e2fbb6f6d960f4292d4dcf4d1bf3815f82cf8470.

Prasianakis, N.I., Curti, E., Kosakowski, G., Poonoosamy, J. & Churakov, S.V. (2017): Deciphering pore-level precipitation mechanisms. Scientific Reports 7/1, p. 13765. DOI: 10.1038/s41598-017-14142-0.

Prasianakis, N.I., Kosakowski, G., Gimmi, T., Miron, G.D., Pfingsten, W. & Churakov, S.V. (2022): Cement-Clay Synthesis of transport across the cement-clay interface. Nagra Arbeitsbericht NAB 22-034.

Prieto, M. (2014): Nucleation and supersaturation in porous media (revisited). Mineralogical Magazine 78/6, 1437-1447. DOI: 10.1180/minmag.2014.078.6.11.

Putnis, A. (2015): Transient Porosity Resulting from Fluid–Mineral Interaction and its Consequences. Reviews in Mineralogy and Geochemistry 80/1, 1-23. DOI: 10.2138/rmg.2015.80.01.

Putnis, A. & Fernandez-Diaz, L. (1990): Factors controlling the kinetics of crystallization: Supersaturation evolution in a porous medium. Application to barite crystallization. Geological Magazine 127/6, 485-495. DOI: 10.1017/S0016756800015417.

Rad, M.N. (2014): Pore-Scale Investigation of Salt Precipitation during Evaporation from Porous Media. PhD Thesis. University of Manchester.

Reichardt, C. (2007): Solvents and Solvent Effects: An Introduction. Org. Process Res. Dev. 11/1, 105-113. DOI: 10.1021/op0680082.

Roberge, P.R. (2019): Handbook of Corrosion Engineering, Third Edition. 3rd editio, New York. McGraw-Hill Education, available online at https://www.accessengineeringlibrary.com/content/book/9781260116977.

Rodríguez-Valverde, M.Á. & Tirado Miranda, M. (2011): Derivation of Jurin's law revisited. Eur. J. Phys. 32/1, 49-54. DOI: 10.1088/0143-0807/32/1/005.

Romero, E. (2013): A microstructural insight into compacted clayey soils and their hydraulic properties. Engineering Geology 165, 3-19. DOI: 10.1016/j.enggeo.2013.05.024.

Romero, E. & Gómez, R. (2013): Water and air permeability tests on deep core samples from Schlattingen SLA-1 borehole. Nagra Arbeitsbericht NAB 13-51.

Romero, E. & Gonzales-Blanco, L. (2018): Hydromechanical processes associated with gas transport in Wyoming granular bentonite – Complementary laboratory experiments carried out at UPC in 2017. Nagra Arbeitsbericht NAB 18-09.

Romero, E. & González-Blanco, L. (2015): Complementary water and air permeability tests on core samples from Schlatingen SLA-1 borehole. Nagra Arbeitsbericht NAB 15-06.

Romero, E. & Gonzalez-Blanco, L. (2017): Hydro-mechanical processes associated with gas transport in MX-80 bentonite in the context of Nagra's RD&D programme. Nagra Arbeitsbericht NAB 17-09.

Romero, E., Senger, R., Marschall, P. & Gómez, R.: Air Tests on Low-Permeability Claystone Formations. Experimental Results and Simulations. Keynote lecture. Proc. Int. Workshop on Advances in Multiphysical Testing of Soils and Shales, Lausanne, Switzerland, September 2012. In: Multiphysical Testing of Soils and Shales. L. Laloui & A. Ferrari (eds.). Springer Series in Geomechanics & Geoengineering. Springer-Verlag, Berlin: 69-83.

Ruan, K. & Fu, X.-L. (2021): A modified Kozeny–Carman equation for predicting saturated hydraulic conductivity of compacted bentonite in confined condition. Journal of Rock Mechanics and Geotechnical Engineering. DOI: 10.1016/j.jrmge.2021.08.010.

Russell, D., Basheer, P.A.M., Rankin, G.I.B. & Long, A.E. (2001): Effect of relative humidity and air permeability on prediction of the rate of carbonation of concrete. Proceedings of the Institution of Civil Engineers - Structures and Buildings 146/3, 319-326. DOI: 10.1680/stbu.2001.146.3.319.

Savage, D. & Cloet, V. (2018): A review of Cement-Clay Modelling. Nagra Arbeitsbericht NAB 18-24.

Šavija, B. & Luković, M. (2016): Carbonation of cement paste: Understanding challenges and opportunities. Construction and Building Materials 117, 285-301. DOI: 10.1016/j.conbuildmat.2016.04.138.

Schanz, T. (ed.) (2007): Moisture effects on argillaceous rocks. Zhang, C. L.; Rothfuchs, T. 2nd International Conference of Mechanics of Unsaturated Soils. Springer Proceedings in Physics, 12. springer.

Schönlin, K. & Hilsorf, H.K. (1988): Permeability as a Measure of Potential Durability of Concrete-Development of a Suitable Test Apparatus. SP-108: Permeability of Concrete.

Schramm, L.L. (1994): The Language of Colloid and Interface Science. Environmental Science and Technology 28/13. DOI: 10.1021/es00062a732.

Scott, S.W. & Driesner, T. (2018): Permeability Changes Resulting from Quartz Precipitation and Dissolution around Upper Crustal Intrusions. Geofluids 2018, 1-19. DOI: 10.1155/2018/6957306.

Scrivener, K.L., Crumbie, A.K. & Laugesen, P. (2004): The Interfacial Transition Zone (ITZ) Between Cement Paste and Aggregate in Concrete. Interface Science 12/4, 411-421. DOI: 10.1023/B:INTS.0000042339.92990.4c.

Seigneur, N., Mayer, K.U. & Steefel, C.I. (2019): Reactive Transport in Evolving Porous Media. Reviews in Mineralogy and Geochemistry 85/1, 197-238. DOI: 10.2138/rmg.2019.85.7.

Seiphoori, A. (2015): Thermo-hydro-mechanical characterisation and modelling of Wyoming granular bentonite. Nagra Technischer Bericht NTB 15-05.

Sellin, P. & Leupin, O. (2013): The use of clay as an engineered barrier in radioactive-waste management – A review. Clays and Clay Minerals 61, 477-498.

Senger, R., Papafotiou, A. & Marschall, P. (2013): Gas related property distributions in the proposed host rock formations of the candidate siting regions in Northern Switzerland and in the Helvetic Zone. Nagra Arbeitsbericht NAB 13-83.

Senger, R., Papafotiou, A. & Marschall, P. (2014a): Thermo-hydraulic simulations of the nearfield of a SF/HLW repository during early- and late-time post-closure period. Nagra Arbeitsbericht NAB 14-11.

Senger, R., Romero, E., Ferrari, A.K. & Paul Marschall (2014b): Characterization of gas flow through low-permeability claystone: laboratory experiments and two-phase flow analyses. Geological Society, London, Special Publications 400, 1-13, available online at DOI: 10.1144/SP400.15.

Senger, R.K. & Ewing, J. (2009): Gas-L/ILW: Gas pressure buildup and transport in a deep geologic L/ILW repository in Opalinus Clay using large-scale and local-scale models. Nagra Arbeitsbericht NAB 09-17.

Senger, R.K., Papafotiou, A. & Namhata, A. (2018): Gas-test interpretation incorporating sub-scale information in bentonite. Nagra Arbeitsbericht NAB 18-33.

Shafizadeh, A., Gimmi, T., van Loon, L.R., Kaestner, A., Lehmann, E., Mäder, U.K. & Churakov, S.V. (2015): Quantification of water content across a cement-clay interface using high resolution neutron radiography. Physics Procedia 69/October 2014, 516-523. DOI: 10.1016/j.phpro.2015.07.073.

Shafizadeh, A., Gimmi, T., van Loon, L.R., Kaestner, A.P., Mäder, U.K. & Churakov, S.V. (2020): Time-resolved porosity changes at cement-clay interfaces derived from neutron imaging. Cement and Concrete Research 127/October 2019, p. 105924. DOI: 10.1016/j.cemconres.2019.105924.

Small, J. (2019): Final synthesis report for MIND WP1. Deliverable D1.9. Edited by European Commission, MIND Project (Microbiology in Nuclear Waste). Grant Agreement: 661880.

Soler, J.M. (2013): Reactive transport modeling of concrete-clay interaction during 15 years at the Tournemire Underground Rock Laboratory. European Journal of Mineralogy 25/4, 639-654. DOI: 10.1127/0935-1221/2013/0025-2324.

Stack, A.G. (2015): Precipitation in Pores: A Geochemical Frontier. Reviews in Mineralogy and Geochemistry 80/1, 165-190. DOI: 10.2138/rmg.2015.80.05.

Stefanoni, M., Angst, U. & Elsener, B. (2018): Corrosion rate of carbon steel in carbonated concrete – A critical review. Cement and Concrete Research 103, 35-48. DOI: 10.1016/j.cemconres.2017.10.007.

Tang, Y., Yao, X., Chen, Y., Zhou, Y., Zhu, D.Z., Zhang, Y., Zhang, T. & Peng, Y. (2020): Experiment research on physical clogging mechanism in the porous media and its impact on permeability. Granular Matter 22/2, p. 37. DOI: 10.1007/s10035-020-1001-8.

Tashiro, S., Fujiwara, A. & Senoo, M. (1998): Study on the permeability of engineered barriers for the enhancement of a radioactive waste repository system. Nuclear Technology 121/1, 14-23.

Taylor, H.F.W. (1997): Cement Chemistry. 2nd. ed., London UK. Thomas Telford.

Tinseau, E., Bartier, D., Hassouta, L., Devol-Brown, I. & Stammose, D. (2006): Mineralogical characterization of the Tournemire argillite after in situ interaction with concretes. Waste Management 26/7, 789-800. DOI: 10.1016/j.wasman.2006.01.024.

Torkzaban, S., Bradford, S.A., Vanderzalm, J.L., Patterson, B.M., Harris, B. & Prommer, H. (2015a): Colloid release and clogging in porous media: Effects of solution ionic strength and flow velocity. Journal of Contaminant Hydrology 181, 161-171. DOI: 10.1016/j.jconhyd.2015.06.005.

Torkzaban, S., Vanderzalm, J., Treumann, S. & Amirianshoja, T. (CSIRO) (2015b): Understanding and quantifying clogging and its management during re-injection of CSG water permeates, brines and blends, Australia.

Tournassat, C. & Appelo, C. (2011): Modelling approaches for anion-exclusion in compacted Na-bentonite. Geochimica et Cosmochimica Acta 75/13, 3698-3710. DOI: 10.1016/j.gca.2011.04.001.

Tournassat, C. & Steefel, C.I. (2015): Ionic Transport in Nano-Porous Clays with Consideration of Electrostatic Effects. Reviews in Mineralogy and Geochemistry 80/1, 287-329. DOI: 10.2138/rmg.2015.80.09.

Tournassat, C. & Steefel, C.I. (2019): Reactive Transport Modeling of Coupled Processes in Nanoporous Media. Reviews in Mineralogy and Geochemistry 85/1, 75-109. DOI: 10.2138/rmg.2019.85.4.

Trotignon, L., Thouvenot, P., Munier, I., Cochepin, B., Piault, E., Treille, E., Bourbon, X. & Mimid, S. (2011): Numerical Simulation of Atmospheric Carbonation of Concrete Components in a Deep Geological Radwaste Disposal Site During Operating Period. Nuclear Technology 174/3, 424-437. DOI: 10.13182/NT11-A11750.

Tyagi, M., Gimmi, T. & Churakov, S.V. (2013): Multi-scale micro-structure generation strategy for up-scaling transport in clays. Advances in Water Resources 59, 181-195. DOI: 10.1016/j.advwatres.2013.06.002.

Valkó, P. (2013): Hydraulic Fracturing. *In:* Inc, J. W. &. S., Kirk, R. E. & Othmer, D. F.(eds.): Kirk-Othmer Encyclopedia of Chemical Technology. (Wiley online library). New York: Wiley, 1-24.

van Brakel, J. & Heertjes, P.M. (1974): Analysis of diffusion in macroporous media in terms of a porosity a tortuosity and a constrictivity factor. International Journal of Heat and Mass Transfer 17/9, 1093-1103. DOI: 10.1016/0017-9310(74)90190-2.

van Loon, L.R., Soler, J.M., Müller, W. & Bradbury, M.H. (2004a): Anisotropic Diffusion in Layered Argillaceous Rocks: A Case Study with Opalinus Clay. Environmental science & technology 38/21, 5721-5728. DOI: 10.1021/es049937g.

van Loon, L.R., Wersin, P., Soler, J.M., Eikenberg, J., Gimmi, T., Hernán, P., Dewonck, S. & Savoye, S. (2004b): In-situ diffusion of HTO $^{22}Na^{+}$ Cs^{+} and I^{-} in Opalinus Clay at the Mont Terri underground rock laboratory. Radiochimica Acta 92/9–11, 757-763. DOI: 10.1524/ract.92.9.757.54988.

Villani, C., Loser, R., West, M.J., Di Bella, C., Lura, P. & Weiss, W.J. (2014): An inter lab comparison of gas transport testing procedures: Oxygen permeability and oxygen diffusivity. Cement and Concrete Composites 53, 357-366. DOI: 10.1016/j.cemconcomp.2014.05.004.

Vinsot, A., Appelo, C.A.J., Lundy, M., Wechner, S., Cailteau-Fischbach, C., Donato, P. de, Pironon, J., Lettry, Y., Lerouge, C. & Cannière, P. de (2017): Natural gas extraction and artificial gas injection experiments in Opalinus Clay Mont Terri rock laboratory (Switzerland). Swiss Journal of Geosciences 110/1, 375-390. DOI: 10.1007/s00015-016-0244-1.

Vinsot, A., Appelo, C.A.J., Lundy, M., Wechner, S., Lettry, Y., Lerouge, C., Fernández, A.M., Labat, M., Tournassat, C., Canniere, P. de, Schwyn, B., Mckelvie, J., Dewonck, S., Bossart, P. & Delay, J. (2014): In situ diffusion test of hydrogen gas in the Opalinus Clay. Geological Society, London, Special Publications 400/1, 563-578. DOI: 10.1144/SP400.12.

Wagner, M. (2019): DGMK 06 microbiological aspects of hydrogen storage in porous underground storages. *In:* EAGE/DGMK Joint Workshop on Underground Storage of Hydrogen, vol. 2019: European Association of Geoscientists and Engineers, EAGE, 1-3, available online at https://www.earthdoc.org/content/papers/10.3997/2214-4609.201900260.

Wantanaphong, J., Mooney, S.J. & Bailey, E.H. (2006): Quantification of pore clogging characteristics in potential permeable reactive barrier (PRB) substrates using image analysis. Journal of Contaminant Hydrology 86/3–4, 299-320. DOI: 10.1016/j.jconhyd.2006.04.003.

Warthmann, R., Mosberger, L. & Baier, U. (2013): Langzeit-Degradation von organischen Polymeren unter SMA-Tiefenlagerbedingungen. Nagra Technischer Bericht NTB 13-04.

Watkinson, D. & Lewis, M. (2004): ss Great Britain iron hull: modelling corrosion to define storage relative humidity. *In:* Metal 2004, vol. 44, 88-102, available online at http://www.recollections.nma.gov.au/shared/libraries/attachments/publications/metal_04_proceedings/section_1_preventive_conservation/files/7822/NMA_metals_s1_p7_ss_great_britian_iron_hull.pdf.

Wellman, H.W. & Wilson, A.T. (1965): Salt weathering a neglected geological erosive agent in coastal and arid environments [6]. Nature 205/4976, 1097-1098. DOI: 10.1038/2051097a0.

Wigger, C., Plöze, M. & van Loon, L.R. (2018): Pore Geometry as a Limiting Factor for Anion Diffusion in Argillaceous Rocks. Clays and Clay Minerals 66/4, 329-338. DOI: 10.1346/CCMN.2018.064101.

Wilson, J., Bateman, K. & Tachi, Y. (2021): The impact of cement on argillaceous rocks in radioactive waste disposal systems: A review focusing on key processes and remaining issues. Applied Geochemistry 130/January, p. 104979. DOI: 10.1016/j.apgeochem.2021.104979.

Winter, N.B. (2009): Understanding Cement: An introduction to cement production, cement hydration and deleterious processes in concrete, Woodbridge UK. WHD Microanalysis Consultants.

Xie, M., Mayer, K.U., Claret, F., Alt-Epping, P., Jacques, D., Steefel, C., Chiaberge, C. & Simunek, J. (2015): Implementation and evaluation of permeability-porosity and tortuosity-porosity relationships linked to mineral dissolution-precipitation. Comput Geosci 19/3, 655-671. DOI: 10.1007/s10596-014-9458-3.

Yan, H., Sedighi, M. & Jivkov, A. (2021): Modelling the effects of water chemistry and flowrate on clay erosion. Engineering Geology 294, p. 106409. DOI: 10.1016/j.enggeo.2021.106409.

Yang, Y., Wu, Y., Lu, Y., Shi, M. & Chen, W. (2021): Microorganisms and their metabolic activities affect seepage through porous media in groundwater artificial recharge systems: A review. Journal of Hydrology 598. DOI: 10.1016/j.jhydrol.2021.126256.

Yokoyama, S., Shimbashi, M., Minato, D., Watanabe, Y., Jenni, A. & Mäder, U. (2021): Alteration of bentonite reacted with cementitious materials for 5 and 10 years in the Mont Terri rock laboratory (CI experiment). Minerals 11/3, 1-17. DOI: 10.3390/min11030251.

Young, J. (1988): Review of the Pore Structure of Cement Paste and Concrete and its Influence on Permeability. undefined, available online at https://www.semanticscholar.org/paper/Review-of-the-Pore-Structure-of-Cement-Paste-and-on-Young/d726a7f0d06a1501b2cc8b77ff5200b52f95cb38.

Youssef, N., Elshahed, M.S. & Mcinerney, M.J. (2009): Chapter 6 - Microbial Processes in Oil Fields: Culprits, Problems, and Opportunities. Advances in Applied Microbiology 66, 141-251. DOI: 10.1016/S0065-2164(08)00806-X.

Yuan, Y. & Rezaee, R. (2019): Comparative Porosity and Pore Structure Assessment in Shales: Measurement Techniques Influencing Factors and Implications for Reservoir Characterization. Energies 12/11, p. 2094. DOI: 10.3390/en12112094.

Zehnder, K. & Arnold, A. (1989): Crystal growth in salt efflorescence. Journal of Crystal Growth 97/2, 513-521. DOI: 10.1016/0022-0248(89)90234-0.

App. A Description of the seals

The basic design concept is broadly similar for all types of seals (see Fig. 2-2). Nonetheless, as explained in this appendix, there are differences, resulting from the different roles of each seal type within the repository system. The provisional designs for the repository seals presented in this appendix according to Nagra (2021) have been selected such that they:

- are judged likely to satisfy the demands of engineering feasibility and of operational and long-term safety
- respect boundary conditions, notably the specifications of the waste to be disposed of and the characteristics of the selected site

A.1 SF/HLW emplacement drifts seals (V1-HLW)

A V1-HLW seal is to be installed at the open end of each HLW emplacement drift immediately after it is backfilled. The prompt sealing of the HLW emplacement drifts ensures the rapid isolation of the radioactive waste.

The lining installed along the drifts will be fully or partially removed where the seals are to be emplaced. Possible variants could include leaving parts of the lining in place. For a detailed discussion see Section 5 in Nagra (2021).

The sealing elements will be constructed with bentonite material, which is emplaced as pellets or granules. The target dry emplacement density is 1.45 kg/m^3. The current target intrinsic permeability for water of the seals is 10^{-18} to 10^{-19} m^2 (see Tab. 2-1). The provisional length of each sealing elements is about 10 m (ca. three times the tunnel diameter; 2.8 m inner diameter and 3.5-3.7 m with robbed tunnel support).

Each sealing element is enclosed by two abutments consisting of non-reinforced, structural concrete, with transition layers of sand, gravel, masonry, etc. on either side of each of the abutments. The entire sealing structure has a provisional length of 20.0 m to 25.0 m, calculated with ca 4.0 m length for each of the two abutments and about 1.0 m to 1.5 m for each of the four transition layers, together with their formworks (Fig. A-1).

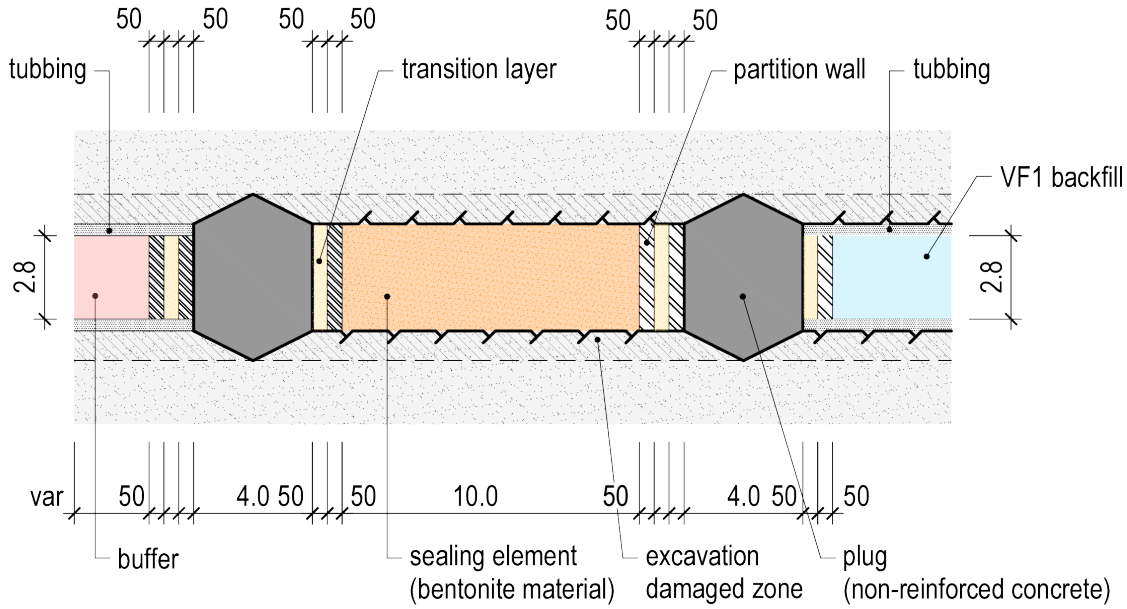

Fig. A-1: Longitudinal section of a provisional V1-HLW seal
Adapted from Nagra (2021)

A.2 L/ILW emplacement cavern seals (V1-L/ILW)

Each L/ILW disposal cavern will be closed with a V1-L/ILW seal which is constructed in the branch tunnel that connects the cavern to the operation tunnel (Fig. A-2).

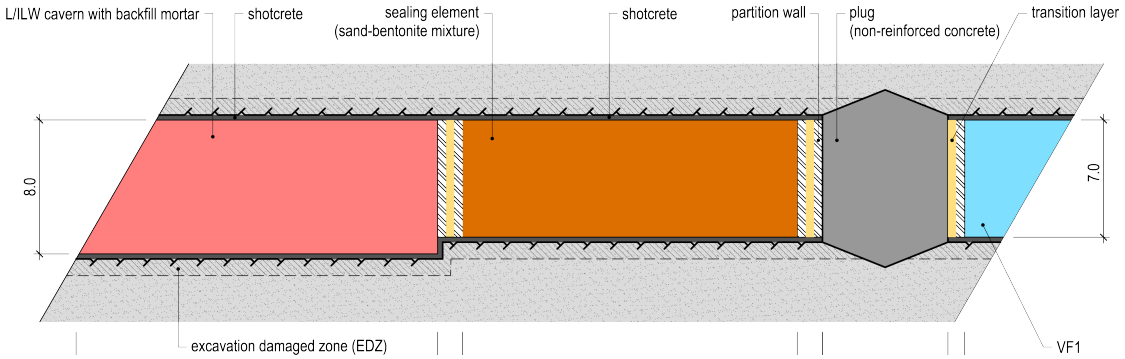

Fig. A-2: Longitudinal section of a provisional V1-L/ILW seal
Adapted from Nagra (2021).

As in the case of the V1-HLW seal, rock support will be fully or partially removed where the seals are to be emplaced.

The sealing element separates the loose VF1 backfill from the storage field of the L/ILW cavern. A sand-bentonite mixture in a weight-ratio of ca. 80:20 is used, which provides the required intrinsic permeability to water of 10^{-17} to 10^{-18} m^2 (Tab. 2-1). This permeability ensures gas pressure equalisation between the L/ILW emplacement cavern and the VF1 backfill, which has the role of providing additional gas storage volume.

On the cavern side of the seal, instead of a concrete abutment, the porous backfill mortar serves to contain the sealing element and is separated from the sealing element by a transition layer. A concrete abutment is placed on the other side of the sealing element, with a transition layer on either side. The dimensioning of the seal, based on a branch tunnel diameter of approximately 6.5 – 7 m, results in a length of ca. 30 m.

A.3 Disposal area seals (V2)

The V2 seals serve to close the L/ILW and HLW disposal areas and the access to the pilot facilities. The seals are constructed after all waste has been emplaced and the tunnels are backfilled with VF1.

The V2 seals for the HLW and L/ILW repository have the same dimensions and components (Fig. A-3) but may differ in the material used for the sealing element (see below). Tunnel sections several decametres in length are required for each of these seals.

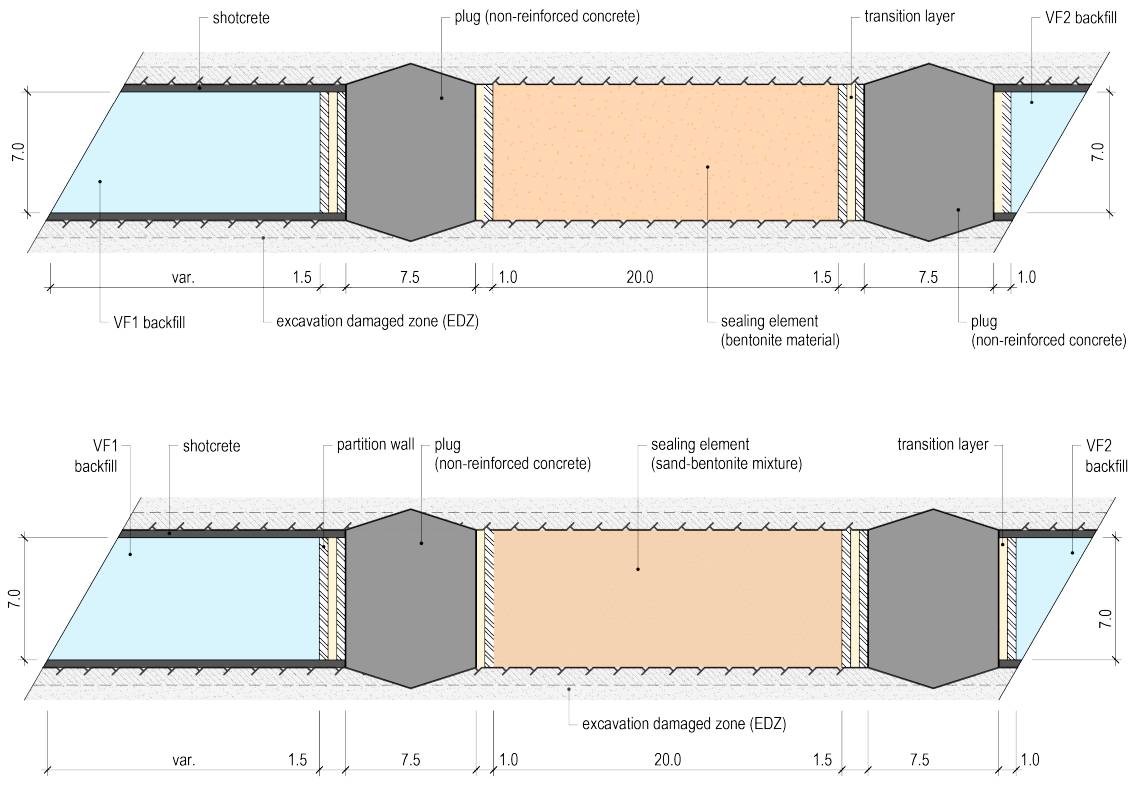

Fig. A-3: Longitudinal section of a provisional V2-HLW seal (above) and a provisional V2-L/ILW seal (below), assuming compacted bentonite is used for the sealing element of the formed, and sand-bentonite for the latter

Adapted from Nagra (2021)

According to the current design, a sand-bentonite mixture will be used for the V2-L/ILW sealing element, with an intrinsic permeability to water of 10^{-17} to 10^{-18} m^2 (Tab. 2-1). This permeability ensures gas pressure equalisation between the VF1 backfill and the VF2 backfill, providing additional gas storage volume. In the case of a combined repository, as well as for a separate HLW repository, the V2-HLW sealing element will have a lower intrinsic permeability of 10^{-17} to 10^{-19} m^2 to prevent or hinder the flow of gas from the L/ILW disposal section to the VF1 backfill of the HLW disposal section, and thus reduce a major potential source of interaction between the two disposal sections of the combined repository. The rock support in the tunnel sections containing sealing elements could be partially or completely removed.

Each sealing element is enclosed by two abutments consisting of high-quality structural concrete, with transition layers of sand, gravel, masonry, etc. on either side of each of the abutments. The tunnel diameter in which the seals are installed is expected to be ca. 6.5 to 7 m. According to the current design, the pre-dimensioning of the abutment suggests they will each require a length of approx. 7.5 m. The sealing elements have a length of about 20.0 m, which corresponds to about three times the tunnel diameter. The entire sealing structure has a length of about 40 m, calculated with about 1.0 m to 1.5 m for each of the four transition layers, together with their formworks (Fig. A-3).

A.4 Shaft seals (V3)

The V3 seals serve to seal the shafts up to the top of the Opalinus Clay, preventing the ingress of water from the aquifers above and limiting the release of radionuclides from the repository. Once the V3 seals are constructed, the repository is transferred to a passive state.

The design of the V3 seals, which is shown in Fig. A-4, is based on the following three assumptions (Nagra 2021):

- The geological repository is located approximately in the middle of the Opalinus Clay host rock. Approximately half the thickness of the Opalinus Clay is therefore available for the construction of the V3 seals.
- Rock support elements will be dismantled before seal construction to maximise the hydraulic resistance provided by the seals. Only intermittent or linear securing elements will remain in the rock to support any zones of weakness.

According to the current design Nagra (2021), the sealing elements will be constructed using bentonite material in the form of granules, pellets, shaped blocks or a combination of these, with a target intrinsic permeability for water of 10^{-18} to 10^{-19} m^2 (see Tab. 2-1). Every ten metres, the sealing elements are interrupted by filter layers of fine sand, each with a thickness of about half a metre. These will tend to saturate with water uniformly, thus favouring evenly-distributed saturation and swelling of the bentonite material as a whole, and the breaking up any preferential transport pathways.

Each sealing element is enclosed on either side by abutments. The material used for the lower abutment should retain its integrity in the long term and not detrimentally affect the chemical environment, avoiding any chemical alteration of the bentonite. For these reasons, cement-based construction material is not used. Candidate materials include, for example, hard-rock ballast (limestone rubble). The lower abutment fills the entire shaft sump, so that small amounts of water entering through the shaft would be initially collected here. The lower abutment extends vertically upwards to over three times the height of the tunnel at the base of the shaft. A wedge with a gradient of about 20° is created where the tunnel joins the shaft to improve the rock mechanical conditions and to facilitate backfilling with ballast. A target installation density for the ballast is set that provides a stiffness (elastic modulus) of between 200 and 300 MPa. Together with load transfer via the silo effect, this is sufficient to guarantee the serviceability of the sealing element.

In addition to its own weight, the lower abutment absorbs the swelling pressure from the sealing element.

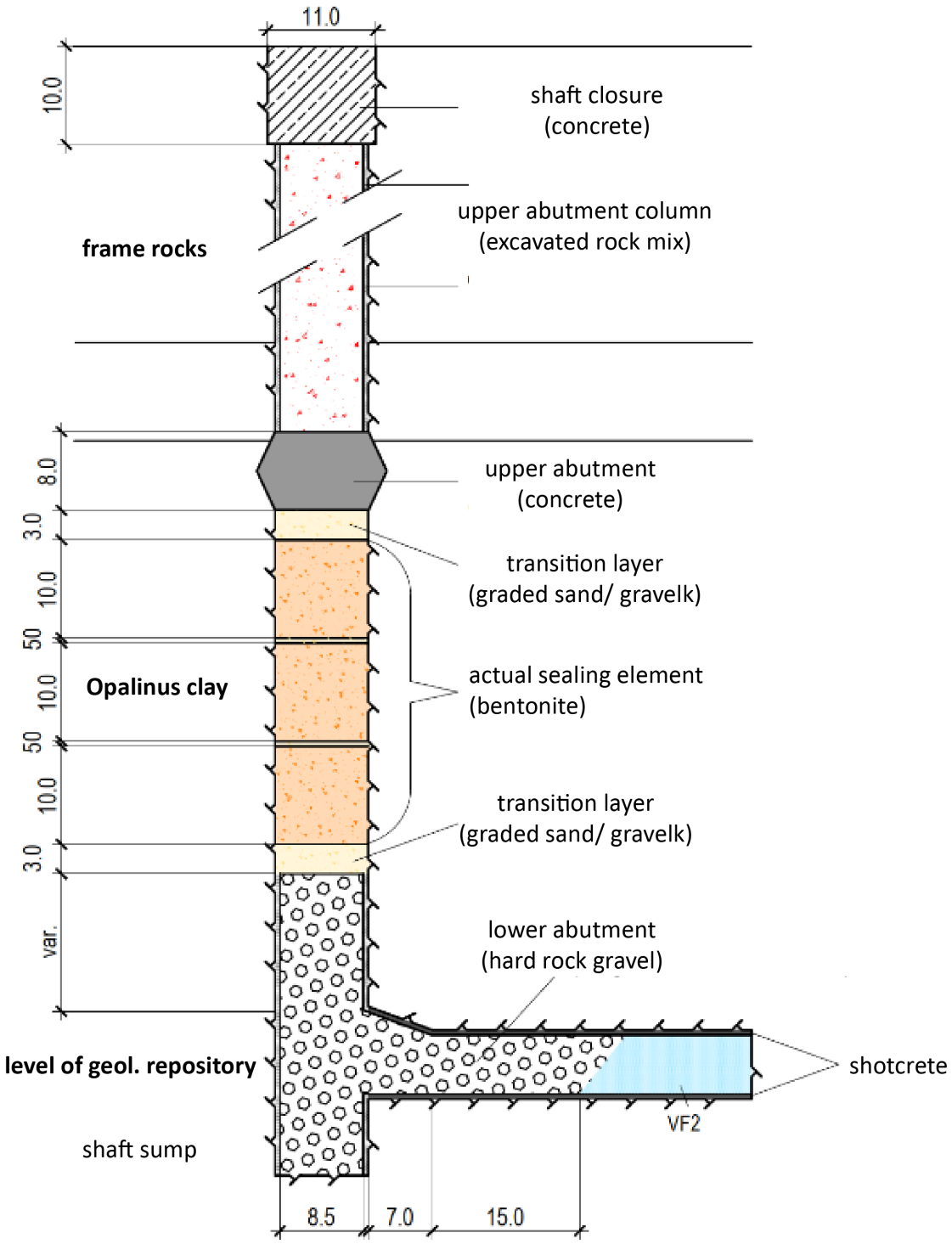

Fig. A-4: Longitudinal section of a V3 seal
Adapted from Nagra (2021)

The upper abutment is composed of non-reinforced, high-quality structural concrete. For static reasons, load transfer into the surrounding rock occurs preferentially via normal stresses, and, to ensure positional stability, the abutment has a double-conical shape, which has proven successful in shaft closures elsewhere (e.g., Dixon et al. 2014). In order to avoid stress increases from bending, the height of the upper abutment corresponds approximately to its diameter. The widening angle of 25° supports load transfer sufficiently via normal stresses into the rock and also simplifies excavation and concreting during construction. In addition to its own weight, the upper abutment absorbs the swelling pressure from the sealing element from below and the hydrostatic pressure of the overburden water from above.

Transition layers, about 3 m in thickness, are used to separate both abutments from the sealing element. The lower transition layer is composed of four to six individual layers that together create the transition from coarse-grained hard rock gravel to bentonite while maintaining filter stability. According to the current design, geotextiles can be considered as an option for these layers (Nagra 2021).

A.5 References

Dixon, D.A., Priyanto, D.G., Martino, J.B., De Combarieu, M., Johnsson, R, Korkeakoski, P. & Villagran, J. (2014): Enhanced Sealing Project (ESP): Evolution of a full-sized bentonite and concrete shaft seal. In: Geological Society, London, Special Publications 400 (1), 63-70.

Nagra (2021): Verschlusskonzept für ein geologisches Tiefenlager. Nagra Arbeitsbericht NAB 21-12.

App. B Gas transport mechanisms

Phenomenological considerations suggest the following subdivision of the basic gas transport mechanisms, as illustrated for the Opalinus Clay in Chapter 5, Fig. 5-1:

- advective-diffusive transport of gas dissolved in pore water
- visco-capillary two-phase flow
- dilatancy-controlled gas flow
- gas transport along macroscopic tensile fractures (hydro- and gas-fracturing)

An overview of gas transport mechanisms is given in Sections 5.1.1 to 5.1.4; a more detailed description is provided in this following appendix.

B.1 Transport of gas dissolved in pore water

Advective and diffusive transport of gas dissolved in pore water is characterised by three fundamental laws (Helmig 1997):

- Darcy's law, which describes advective groundwater flow under the impact of pressure and gravitational forces
- Fick's law, which represents the diffusion of dissolved gas due to the concentration gradients in the pore water
- Henry's law, which describes the solubility of gas in pore water

Darcy's law represents the general basis for the quantitative descriptions of groundwater flow. It denotes the linear correlation between the specific discharge (Darcy velocity) through a representative elementary volume and the hydraulic gradient. The proportionality constant for the relationship is provided by the hydraulic conductivity. Darcy's law is applicable only within certain limits (Nagra 2008).

Diffusion in a porous medium in its simplest form can be described by Fick's first law (Domenico & Schwarz 1990):

$$J = -D_d \,\mathrm{grad}(C)$$

with J being the diffusive flux [mol/L^{2}T]; D_d the effective diffusion coefficient [L^2/T] and C the concentration [mol/L^3] of a species. The effective diffusion coefficient depends on the molecular diffusion of a species in free solution and the porous medium structure which is typically expressed in terms of the porosity and the tortuosity (see Greenkorn 1972, Millingon & Quirk 1961).

Gas dissolution and exsolution can transfer significant quantities of mass between the gas phase and the pore water in a porous medium. According to Henry's law, the partial pressure of an ideal gas in the gas phase is proportional to the concentration of the gas in the aqueous phase (Domenico & Schwarz 1990):

$$K_H = \frac{(\mathrm{gas})_{aq}}{P_{gas}}$$

where K_H is the Henry's law constant [mol Pa^{-1}], P_{gas} is the partial pressure of the gas in the gas phase [Pa] and $(gas)_{aq}$ is the molar concentration of the gas in solution.

B.2 Visco-capillary two-phase flow

In visco-capillary flow, gas transport is controlled by the interaction between the visco-capillary forces, gravity/buoyancy, solubility and diffusion, and the connectivity and spatial variability of the pore network. Lenormand et al. (1988) identified three major flow regimes, namely viscous fingering, capillary fingering, and stable displacement. The capillary number, defined as the ratio of viscous and capillary forces, and the viscous ratio, defined as the ratio of the viscosities of the defending and invading fluid, determine the transition between these flow regimes (Lenormand et al. 1988). Additional two-phase flow phenomena, such as migration (buoyancy-controlled transport), fragmentation (competition between capillary and buoyancy effects), and coalescence (interaction with trapped gas), are described by a third dimensionless number, which is defined as the ratio between viscous and hydrostatic forces.

In its conventional form, visco-capillary two-phase flow is described as a transport process whereby pore water in the pore volume of a rock formation is displaced by gas under the influence of viscous and capillary forces (e.g., Bear 1972). Visco-capillary two-phase flow accounts for the individual phase fluxes, given by the multiphase version of Darcy's law:

$$v_\beta = -\boldsymbol{k} \cdot \frac{k_{r\beta} \cdot \rho_\beta}{\mu_\beta} \left(\nabla p_\beta - \rho_\beta \cdot g\right)$$

where v_β is the Darcy velocity (volume flux) in phase β, k is the intrinsic permeability[1], $k_{r\beta}$ is the relative permeability (a function of saturation; see below) to phase β , μ_β is the viscosity, ρ_β is the density, and p_β is the fluid pressure of phase β. The coefficient g is the gravitational acceleration.

In a geomechanical sense, the rock mass is assumed to behave like an elastic medium, characterised by porosity and rock compressibility. The controlling factor for gas/water the two-phase flow characteristics of a porous medium is the capillary strength (also known as the gas entry pressure or capillary threshold pressure), which represents the difference between gas pressure and water pressure needed to displace the pore water from the initially fully saturated medium. Once the gas entry pressure has been exceeded, gas flow is mostly controlled by the intrinsic permeability (k)[12] of the medium, the permeability-saturation relationship (commonly known as relative permeability), and the relationship between the capillary pressure and the water saturation (also known as suction or water retention curve). The functional dependency between pore space saturation and the relative permeability or the capillary pressure is commonly described with parametric models as e.g., those of the Van Genuchten approach. According to van Genuchten (1980), the parametric relationship between water saturation and capillary pressure is given as:

---

[12] Intrinsic permeability is a tensorial quantity (in m^2) that describes the permeability of a material for a given phase when no other phases are present (single-phase conditions). In general, it is a measure of the ability of the porous material to allow a fluid to pass through it. It is considered predominantly a property of the porous medium pore space but may also depend on the properties of the fluid, so that intrinsic permeability of a material may differ i.e., for gas and water.

$$p_c = p_g - p_w = \frac{1}{\alpha} \cdot \left(S_e^{\frac{n}{1-n}} - 1 \right)^{\frac{1}{n}}$$

where p_c, p_g, and p_w represent the capillary pressure, gas pressure, and water pressure, respectively. $1/\alpha$, the inverse of van Genuchten's α parameter, is the capillary strength and n is a shape factor (pore size distribution index).

The pore water effective saturation, S_e , is the normalised volume of pore water, defined in terms of the pore water saturation, S_w and the liquid residual saturation, S_{wr}:

$$S_e = \frac{S_w - S_{wr}}{1 - S_{wr}}$$

In practical terms, the functional relationship between capillary pressure and saturation state of a porous medium is a measure of suction, or, in other words, of the saturation state for any given pressure difference between the fluid phases.

An example is shown in Fig. B-1, where *Material I* is assumed to have a lower capillary strength than *Material II*. At the boundary between the two materials, the pressure has to be continuous and corresponds to value $P_{c,y}$. There are, however, two different saturation values on either side of the interface, $S_{W,I}$ and $S_{W,II}$. *Material I* has lower suction and thus more gas is present in its pores (saturation $S_{W,I}$). *Material II* has higher suction and will maintain a higher liquid saturation ($S_{W,II}$).

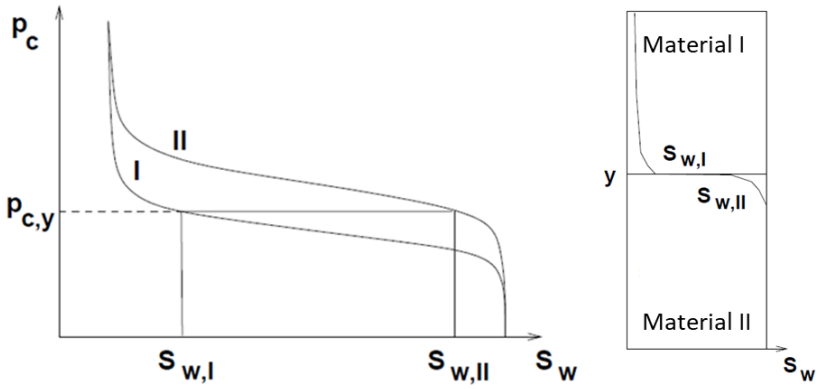

Fig. B-1: Capillary pressure and saturation difference at the boundary between two materials with different capillary strengths

The relative gas/water permeabilities $k_{r,g}$ and $k_{r,w}$ of a porous media can be described by the model given in Mualem (1976) (see also Helmig 1997):

$$k_{r,g} = \left(1 - S_{ekg}\right)^{\gamma} \cdot \left(1 - S_{ekg}^{\frac{n}{n-1}}\right)^{2(1-1/n)}$$

$$k_{r,w} = S_e^{\varepsilon} \cdot \left[1 - \left(1 - S_e^{\frac{n}{n-1}}\right)^{\frac{n-1}{n}}\right]^2$$

S_e and S_{ekg} are the effective saturations for water and gas, respectively, and ε and γ are empircal shape factors representing the pore connectivity of the medium. Typically, these are set to $\varepsilon = 1/2$ and $\gamma = 1/3$ (Luckner et al. 1989).

According to the Mualem approach, the definition of the effective saturation S_{ekg} for gas is defined using the residual gas saturation S_{gr}.

$$S_{ekg} = \frac{S_w}{1 - S_{gr}}$$

B.3 Pathway dilation

Dilatancy-controlled flow (or "pathway dilation", after Horseman 1996; Fig. 4-1) is a transport mechanism of special importance for argillaceous media with low tensile strength. Clay-rich rock cannot withstand long-term gas pressures with a magnitude greater than the minimum principal stress acting on the rock mass. Due to the expected micro-scale variability of the geomechanical rock properties, it is plausible that microfractures will form before yielding (ductile fracturing). The process of gas-driven micro-fracturing leads to an increase of the void space, which is accompanied by a detectable increase in intrinsic permeability and a change in the capillary pressure-saturation relationship. Gas flow is still controlled by visco-capillary forces; the main difference compared with conventional two-phase flow is that the transport properties of the solid phase can no longer be viewed as invariants, since they depend on the state of deformation of the rock, i.e., on state variables such as pressure. A comprehensive literature review on empirical investigations and phenomenological descriptions of dilatancy-controlled gas flow is provided in Nagra (2008).

The well-established critical state theory (e.g., Wood 1990, Azizi 2000) forms the foundation for the conceptualisation of rock deformation due to gas transport processes. Coupling of hydraulic and mechanical state parameters (gas / water pressure, rock stress, water saturation) is expressed in terms of an effective stress formulation (e.g., Azizi 2000). Furthermore, empirical relationships are introduced to link rock deformation with porosity and permeability. A consequence of this conceptual framework is that a smooth transition is expected between conventional two-phase flow and dilatancy controlled gas flow (c.f., Fig. 5-1), when the geomechanical state of the porous medium changes from poro-elastic towards a plastic deformation. Flow and transport processes in a deformable porous medium are still controlled by visco-capillary forces, which can be expressed by a capillary pressure and relative permeability relationships, respectively. Other parameters, however, such as the intrinsic permeability and the gas entry pressure (capillary strength) are no longer seen as invariants, but depend on the state of deformation of the porous medium.

Alonso et al. (2006) developed a hybrid formulation for pathway dilation, expressing the effective permeability of the rock as the superposition of an intrinsic matrix permeability and a stress dependent fracture transmissivity (embedded fracture approach). The approach was tested successfully for soft clays (bentonite) and for claystone. An even simpler approach has been introduced by Senger et al. (2008), which uses a pressure dependent permeability multiplier to calculate an enhanced permeability:

$$k' = k\left[1 + \left(k_{factor} - 1\right)\frac{P - P_1}{P_2 - P_1}\right]$$

where k_{factor} is a scaling factor, P_1 is the characteristic pressure for the onset of dilation and P_2 is the maximum pressure corresponding to the maximum enhanced permeability. Accordingly, capillary strength of the porous medium under dilatant conditions can be scaled through Leverett's function as:

$$P_0' = P_0\sqrt{\frac{k}{k'}}.$$

Papafotiou & Senger (2014) performed analyses of gas induced effects in a generic L/ILW repository, assuming an onset of dilation at 80% of the lithostatic stress at repository level and an enhancement factor of 10 between the onset (80%) and the lithostatic stress (100%). An important feature of this implementation is that permeability and capillary strength revert to their original values once pressure has dissipated.

B.4 Gas transport along macroscopic tensile fractures (hydro- and gas-fracturing)

As a rule of thumb, a macroscopic tensile fracture (hydrofrac/gasfrac) develops when the gas pressure is larger than the sum of the minimal principal stress and the tensile strength of the rock. The brittle fracture is initiated quasi-instantaneously without precursory plastic deformation and propagates at about the velocity of a shear wave (e.g., Gross 2007). Gas flow in such a macroscopic tensile fracture can be seen as a single-phase process. The propagation comes to a halt when the gas pressure in the fracture becomes less than the value of the minimum principal stress (shut-in pressure). In a rock with low tensile strength, a macroscopic fracture develops only when the gas pressure build-up is rapid, i.e., when the combined effect of pore water displacement and formation of small-scale fractures (dilatancy) no longer counterbalances the gas production rate. This is not the case in the post closure period of the geological repository, because the initial gas storage capacity of the backfilled underground structures is sufficiently high to damp the pressure build-up during the early post closure period when the high gas generation rates are expected. In the late post closure period, the gas generation rates decrease significantly and the gas transport capacity of the host rock and the sealing system is sufficient to accommodate the generated gas. Therefore, hydro- and gas-fracs are not expected under the conditions relevant for the geological repository. This has been elucidated in Chapter 7.

B.5 References

Alonso, E., Olivella, S. & Arnedo, D. (2006): Mechanisms of gas transport in clay barriers. Journal of Iberian Geology/32(322), 175-196, available online at https://www.semanticscholar.org/paper/Mechanisms-of-gas-transport-in-clay-barriers-Alonso-Olivella/8dbeacb5188f04e21ebb6a9f5c0d0ef449e24488.

Azizi, F. (1999): Applied analyses in geotechnics. First edition, Boca Raton, FL. CRC Press, an imprint of Taylor and Francis.

Bear, J. (1972): Dynamics of Fluids in Porous Media. Elsevier.

Coussy, O. (2004): Poromechanics. 2nd ed., Chichester. Wiley, available online at https://onlinelibrary.wiley.com/doi/book/10.1002/0470092718.

Domenico, P.A. & Schwartz, F.W. (1998): Physical and chemical hydrogeology. 2. ed., paperback, New York, Weinheim. Wiley, available online at http://www.loc.gov/catdir/description/wiley034/97021776.html.

Greenkorn, R.A. (1972): Transfer operations, New York, Maidenhead. McGraw-Hill.

Gross, D. (2007): Bruchmechanik. Mit einer Einführung in die Mikromechanik. 4., bearb. Aufl. 2007, Berlin, Heidelberg. Springer Berlin Heidelberg, available online at http://nbn-resolving.org/urn:nbn:de:bsz:31-epflicht-1551365.

Helmig, R. (1998): Multiphase flow and transport processes in the subsurface. A contribution to the modeling of hydrosystems. xvi, 367p. Berlin: Springer-Verlag, 1997. Price £49.00. J. Mar. Biol. Ass. 78/1, p. 349. DOI: 10.1017/S0025315400040170.

Horseman, S.T. (Nuclear Energy Agency) (1996): Water, gas and solute movement through argillaceous media. OECD publications, 79325, Paris. OECD.

Lenormand, R., Touboul, E. & Zarcone, C. (1988): Numerical models and experiments on immiscible displacements in porous media. J. Fluid Mech. 189, 165-187. DOI: 10.1017/S0022112088000953.

Luckner, L., Genuchten, M. & Nielsen, D.R. (1989): A consistent set of parametric models for the two-phase flow of immiscible fluids in the subsurface. undefined, available online at https://www.semanticscholar.org/paper/A-consistent-set-of-parametric-models-for-the-flow-Luckner-Genuchten/9ca9007c6ca30c09198af1dff4e059d10a945c73.

Millington, R.J. & Quirk, J. (1961): Permeability of porous solids. Trans. Faraday Soc. 57, 1200-1207. DOI: 10.1039/tf9615701200.

Mualem, Y. (1976): A new model for predicting the hydraulic conductivity of unsaturated porous media. Water Resources Research 12/3, 513-522. DOI: 10.1029/WR012i003p00513.

Nagra (2008a): Effects of post-disposal gas generation in a repository for low- and intermediate-level waste sited in the Opalinus Clay of Northern Switzerland. Nagra Technischer Bericht NTB 08-07.

Nagra (2008b): Vorschlag geologischer Standortgebiete für ein SMA- und ein HAA-Lager: Begründung der Abfallzuteilung, der Barrierensysteme und der Anforderungen an die Geologie (Bericht zur Sicherheit und Machbarkeit). Nagra Technischer Bericht NTB 08-05.

Papafotiou, A. & Senger, R.K. (2014): Sensitivity analyses of gas release from a L/ILW repository in the Opalinus Clay in the candidate siting regions of Northern Switzerland. Nagra Arbeitsbericht NAB 13-92.

Senger, R., Lanyon, B., Marschall, P.V.S. & Fujiwara, A. (2008): Numerical modeling of the gas migration test at the Grimsel Test Site (Switzerland). Nuclear Technology 164/2, 155-168.

Valkó, P. (2013): Hydraulic Fracturing. In John Wiley &. Sons Inc, Raymond Eller Kirk, Donald F. Othmer (Eds.): Kirk-Othmer Encyclopedia of Chemical Technology. (Wiley online library). New York: Wiley, 1-24.

van Genuchten, M.T. (1980): A Closed-form Equation for Predicting the Hydraulic Conductivity of Unsaturated Soils. Soil Science Society of America Journal 44/5, 892-898. DOI: 10.2136/sssaj1980.03615995004400050002x.

Wood, D.M. (1990): Soil Behaviour and critical state soil mechanics. Edited by Cambridge University Press.